# UNIVERSIDAD DE INVESTIGACIÓN DE TECNOLOGÍA EXPERIMENTAL YACHAY

## Escuela de Ciencias Químicas e Ingeniería

## TÍTULO: A REVIEW ON CHITOSAN-BASED COMPOSITE FILM REINFORCED WITH CELLULOSE: MORPHOLOGY AND MECHANICAL PROPERTIES

Trabajo de integración curricular presentado como requisito para la obtención del título de Ingeniero de Polímeros

**Autor:**

Sengés Bravo Alejandro Iván

**Tutor:**

PhD. Michell Uribe Rose Mary Rita

MSc. De Lima Eljuri Lola María

Urcuquí, junio 2021

**SECRETARÍA GENERAL**
**(Vicerrectorado Académico/Cancillería)**
**ESCUELA DE CIENCIAS QUÍMICAS E INGENIERÍA**
**CARRERA DE POLÍMEROS**
**ACTA DE DEFENSA No. UITEY-CHE-2021-00005-AD**

A los 10 días del mes de junio de 2021, a las 14:00 horas, de manera virtual mediante videoconferencia, y ante el Tribunal Calificador, integrado por los docentes:

| | |
|---|---|
| **Presidente Tribunal de Defensa** | Dra. LOPEZ GONZALEZ, FLORALBA AGGENY , Ph.D. |
| **Miembro No Tutor** | Dra. GONZALEZ VAZQUEZ, GEMA , Ph.D. |
| **Tutor** | Dra. MICHELL URIBE, ROSE MARY RITA , Ph.D. |

El(la) señor(ita) estudiante **SENGES BRAVO, ALEJANDRO IVAN**, con cédula de identidad No. **1316288164**, de la **ESCUELA DE CIENCIAS QUÍMICAS E INGENIERÍA**, de la Carrera de **POLÍMEROS**, aprobada por el Consejo de Educación Superior (CES), mediante Resolución **RPC-SO-41-No.476-2014**, realiza a través de videoconferencia, la sustentación de su trabajo de titulación denominado: **A REVIEW ON CHITOSAN-BASED COMPOSITE FILM REINFORCED WITH CELLULOSE: MORPHOLOGY AND MECHANICAL PROPERTIES**, previa a la obtención del título de **INGENIERO/A DE POLÍMEROS**.

El citado trabajo de titulación, fue debidamente aprobado por el(los) docente(s):

| | |
|---|---|
| **Tutor** | Dra. MICHELL URIBE, ROSE MARY RITA , Ph.D. |
| **Co - Tutor** | Mgs. DE LIMA ELJURI, LOLA MARIA |

Y recibió las observaciones de los otros miembros del Tribunal Calificador, las mismas que han sido incorporadas por el(la) estudiante.

Previamente cumplidos los requisitos legales y reglamentarios, el trabajo de titulación fue sustentado por el(la) estudiante y examinado por los miembros del Tribunal Calificador. Escuchada la sustentación del trabajo de titulación a través de videoconferencia, que integró la exposición de el(la) estudiante sobre el contenido de la misma y las preguntas formuladas por los miembros del Tribunal, se califica la sustentación del trabajo de titulación con las siguientes calificaciones:

| Tipo | Docente | Calificación |
|---|---|---|
| Miembro Tribunal De Defensa | Dra. GONZALEZ VAZQUEZ, GEMA , Ph.D. | 9,5 |
| Tutor | Dra. MICHELL URIBE, ROSE MARY RITA , Ph.D. | 10,0 |
| Presidente Tribunal De Defensa | Dra. LOPEZ GONZALEZ, FLORALBA AGGENY , Ph.D. | 10,0 |

Lo que da un promedio de: **9.8 (Nueve punto Ocho)**, sobre 10 (diez), equivalente a: **APROBADO**

Para constancia de lo actuado, firman los miembros del Tribunal Calificador, el/la estudiante y el/la secretario ad-hoc.

Certifico que *en cumplimiento del Decreto Ejecutivo 1017 de 16 de marzo de 2020, la defensa de trabajo de titulación (o examen de grado modalidad teórico práctica) se realizó vía virtual, por lo que las firmas de los miembros del Tribunal de Defensa de Grado, constan en forma digital.*

SENGES BRAVO, ALEJANDRO IVAN
**Estudiante**

Dra. LOPEZ GONZALEZ, FLORALBA AGGENY , Ph.D.
**Presidente Tribunal de Defensa**

FLORALBA AGGENY LOPEZ GONZALEZ
Digitally signed by FLORALBA AGGENY LOPEZ GONZALEZ
Date: 2021.06.11 09:22:47 -05'00'

ROSE MARY
RITA MICHELL
URIBE

Firmado digitalmente por
ROSE MARY RITA MICHELL
URIBE
Fecha: 2021.06.11 11:04:17
-05'00'

Dra. MICHELL  URIBE, ROSE MARY  RITA , Ph.D.
**Tutor**

GEMA GONZALEZ
VAZQUEZ

Digitally signed by GEMA
GONZALEZ VAZQUEZ
Date: 2021.06.11 14:00:29 -05'00'

Dra. GONZALEZ VAZQUEZ, GEMA , Ph.D.
**Miembro No Tutor**

CARLA SOFIA

Digitally signed by CARLA
SOFIA YASELGA NARANJO

YASELGA NARANJO  Date: 2021.06.11 08:56:20
-05'00'

YASELGA  NARANJO, CARLA
**Secretario Ad-hoc**

# AUTORÍA

Yo, **ALEJANDRO IVÁN SENGÉS BRAVO**, con cédula de identidad 1316288164, declaro que las ideas, juicios, valoraciones, interpretaciones, consultas bibliográficas, definiciones y conceptualizaciones expuestas en el presente trabajo; así cómo, los procedimientos y herramientas utilizadas en la investigación, son de absoluta responsabilidad de el/la autora (a) del trabajo de integración curricular. Así mismo, me acojo a los reglamentos internos de la Universidad de Investigación de Tecnología Experimental Yachay.

Urcuquí, junio 2021.

_____

Alejandro Iván Sengés Bravo
CI: 1316288164

# AUTORIZACIÓN DE PUBLICACIÓN

Yo, **ALEJANDRO IVÁN SENGÉS BRAVO,** con cédula de identidad 1316288164, cedo a la Universidad de Investigación de Tecnología Experimental Yachay, los derechos de publicación de la presente obra, sin que deba haber un reconocimiento económico por este concepto. Declaro además que el texto del presente trabajo de titulación no podrá ser cedido a ninguna empresa editorial para su publicación u otros fines, sin contar previamente con la autorización escrita de la Universidad.

Asimismo, autorizo a la Universidad que realice la digitalización y publicación de este trabajo de integración curricular en el repositorio virtual, de conformidad a lo dispuesto en el Art. 144 de la Ley Orgánica de Educación Superior

Urcuquí, junio 2021.

_____

Alejandro Iván Sengés Bravo
CI: 1316288164

**DEDICATORIA**

*A mis padres,*

*A mis hermanos.*

Alejandro Iván Sengés Bravo

# AGRADECIMIENTOS

Agradezco a mis padres por haberme apoyado todo el tiempo. Por ser el soporte y guía que necesitaba para mi formación.

Mi mayor gratitud hacia mi tutora PhD. Rose Mary Michell por brindarme su tiempo, guía, y motivación durante la realización de esta investigación. Además, por el gran aprendizaje que me llevo de sus clases. También a mi tutora MSc. Lola De Lima por su dedicación en este trabajo.

Me siento afortunado por haber tenido excelentes profesores. Cada uno de ellos enseñaba con pasión y era experto en la que hacía. Gracias a mis profesores Alex Palma, Juan Pablo Tafur, Hortensia Rodríguez, Alfredo Viloria, Alicia Sommer y Antonio Díaz.

De esta universidad me llevo grandes recuerdos y experiencias. Gracias a todos los que conformaron parte de esta etapa, y especialmente a mis amigos: Diana, David, Bryan, Michelle y Cindhy. Ustedes hicieron más llevadero estos últimos 5 años. No solo fueron largas noches de estudio juntos, también noches del "árbol de la vida", noches del Café y noches de Risk.

Alejandro Iván Sengés Bravo

# RESUMEN

En el presente trabajo se realizó una revisión bibliográfica respecto a películas de compósitos basados en quitosano y reforzados con celulosa. Este refuerzo involucraba celulosa micro fibrilada, celulosa microcristalina, nanofibras de celulosa y nanocristales de celulosa. Las propiedades analizadas de los compósitos fueron la morfología superficial y el desempeño mecánico.

Para llevar a cabo la investigación, se recolectó información de los últimos 5 años (2015-2020), y luego fue resumida y clasificada en tablas según el tipo de celulosa. La información de las tablas fue usada para obtener tendencias generales sobre la morfología superficial y las propiedades mecánicas de los compósitos a medida que el contenido del refuerzo incrementaba. Además, con ejemplos seleccionados de las tablas, se construyeron figuras para ilustrar mejor las tendencias del desempeño mecánico.

La adición de celulosa dio como resultado películas de compósitos con una morfología superficial donde el refuerzo estaba cubierto por la matriz y uniformemente distribuido. La dispersión del refuerzo era adecuada siempre y cuando este no estuviera en exceso. Por encima del punto de umbral, las interacciones celulosa-celulosa eran más fuertes que las de celulosa-matriz, formando aglomeraciones. Este evento fue más notorio con la adición de las micropartículas, ya que con estas la formación de agregados ocurría más tempranamente. En cuanto a las propiedades mecánicas, todos los refuerzos mejoraron la resistencia a la tensión y el módulo de Young, mientras que la elongación a la rotura fue disminuida. Las razones de esto se debieron principalmente a los fuertes enlaces intermoleculares de hidrógeno y a las interacciones electrostáticas entre el refuerzo y la matriz; además, debido a la naturaleza rígida de la celulosa, que en consecuencia redujo el alargamiento a la rotura de las películas. Considerando que la celulosa aumentó la resistencia y rigidez de los materiales, y redujo la flexibilidad, con nanofibras de celulosa las películas compuestas alcanzaron los mejores valores. Si bien es cierto que este material podría considerarse frágil, su aplicación estaría destinada para usos donde la ductilidad no sea requerida. Además, los otros rellenos podrían considerarse buenas opciones, dependiendo de la aplicación que se le quiera dar a la película.

**Palabras Claves**: quitosano, celulosa, biopolímeros.

# ABSTRACT

In the present work, a bibliographic review was carried out on chitosan-based composite films reinforced with cellulose. This reinforcement involved microfibrillated cellulose, microcrystalline cellulose, cellulose nanofibers, and cellulose nanocrystals. The analyzed properties of the composites were the surface morphology and mechanical performance.

To carry out the research, information from the last 5 years (2015-2020) was collected, and then it was summarized and classified in tables according to the type of cellulose. The information in tables was used to obtain general tendencies about the surface morphology and mechanical properties of the composites as the reinforcement content increased. Also, with examples selected from tables, figures were constructed to illustrate the mechanical performance tendencies better.

The addition of cellulose resulted in composite films with a surface morphology where the reinforcements were embedded within the matrix and evenly distributed. The dispersion of the reinforcements was adequate as long as the amount of filler was not excessive. Above the threshold point, cellulose-cellulose interactions were stronger than cellulose-matrix, forming agglomerates. This event was more noticeable with the addition of the microparticles since, with these, the formation of agglomerates occurred earlier. Regarding the mechanical properties, all the fillers improved the tensile strength and Young's modulus, while the elongation at the break decreased. This behavior was mainly due to strong intermolecular hydrogen bonds and electrostatic interactions between the reinforcement and the matrix; also, due to the rigid nature of cellulose, which consequently reduced the elongation at break of the films. Considering that cellulose increased the strength and rigidity of the materials, and reduced flexibility, with cellulose nanofibers, the composite films reached the highest values. Although this material could indeed be considered brittle, its application would be intended for use where ductility is not required. Furthermore, the other fillers could be considered good options, depending on the intended film application.

**Keywords:** chitosan, cellulose, biopolymers.

# CONTENT

# LIST OF FIGURES

# LIST OF TABLES

# LIST OF ABBREVIATIONS AND ACRONYMS

| | | | |
|---|---|---|---|
| **AFM** | Atomic Force Microscope | **MEF** | Moderate electric fields |
| **BC** | Bacterial cellulose | **MFC** | Microfibrillated cellulose |
| **CH** | Conventional Heating | **MIC** | Microfluidization |
| **CNCs** | Cellulose nanocrystals | **MW** | Molecular weight |
| **CNFs** | Cellulose nanofibers | **RMS** | Root means square |
| **D** | Diameter | **SEM** | Scanning Electron Microscope |
| **DDA** | Degree of deacetylation | **TEM** | Transmission Electron Microscope |
| **DES** | Deep Eutectic Solvents | | |
| **EB** | Elongation at break | **TS** | Tensile strength |
| **FTIR** | Fourier-Transform Infrared Spectroscopy | **UB** | Ultrasonic bath |
| **GA** | Glutaraldehyde | **XCNCs** | X wt.% CNCS |
| **L** | Length | **XCNFs** | X wt.% CNFs |
| **MC** | Microwave | **XMCC** | X wt.% MCC |
| **MCC** | Microcrystalline cellulose | **XMFC** | X wt.% MFC |
| **MECH** | Mechanical stirring | **YM** | Young's modulus |

# CHAPTER I:

# General Introduction

## 1.1. Introduction

The wide production of synthetic plastics is due to their different fields of applications, such as medical, food industries, and others [1], [2]. The development and growth of technologies involved in obtaining these traditional polymers have turned them into economically viable products. Additionally, this kind of plastics has excellent mechanical properties that offer good performance even under unfavorable conditions. However, they are non-biodegradable and can remain in the environment for years [3]. The environmental problems caused by the use of synthetic polymers have motivated researchers into looking for alternative materials based on natural polymers since they are biodegradable, biocompatible, abundant, and come from renewable sources [4], [5].

Among natural polymers, chitosan is a polysaccharide that has been of interest to science and industry as a promising biopolymer that could replace synthetic plastics in some applications. This natural polymer is obtained through the deacetylation of chitin, which is the second most abundant polysaccharide on earth [6]. It is characterized by its biodegradability, biocompatibility, non-toxicity, flocculating capacity, antioxidant and antimicrobial activity [7]. These properties have made attractive the production of chitosan-based films for biomedical, food packaging, waste water treatment, cosmetics, electrical uses, and many others [8], [9].

Chitosan-based films can convert water vapor to electrical power making possible its application for electrical purposes [10]. Its ability to prevent the proliferation of foodborne pathogens and fungal attacks makes it useful for food packaging. The film could preserve the quality and improve the shelf life of edible products [2], [11]. Additionally, its mucoadhesive and carrier property allow it to be the main component of a drug delivery system [12]. On the other hand, despite all these unique characteristics,

chitosan-based films have deficiencies in some properties that are necessary to meet current industry standards.

Although chitosan has an excellent film-forming ability, its mechanical properties are insufficient compared to synthetic polymers [13]. Consequently, chitosan-based films have been blended with other polymers to obtain composite films with better performance [14]. The addition of cellulose as a reinforcement agent has been tested in many researches. It has been used modified cellulose, derivatives, and cellulose with different dimensions (micrometric and nanometric), i.e., cationic dialdehyde cellulose, carboxymethyl cellulose, methyl cellulose, cellulose nanofibers, cellulose nanocrystals, microcrystalline cellulose, and others [1], [15]–[18].

Cellulose is a semi-crystalline polymer consisting of D-glucopyranosyl units linked together by -(1,4)-glucosidic bonds [19]. This natural polymer is abundant, biodegradable, biocompatible, has a low density and cost [20]. It is the most abundant biopolymer on earth and is the main constituent of plants. Cellulose is mainly obtained from natural resources such as grass, straw fibers (wheat, rice, barley straw), leaf fibers, marine animals, fungi, algae, and bacteria [21], [22].

The potential of cellulose as a reinforcement is due to its barrier and high mechanical properties [23]. In a comparative study, chitosan and cellulose films were subjected to a tensile test, and it was found that the strength of cellulose was almost twice that of the chitosan film [24]. It is well known that the drawback of chitosan films is their low mechanical properties [21]. Thus, the elaboration of chitosan-based composite films reinforced with cellulose has resulted in a synergistic effect, in which chitosan gets properties that it could not have individually.

## 1.2. Problem Statement

Cellulose reinforced chitosan-based composite films have been shown as a promising material to be used in a drug delivery system, wound healing, food packaging, water treatment, and electrical applications [10], [25]–[28]. The chemical nature and similar structure of both polysaccharides have made possible good compatibility between them. As a result of forming good interactions, this fully bio-sourced material is owned of excellent mechanical properties [28]. Therefore, this work aims to carry out a literature review of the last five years (2015-2020) on chitosan-based composite films reinforced with cellulose, including modifications, derivatives, and different sizes of cellulose. A

particular emphasis will be placed on the mechanical and morphological properties without neglecting other important properties of the films, such as the barrier, antimicrobial and optical properties. To our knowledge, there is not a review focus on cellulose as a reinforcement of chitosan. Thus, it will be possible to determine what might be the best reinforcement for chitosan.

## 1.3. Objectives

### 1.3.1. General Objective

To review the literature of the last 5 years on cellulose reinforced chitosan-based composite films.

### 1.3.2. Specific Objective

- To analyze the surface morphology of chitosan-based films by incorporating cellulose nanocrystals, cellulose nanofibers, microfibrillated cellulose, or microcrystalline cellulose.
- To analyze the mechanical performance of chitosan-based films by incorporating cellulose nanocrystals, cellulose nanofibers, microfibrillated cellulose or microcrystalline cellulose.
- To study the effects on cellulose reinforced chitosan-based composite films by incorporating plasticizers, cross-linking agents, and the substitution of the reinforcement by modified cellulose.
- To determine the best filler for chitosan-based films.

# CHAPTER II:

# Chitosan

Chitosan is a polysaccharide derived by the deacetylation of chitin, which is the most abundant natural polymer after cellulose [6]. It is characterized by its biodegradability, biocompatibility, non-toxicity, antioxidant and antimicrobial activity. The fields of chitosan application are biotechnology, pharmaceutical, agriculture, food, and cosmetics [4], [8]. It can be used as a fertilizer, dietary supplement, paper manufacturing, flocculating agent for water treatment, substitute for hyaluronic acid in cosmetics, coatings or packaging in food, wound dressing, drug delivery vehicles, tissue engineering, manufacture of artificial skin, gene delivery, adjuvant in vaccines and many others[8], [29].

## 2.1. From Chitin to chitosan

Chitin is a semi-crystalline homopolymer made up of N-acetyl-d-glucosamine units linked by β,1-4 glycosidic bonds [30]. It is known as a structural polymer found in the cell walls of fungi and the exoskeleton of crustaceans [2], [31]. Also, it is present in the cuticles of insects, wings of cockroach, grasshopper species, and aquatic invertebrates, although commercially, it is mainly extracted from crabs, shrimps, krill shells, and fungi since they are part of the waste of food industries [21], [31].

According to the literature, the seafood processing industry generates approximately 8.5 million tons of waste, but not all can be considered chitin. For example, in crustaceans shells, 20-40% protein, 20-50% calcium and magnesium carbonate, 15-40% chitin, and other minor components [31]–[33]. There are two possible methods for the extraction of chitin from animal waste: chemical and biological. The most common industrial process is the chemical way, and it consists of three steps (Figure 1): demineralization, deproteinization, and depigmentation [34].
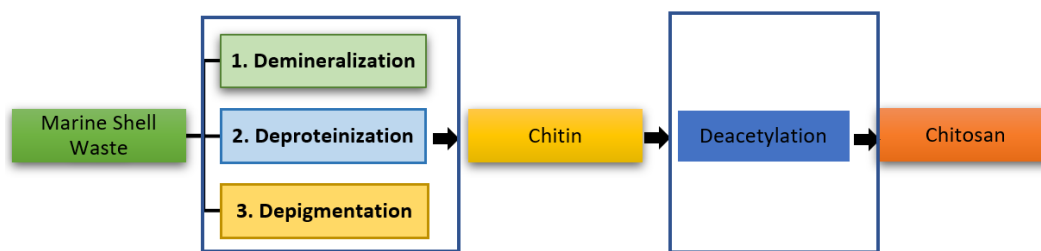
Figure 1. Overview of production of chitin and chitosan from marine shell waste

The demineralization process consists of removing calcium carbonate and other minerals by treating the raw material with an acidic solution. First, the shell wastes are washed and ground to a smaller size. Then, they are placed into the acidic solution at room temperature and constant stirring. After a time (1-48 h), calcium carbonate breaks down into water-soluble calcium salts with carbon dioxide release. A similar reaction occurs with the other minerals, and all the salts are separated by filtration of the solid chitin phase. The acid used in this step can be $HNO_3$, $H_2SO_4$, $HCOOH$, $CH_3COOH$, or $HCl$, the latter being the most used with a concentration between 0.275 and 2 M [32], [35]. After demineralization, the sample is washed until it reaches a neutral pH. Then it is dried [11], [35].

The deproteinization process consists of the removal of proteins by solubilizing the dried decalcified shells in a dilute aqueous sodium hydroxide (NaOH) [11], [31]. There are other deproteinization reagents such as $Na_2CO_3$, $NaHCO_3$, $KOH$, $K_2CO_3$, $Ca(OH)_2$, $Na_2SO_3$, $NaHSO_3$, $CaHSO_3$, $Na_3PO_4$, and $Na_2S$, although sodium hydroxide is the most used. This process is carried out with constant stirring for 1-72 hours at temperatures ranging from 65 to 100 °C [11], [30], [32].

The depigmentation is responsible for removing leftover pigment and obtaining a less color product. In this process, the sample is treated again with an alkaline solution [34], [36].

After the three steps, chitin is obtained as the final product. However, these treatments must be adapted to each chitin source. Furthermore, the deproteinization and demineralization would carry out by an enzymatic method instead of the chemical. In an enzymatic way, lactic acid-producing bacteria and proteases from bacteria for demineralization and deproteinization steeps, respectively. This different route implies

that the residual protein and the reaction time are higher than in the chemical method; therefore, it is not applied industrially [35], [37].

On the other hand, for chitosan production, there are also two available processes. Chitin can be converted into chitosan by an enzymatic or chemical method. In the first case, the enzyme used is chitin deacetylase, being this an ecofriendly method. However, again it takes several days and is limited to laboratory-scale studies. Regarding the chemical method, this is the most common due to its suitability for mass production [34], [37]. Therefore, the following process will be based on this.

To the production of chitosan, the isolated chitin is deacetylated. It is treated with concentrated NaOH or KOH solution (40-50 %), commonly at 100 °C for a few hours. During that time, the acetyl groups from the chitin are hydrolyzed. The N-acetyl-D-glucosamine units are converted to D-glucosamine units with free amine groups (Figure 2). The deacetylation degree of chitosan is influenced by the alkali concentration, time, and temperature at which its production is carried out [11], [38]. In some cases, the deacetylation process would be repeated to get higher values. A deacetylation degree between 75 and 95% is expected since the physical and chemical properties of chitosan mainly depend on [21], [39].
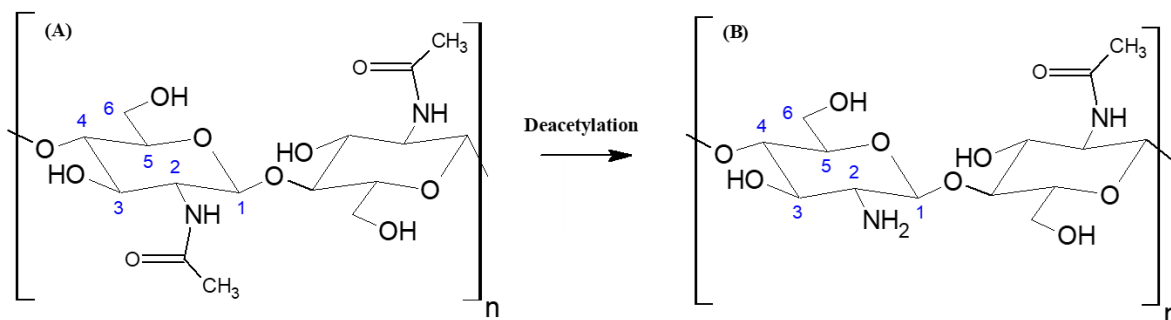


Figure 2. (A) Chitin and (B) Chitosan structure [32]

## 2.2. Chitosan Structure

The chemical structure of chitosan consists of two monomeric units. This copolymer is composed of D-glucosamine and N-acetyl-D-glucosamine units linked linearly via 1,4-glycosidic bonds [2], [40]. The proportion in which they are present depends on the alkaline treatment, and it is quantified as deacetylation degree [31]. D-glucosamine

content is expected to be between 75-95%. If the biopolymer comprises a majority proportion of N-acetyl-D-glucosamine, the polymer is chitin [30].

The repeating unit of chitosan consists of three reactive functional groups (Figure 2). It has one primary amine or acetamide group and a primary and secondary hydroxyl group at C-2, C-3, and C-6 positions, respectively [30]. These functional groups make the polymer flexible for molecularly imprinted polymers and more prone to undergo chemical modifications [2], [41]. They also influence some critical characteristics of chitosan, including solubility, antibacterial activity, and mechanical attributes that will be discussed in the next section [2].

Since chitosan is a partially deacetylated product of chitin, at the C-2 position, there will be two possible functional groups, the primary amine being the most frequent at the site. This group makes chitosan soluble in aqueous acidic solutions [21]. When the polymer is in acidic media, the amino groups present in the chain get protonated, and the chitosan becomes cationic [11]. The cationic sites formed increase solubility by increasing polarity and the degree of electrostatic repulsion [31]. Simultaneously, positively charged amines can electrostatically interact with anionic groups present on the surface of bacterial cells, inhibiting bacterial growth or inducing cell death [21].

### 2.3. Chitosan Properties

#### 2.3.1. Molecular weight

The molecular weight (MW) of chitosan is defined as the number of sugar units per polymer molecule [31]. It varies between 50 and 2000 kDa [30]. Physical and chemical properties as viscosity, solubility, adsorption on solids, elasticity, tear strength, and bio-activities depend on MW [2], and according to the requirements, its value can be modified.

Increasing MW can affect the crystal size and antimicrobial activity of the biopolymer. With high values, the membrane crystallinity was found to decrease [31]. Also, chitosan could not pass through a microbial membrane. Consequently, it does not block the transport of vital solutes to the microorganism and, bacterial growth is not inhibited [42]. For a good penetration, the MW of chitosan must be less than 5000 kDa [30], and when it is exceeding, MW can be lowered by acidic or enzymatic depolymerization [36].

### 2.3.2. Degree of deacetylation (DDA) and distribution of acetyl groups

The degree of deacetylation (DDA) of chitosan is referred to as the content of the acetyl group in the structure [36]. With high DDA values, there is a low content of N-acetyl-d-glucosamine units; that is, primary amine mostly occupies that C-2 position.

DDA correlates with the solubility and crystallinity of chitosan. Commercially available chitosan has a DDA ranging from 50 to 98% [36]. From 50% DDA, the biopolymer becomes soluble in aqueous acid media [31]. Depending on the application, chitosan will require a higher or lower value of DDA. To increase it, it can be subjected to a repeated alkaline treatment, or for the opposite effect, it is re-acetylated [21], [31].

As DDA increases, chitosan becomes more flexible, and the other mechanical properties tend to be weaker. Also, the polymer forms a random coil with more intramolecular hydrogen bonds within the chain. On the other hand, when the chitosan is less deacetylated, a more extended chain is formed. It has stronger intermolecular interactions and bio-activities such as cell adhesion and proliferation decrease. Other properties like cytocompatibility are not changed by DDA [31], [40].

### 2.3.3. Solubility

Chitosan is insoluble in water but soluble in dilute acid solutions. The nonbonding electron pairs of the amino groups are protonated under acidic conditions, making chitosan a cationic polymer that permits interaction with different molecules. It is soluble in organic acid solutions like acetic, lactic, citric, and hydrochloric [5], [39]. Its ability to become a polyelectrolyte in acidic media is why the large set of applications in different fields (agriculture, medical science, industrial engineering); it is the only pseudo-natural cationic polymer [36].

The protonation of the amino groups occurs in week acid solutions at pH values below 6. At basic pH values, protonation does not occur, and, therefore, the polymer is not solubilized. At a pH value of about 6.5, there is a state of transition between solubility and insolubility [30]. On the other hand, the solubility of chitosan is not only depending on the pH solution. There are many factors [30], [36], [38]:

- The ionic strength of the solvent that guides the salting-out effect
- Ions in the solvent interacting with chitosan and limiting its solubility
- Degree of deacetylation
- Molecular weight

It was found that the amount of acid necessary to dissolve chitosan varies concerning the mass to be dissolved. The concentration of protons needed must be at least equal to the concentration of -NH$_2$ units involved [36]. Furthermore, it is possible to dissolve chitosan in a basic pH solution when it has a medium molecular weight and a degree of deacetylation of 0.5 [38].

In general, all chitosan varieties, neglecting their characteristics, are soluble in a pH solution below 6.

### 2.3.4. Antimicrobial Activity

Chitosan is a natural polymer with an inherent antimicrobial activity. It can inhibit the growth of a wide variety of fungi, yeast, and bacteria [42]. This property depends on its cationic nature, degree of deacetylation, molecular weight, temperature conditions, and type of microbial [38], [43]–[45].

Some investigations have obtained different results regarding the antimicrobial activity of chitosan. As stated above, the performance of chitosan depends on many factors. In some cases, the film antimicrobial activity against Gram-positive bacteria has been greater than against Gram-negative bacteria [46], [47], or the opposite [48], [49]. Furthermore, the characteristics of the polymer will influence differently depending on the type of microorganism. Zhen and others [50] tested the antimicrobial activity of chitosan with different molecular weights. They reported that the antimicrobial activity against Gram-positive bacteria S. aureus was improved with high molecular weights. This result is explained by the fact that chitosan forms a film that inhibits nutrient entry to bacteria. In the same work, the antimicrobial test showed better performance against Gram-negative bacteria E. coli as the molecular weight of the chitosan decreased. In this case, the mechanism proposed is that chitosan penetrates the cell wall of the bacteria to disturb the metabolism of the cell, so if the molecular weight is low, diffusion is more accessible [50], [51].

Some mechanisms have been proposed to describe the antimicrobial activity of chitosan. One of the most accepted is related to the primary amines of its backbone. When the amino groups are protonated, they can interact with anionic groups of the bacterial cell membrane. This interaction causes changes in permeability that lead to the death of the cell by inducing leakage of intracellular components [52], [53]. However, the protonation of the amino groups occurs when chitosan is in an acidic medium. To have a component

with a permanent charge, it is very common to subject chitosan to a structural modification. Chemical modification such as quaternization, carboxymethylation, or cationization gives a chitosan derivative with better antimicrobial activity by the fact that they have a greater amount of positive charges in the form of $-NH_3^+$ [21], [52], [54]. It enhances its ability to interact with the bacterial cell wall.

Below are several hypotheses raised about the antimicrobial activity of chitosan-based films [38], [55].

- Chitosan-based films can act as a protective layer that protects a surface from the attacks of the outer microbial [56].
- Chitosan-based films can act as an oxygen barrier. This characteristic limits the rate transfer of oxygen and, as a result, inhibits the growth of aerobic microbes in a system [45].
- The polycationic nature of chitosan makes possible its absorption on the surface of a microorganism. As a consequence, an impermeable polymeric layer is formed around it and causes blockage. This layer inhibits nutrients and vital solutes from entering the microbial cell, resulting in failure of metabolic machinery and finally cell death [57].
- Protonated chitosan or its derivates with high-density charge can interact with the anionic groups (lipids, proteins, carbohydrates) of a bacterial cell wall, causing distortion and deformation [58].
- Chitosan can pass through the cell wall. The electrostatic interactions between the cationic groups of chitosan and peptidoglycans of a cell wall alter the cytoplasmic membrane of bacteria, leading to leakage of the intercellular components and, consequently, cell death [59].
- Low molecular weight chitosan can penetrate the cell nuclei and inhibit RNA transcription by binding to the DNA [60].

# CHAPTER III:

# Cellulose

Cellulose is a natural polymer that is considered the most abundant polysaccharide on earth, with an annual production of about $1.5 \times 10^{12}$ tons. It can be obtained from different sources such as wood, plants, marine animals, fungi, algae, and bacteria [61]. The primary source of this polysaccharide is from the vegetal kingdom since cellulose is the major constituent of the cell walls, serving as a structural polymer [21]. However, the cellulose from plants is accompanied by hemicellulose, lignin, and small amounts of extractives. This production is not pure, and cellulose must be isolated through different treatments, typically mechanical and chemical [62].

Cellulose characteristics are biodegradability, biocompatibility, renewability, low density and cost, good mechanical properties, and producibility. Products based on cellulose are widely used in textile, sorption media, medical supplies, packaging, biomedical, and many other applications [21], [61].

## 3.1. Cellulose structure

Cellulose is a homopolymer composed of β-glucose molecules. The number of these segments is between 1,000 and 30,000 and depends on the cellulose source [61]. For example, plant cellulose has a degree of polymerization lower than bacterial cellulose (up to 8,000) [63]. The repeat unit of cellulose consists of two anhydroglucose rings that are linked together by β-1,4 glycosidic bonds. In summary, oxygen covalently bonded to C1 of one glucose ring is also linked to C4 of the adjacent ring. This dimmer of glucose is known as cellobiose. [64], [65].

Each anhydroglucose ring is composed of three reactive hydroxyl groups (Figure 3). There are one primary and two secondary hydroxyl groups at C6, C2, and C3 positions, respectively. At the end of the chain, there are two different terminations. One side, the nonreducing end, has an anomeric atom of C connected with the glycosidic bonds. While

the other side, the reducing end, contains a D-glucopyranose unit in equilibrium with the aldehyde function [61].
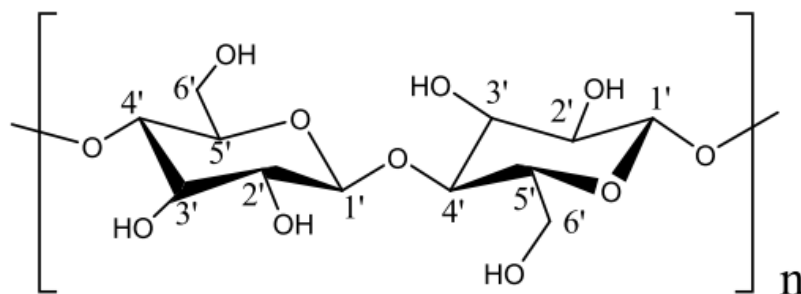


Figure 3. Chemical structure of cellulose [66]

On the other hand, the structure is stabilized by intramolecular and intermolecular interactions. The presence of intra and inter-chain hydrogen bonds between hydroxyl groups and oxygens makes cellulose a relatively stable polymer. Furthermore, the interactions between adjacent molecules drive a parallel stacking of multiple cellulose chains forming longer units known as elemental fibers (protofibrils), which pack into larger units called microfibrils. The microfibrils agglomeration is carried out by Van der Waals forces and hydrogen bonds [62], [64].

The cellulose fibrils are composed of two regions, the crystalline and amorphous zone. The first one is considered as an ordered domain in which cellulose chains are arranged together in crystallites. While the other one represents a disordered domain in which the microfibrils have been distorted due to internal strain (tilt/twist) in the fiber; they are segments of chain dislocations [67].

### 3.2. Cellulose polymorphs

There are several cellulose polymorphs: cellulose $I$, cellulose $II$, cellulose $III$, and cellulose $IV$. These allomorphs depend on the cellulose source, method of extraction, or treatment [64]. Cellulose $I$ is considered as "natural cellulose", and it can be obtained from trees, plants, tunicates, alga, and produced by bacteria. Within this polymorph, there are two suballomorphs: $I_\alpha$ with a triclinic structure and $I_\beta$ with a monoclinic structure. Both coexist in different proportions depending on the cellulose source [62]. When cellulose is produced by bacteria [68] or algae [69], $I_\alpha$ is the principal constituent, while in the case of tunicates [70], [71], or higher plant cellulose [68], $I_\beta$ is predominant. The polymorph $I_\beta$ is more thermodynamically stable than $I_\alpha$ and as a consequence cellulose

12

with a majority of $I_\alpha$ is subjected to thermal treatments in alkaline solutions or in organic solvents in which $I_\alpha$ is partially converted into $I_\beta$ [62].

Cellulose *II* can be obtained from cellulose *I*. It is the most stable to date, and the molecules are more densely packed and strongly interbonded [61]. Cellulose *II* can be produced by two different processes: chemical regeneration and mercerization. In the chemical regeneration, cellulose *I* is dissolved in a solvent and then is recrystallized in water. Solvent includes solutions of cupric hydroxide in aqueous ammonia, ammonium thiocyanate, hydrazine/thiocyanate, ethylenediamine/thiocyanate salt, N-methylmorpholine-N-oxide/water, etc [64], [72], [73]. In mercerization, cellulose *I* is submerged in a swelling agent such as concentrated sodium hydroxide solutions or in nitric acid. Cellulose *II* is obtained after removing the swelling agent [64]. The resultant molecule has a monoclinic structure and has been used to make cellophane, rayon and textile fibers [74].

Cellulose *III* can be obtained from cellulose *I* or cellulose *II* when they are exposed to ammonia (gas or liquefied). Polymorph *IV* may be formed by heating cellulose *III* up to 260 °C in glycerol. As cellulose *I*, cellulose *IV* could be found is some plants, mainly in the primary cell walls [64].

### 3.3. Isolation of cellulose

As mentioned, cellulose fibers may be obtained from different sources such as wood, plants, algae, tunicate, and bacteria. The extraction method depends on the cellulose source, and further treatments influence the desired product. It could be gotten microfibrillated cellulose, microcrystalline cellulose, cellulose nanofibers, and cellulose nanocrystals.

In general, the isolation of cellulose consists of two steps: purification and treatments. This section will focus on cellulose from wood, plants, and bacteria due to the frequent use.

### 3.3.1. Cellulose from plants or wood

The raw material is previously subjected to cutting, washing, drying, and grinding processes [75]. The purification method consists of removing hemicellulose, lignin, and other components from the cellulose matrix. In order to eliminate them, this method includes two pre-treatments, an alkaline, and bleaching. The alkaline pretreatment

consists of immersing the cellulosic material in sodium hydroxide [12], [19], [83]–[85], [75]–[82] or potassium hydroxide [86], [87]. In this remotion, almost all of the hemicellulose is removed, including a small amount of lignin. For bleaching pre-treatment, the material is subjected to a hydrogen peroxide [12], [75], [77], [83], [86] or sodium chlorite [12], [19], [87], [76]–[79], [81], [82], [84], [85] solution. In this part, pigments and considerable amounts of lignin are removed.

The purification step makes it possible to obtain cellulose fibers almost pure. For the second step, the treatments will depend on the size, aspect ratio, crystallinity, crystal structure, morphology, and properties desired for the final product [62]. For the production of microcrystalline cellulose and cellulose nanocrystals, it is very common to hydrolyze the purified fibers in acidic solutions of sulfuric acid [1], [12], [90], [13], [19], [75], [78], [84], [86], [88], [89] or hydrochloric acid [28], [77], [79], [91]. The strongest hydrolysis and additional treatments like ultrasound result in the nanocrystal particles [61]. They are obtained by applying a high shear force to the raw material for cellulose micro or nanofibers. The smallest particles, the nanofibers, would be obtained by subsequent ultrasound application [92]. Also, an alternative method for cellulose nanofibers involves the application of mild acid or enzymatic hydrolysis with high shear mechanical forces (high-pressure homogenizers, ultrasonic homogenizers, or grinders) [5], [76], [93].

The process presented here is general, and additional treatments may be applied. For a better understanding, the production processes are available within the respective references for the following specific cases: microcrystalline cellulose [87], [91], microfibrillated cellulose [81], [82], [85], cellulose nanofibers [79], [86], and cellulose nanocrystals [75], [77].

### 3.3.2. Cellulose from bacterial

Bacterial cellulose is synthesized by many bacteria such as Gluconacetobacter xylinus [94], Komagateibacter xylinus [95], Glucanocetobacter hansenil [96], and many others. Unlike plant cellulose, this does not require a remotion process of lignin and hemicellulose. Furthermore, it presents a higher degree of polymerization, water absorption capacity, hydrophilicity, ultrafine network architecture, good compatibility, non-toxicity, and transparency that can be used in biomedical fields [63], [95], [97].

The synthesis of bacterial cellulose is carried out under special culturing conditions that make possible the secretion of cellulose microfibrils, forming a thick gel [62]. The culture conditions include many variations as temperature, additives, static fermentation, or agitated fermentation. These conditions are adapted to the kind of bacteria and influence the chemical structure, composition and viscosity of the bacterial cellulose [98].

In order to isolate the bacterial cellulose from the culture medium, it is subjected to a purification step. The film formed is placed into a hydroxide sodium solution with periods of stirring. After a time, the material is washed in distilled water until it reaches a neutral pH [95], [99]. The alkaline solution makes possible the elimination of some impurities, including bacteria.

After the purification, bacterial cellulose is obtained. Additional treatments may be applied to obtain a product with specific characteristics. The material could be treated with mechanical methods such as sonication or homogenization [48], [99]. In the nano-bacterial cellulose, the material is subjected to atomization, spray-drying, microfluidization, or hydrolysis process with sulfuric acid [48], [99].

On the other hand, some variables differ in most investigations, such as time and temperature conditions, fermentations, culture medium, substances, techniques used, and others. For a better understanding could be read the information for the following cases: bacterial cellulose [94], [95], [98], [100], [101], and nano-bacterial cellulose [96], [99], [102].

# CHAPTER IV:

## Cellulose/Chitosan Composites

Chitosan and cellulose have a similar polysaccharide structure. The only difference is their functional group at the C-2 position. Chitosan has a primary amine, whereas cellulose has a secondary hydroxyl group [103]. The fact of similarity makes interesting the use of cellulose as a reinforcement of chitosan-based films. Additionally, the possibility of hydrogen bonding between their functional groups would result in good interfacial adhesion between the filler and the matrix, which is crucial to improve the properties of composites [28].

Cellulose as a reinforcement has been used in different ways. It includes cellulose nanocrystals (CNCs), cellulose nanofibers (CNFs), microcrystalline cellulose (MCC), microfibrillated cellulose (MFC), and cellulose derivatives and modifications.

### 4.1. Cellulose Nanocrystals

Nanocellulose is the most common filler in chitosan-based films. Responsible for this is the particle size, as small particles can offer a high surface area for good interfacial adhesion between filler and matrix, and also the stress transfer process is more efficient [3], [103]. The term nanocellulose includes cellulose nanocrystals and cellulose nanofibers. Cellulose nanocrystals (CNCs) are characterized by a high aspect ratio, good mechanical properties, and high crystallinity. Intermolecular hydrogen bonds and electrostatic interactions between cationic and anionic groups of chitosan and CNCs, respectively, promote strong bonding between the two polymers [15], [104].

The morphology of CNCs depends on the source and the preparation process [105], being a rod or needle shape the most common, as shown in Table 1. Also, it exhibits that CNCs are incorporated into the chitosan matrix in low proportions since the composite films have been tested varying the filler content from 1 to 20 wt.% (based on chitosan weight).

Furthermore, Table 1 shows that the dimensions of the filler particles vary from 5 to hundreds of nanometers.

Table 1. CNCs incorporated in chitosan-based films

| Reinforcement | Other components | Cellulose shape | Cellulose size | Cellulose content (wt.%) | References |
|---|---|---|---|---|---|
| Cellulose nanocrystals | | Rod-like | D= 15-20 nm<br>Aspect ratio= 20-25 | 0, 5,10 and 15* | [88] |
| Cellulose nanocrystals | | Rod-like | D= 7.2 nm<br>L= 164 nm<br>Aspect ratio= 23 | 0, 1, 3, 5 and 10* | [106] |
| Cellulose nanocrystals | | Needle-like | D= 5-30 nm<br>L= 100-500 nm | 0, 2, 4, 6 and 8 | [1] |
| Cellulose nanocrystals | | Needle-like | D= 5 nm<br>L= 330 nm<br>Aspect ratio= 66 | 0, 1, 3, 5 and 8* | [107] |
| Cellulose nanocrystals | | Rod-like | D= 4-7 nm<br>L= 120-200 nm | 0, 2.5, 5 and 10 | [108] |
| Cellulose nanocrystals | | Needle-like | Size= 100 nm | 0, 5, 12.5, 25 and 37.5* | [27] |
| Cellulose nanocrystalline I | | | D= 76.8-5560 nm | 0, 5, 10, and 20 | [109] |
| Cellulose nanocrystalline II | | Spherical or irregular | D= 78.8-1480 nm | 0, 5, 10, and 20 | |
| Nanocrystalline cellulose I | | Sheet-like | D< 220 nm | 0, 1, 3, and 5 | [103] |
| Nanocrystalline cellulose II | | Sheet-like | D=255-825 | 0, 1, 3, and 5 | |

| | | | | | |
|---|---|---|---|---|---|
| Cellulose nanocrystals | | Needle-like | D= 5 nm<br>L= 329 nm<br>Aspect ratio= 65 | 0, 1, 3, 5 and 8* | [104] |
| Nanocrystalline cellulose I | | | Particle size distribution:<br>42% with < 122 nm | 0, 1, 3, and 5 | [110] |
| Nanocrystalline cellulose II | | | Particle size distribution:<br>28% with < 122 nm | 0, 1, 3, and 5 | |
| Cellulose nanocrystals | | Rod-like | Width= 9 nm<br>L= 170 nm<br>Aspect ratio= 20 | 0, 1, 2, 5, 10 and 20 | [111] |
| Nanocrystalline cellulose | | | | 0, 5, 7.5, and 10 | [112] |
| Cellulose nanocrystals | | Rod-like | D= 16.2 nm<br>L= 126.3 nm<br>Aspect ratio= 65 | 0, 1, 2, 3, 4 and 5* | [66] |
| Cellulose nanocrystals | | | Particle size= 156 nm | 5 | [113] |
| Cellulose nanocrystals | Glycerol: 20 wt.% | Rod-like | D= 50.3 nm<br>L= 305 nm<br>Aspect ratio= 6.06 | 5, 10, 20 and 30* | [77] |
| Cellulose nanocrystals | Glycerol: 30 wt.% | | | 0, 10, 15, 20 and 30 | [114] |
| Cellulose nanocrystals | Malonic acid: 86.82 wt.%<br>ChCl: 116.21 wt.% | | Average sizes of CNCs:<br>20x100x700 nm | 0, 2, 4 and 6* | [115] |
| Cellulose nanocrystals | Tannic acid: 20 mg | Needle-like | D= 25.81 nm<br>L= 298.46 nm<br>Aspect ratio= 9.94-19.8 | 0 and 11.11 | [116] |

| | | | | | |
|---|---|---|---|---|---|
| Cellulose nanocrystals | Tannic acid: 20 or 40 mg tannic acid/g chitosan | Rod-like | D= 15-40 nm L= 150-450 nm Aspect ratio= 20.9 | 0, 11.11 and 42.86 | [117] |
| Cellulose nanocrystals | Glycerol: 9.98 wt.% Glutaraldehyde: 4.95 wt.% | | | 0,1, 2, 3, 4 and 5 | [3] |
| Cyanoethylated cellulose nanocrystals | | | Size= 35-38 nm | 0, 10, 30 and 50* | [9] |
| Cationic dialdehyde cellulose nanocrystals (Modified NCC | | Rod-like | Particle size= 130 nm | 0, 4, 8, 12, 16 and 20 | [15] |
| Cationic dialdehyde cellulose nanocrystals | | | | 0, 4, 8, 12, 16 and 20 | [118] |
| TEMPO-oxidized cellulose nanocrystals | | Rod-like | D= 4-8 nm L= 120-200 nm | 0, 2.5, 5 and 10 | [108] |
| Dialdehyde cellulose nanocrystals | | Rod-like | D< 11.7 nm L< 229 nm | 0, 1, 3, 5 and 7 | [119] |
| Cationized TEMPO-cellulose nanocrystals | | Rod-like | Width= 6 nm L= 125 nm Aspect ratio= 23 | 0, 1, 2, 5, 10 and 20 | [111] |
| TEMPO-oxidized cellulose nanocrystals | | Irregular cylinder or spheres | D= 3-17 nm | 0, 6.5 and 14 | [105] |
| Cellulose nanocrystals | Curcumin: 450 µg Silver nitrate: 463 µ mol | | D= 40-90 nm | Not available | [120] |
| Cellulose nanocrystals | Tween 80: 5 wt.% Span 80: 5 wt.% | | | 0, 5, and 10 | [121] |

| Cellulose nanocrystals | Combination of oregano and thyme (1:1) essential oils | | 5 | [122] |
|---|---|---|---|---|
| Cellulose nanocrystals | Combination of oregano and thyme (1:1) essential oils: 37.5 wt.% | | 5 | [123] |
| Bacterial cellulose nanocrystals | Glycerol: 30 wt.%* Silver nanoparticles: 1 wt.%* | D= 20-30 nm | 0, 2, 4 and 6* | [48] |

El Achaby et al. [107] worked with CNCs from alfa fibers and used them to improve the tensile properties of chitosan-based films. In order to determine the microstructure and morphology of the filler, it was used TEM and AFM microscopies. The images of the CNCs showed a needle-like shape with an average diameter and length of $5 \pm 3$ nm and $330 \pm 30$ nm, respectively (see Figure 4). These dimensions are within the nanometric fillers range, and their morphology is the most common for CNCs [62], [122]. The aspect ratio of this filler is about 66; value that confirms its potential as a reinforcement for composites since it has been reported that this value should be a minimum of 10 to obtain a good stress transfer from the matrix to the fillers [88], [107].
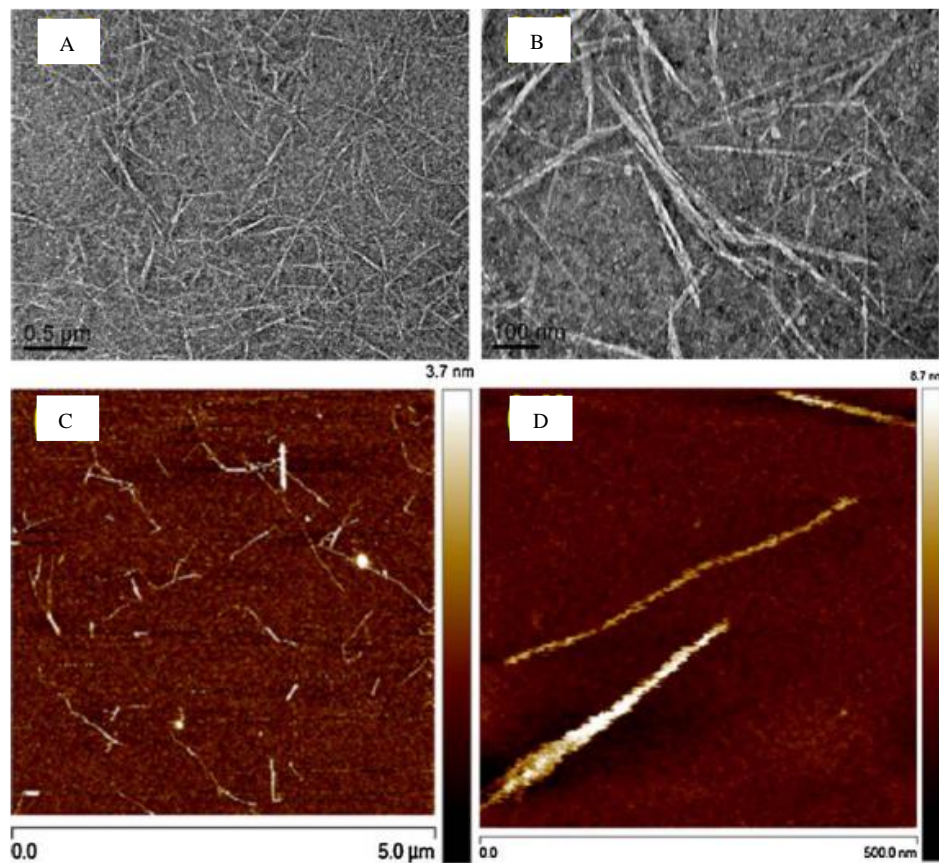


Figure 4. (A, B) TEM and (C, D) AFM images of CNCs [107]

When CNCs are incorporated into a chitosan matrix, they disperse well. However, this behavior may change depending on the amount of reinforcement added. The surface of chitosan-based films is usually smooth, just with minimal roughness. With little addition of CNCs, the roughness of the composite film increases, although they are still well

distributed. If the addition continues to increase, there is a point (threshold) in which the filler forms agglomerations.

Corsello et al. [106] elaborated chitosan films reinforced with CNCs to evaluate changes in morphology and mechanical properties. The morphology of the cross-section of the composite films was observed by SEM varying the content of the filler from 1-10 wt.% (based on chitosan weight). Thus, by observing the fracture surface images (Figure 5), it was concluded that with 1 wt.% of CNCs (1CNCs) the roughness of the composite film was similar to that of chitosan net, but with the incorporation of 3 wt.% of CNCs (3CNCs) the film had a slightly rougher surface. The authors suggested that with amounts greater than 3 wt.%, a phase-segregated system could be generated since by incorporating 5CNCs and 10CNCs the roughness is more noticeable and increases rapidly. It can be inferred that composite films with lower CNCs loading have a more homogeneous material distribution.
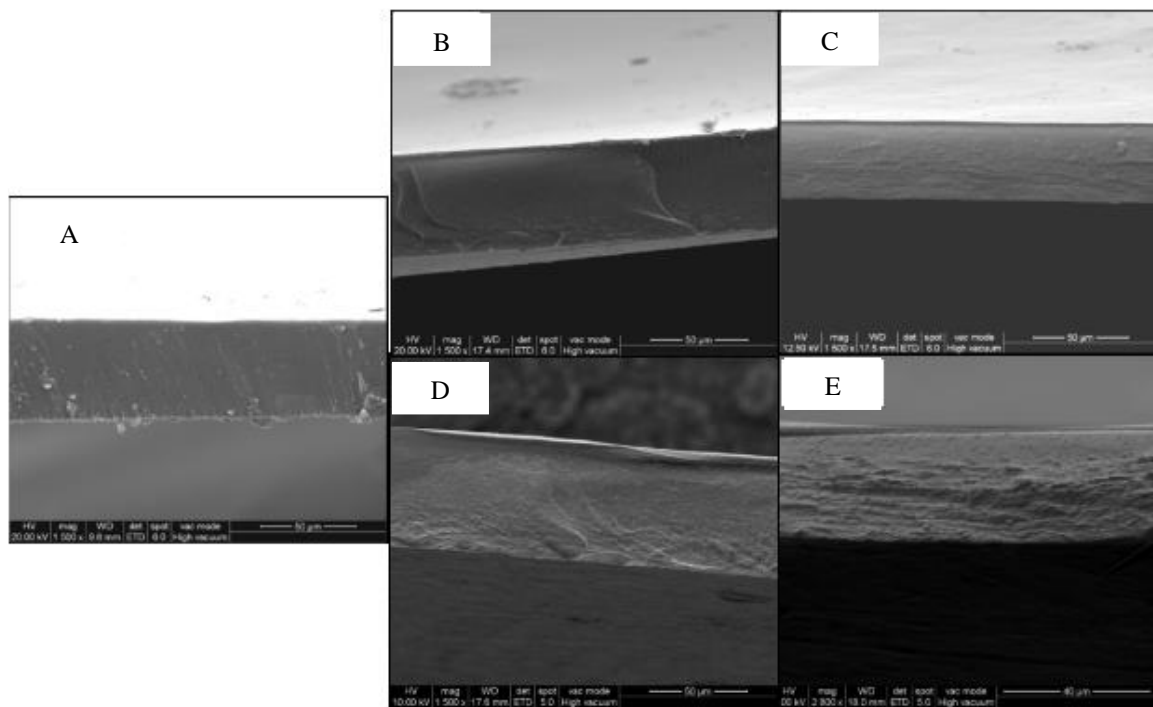


Figure 5. SEM images of the fracture surface of A) chitosan film, B) 1CNCs/chitosan film, C) 3CNCs/chitosan film, D) 5CNCs/chitosan film and E) 10CNCs/chitosan film [106]

Celebi et al. [88] used different methods to disperse CNCs into a chitosan matrix. They reported SEM images of composites in which mechanical stirring with ultrasonication (MECH) or microfluidization (MIC) was applied. Figure 6 represents the morphologies

of the fractured surfaces of the chitosan net, chitosan with 5CNCs and 15CNCs (based on chitosan weight) for both methods. It was described that for the chitosan net film, the surface was relatively smooth without any phase separation. For chitosan loaded with 5CNCs the surface was homogenous, indicating a good dispersion of the filler, which is seen as white dots in the images. Also, it was observed that most of the CNCs are coated by the chitosan matrix, which confirms the good adhesion and compatibility between both polymers. However, as the CNCs content increased, the surface became rougher, and it was observed agglomerations of the filler. As a result, the image of the composite with 15CNCs shows large agglomeration clusters in the matrix. This scenario is the same for both dispersion methods, although the MIC reduced those agglomerations more effectively.
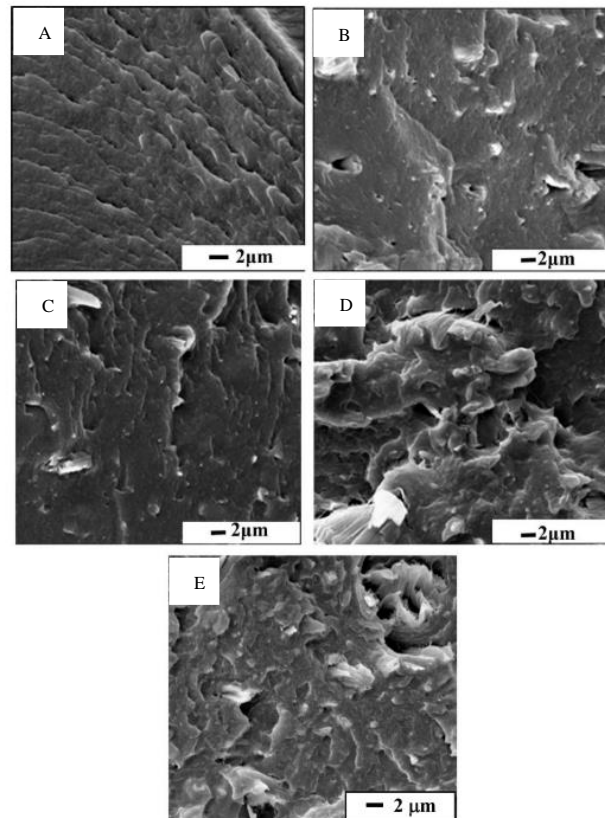


Figure 6. SEM Micrographs (x 5000) of A) chitosan film, B) 5CNCs/chitosan film-MECH, C) 5CNCs/chitosan film-MIC, D) 15CNCs/chitosan film-MECH and E) 15CNCs/chitosan film-MIC [88]

A uniform and homogenous distribution of CNCs is responsible for the enhanced physical and mechanical properties of a chitosan-based film [1]. In most research, the agglomerations of CNCs into a chitosan matrix are influenced by the amount of filler added (see Figure 13). These agglomerations act as a stress concentrator, being the

starting point of a failure in the event of stressing the composite [124]. A CNCs reinforced chitosan composite film will have a smooth surface with some roughness and without any possible phase separation as long as the amount of filler is not excessive.

On the other hand, for the preparation of CNCs/chitosan composite films, plasticizers and cross-linking agents have been added, and modified CNCs have also been used as reinforcement. Plasticizers are small molecules that can reduce brittleness and make the film more processable. These molecules must have a structure similar to that of the polymer, with glycerol being the best-known plasticizer for chitosan films since both present hydrophilic groups [5], [125]. There are two theories related to the activity of plasticizers. The lubrication theory postulates that plasticizers act as internal lubricants by reducing frictional forces between polymer chains. The gel theory says plasticizers break polymer-polymer interactions (hydrogen bonds), promoting second bonds and causing adjacent chains to move apart, thus reducing rigidity and increasing flexibility [126].

Mujtaba et al. [77] study the effect of CNCs on mechanical and barrier properties of chitosan-based films prepared with glycerol. The CNCs content was 0, 5, 10, 20, and 30 wt.% (based on chitosan weight), whereas glycerol was constant in all the samples (20 wt.%; based on chitosan weight). To analyze the surface morphology of the composite films it was used SEM and AFM. Using the AFM images (Figure 7), the root means square (RMS) roughness for all the samples was calculated over an area of 25 $\mu m^2$. As expected, the chitosan net film exhibited a smooth surface morphology with the lowest RMS value corresponding to 5.5 nm. The roughness of the composite films increased with the addition of the CNCs, being the 30CNCs loaded composite which had the highest RMS value.

On the other hand, a uniform and homogeneous distribution of cellulose nanocrystals were observed on the composite films. These results coincide with the conclusions obtained through SEM images (Figure 8). These micrographs showed a homogeneous surface morphology for all the samples. The good compatibility between the two polymers was confirmed by incorporating the CNCs into the matrix.
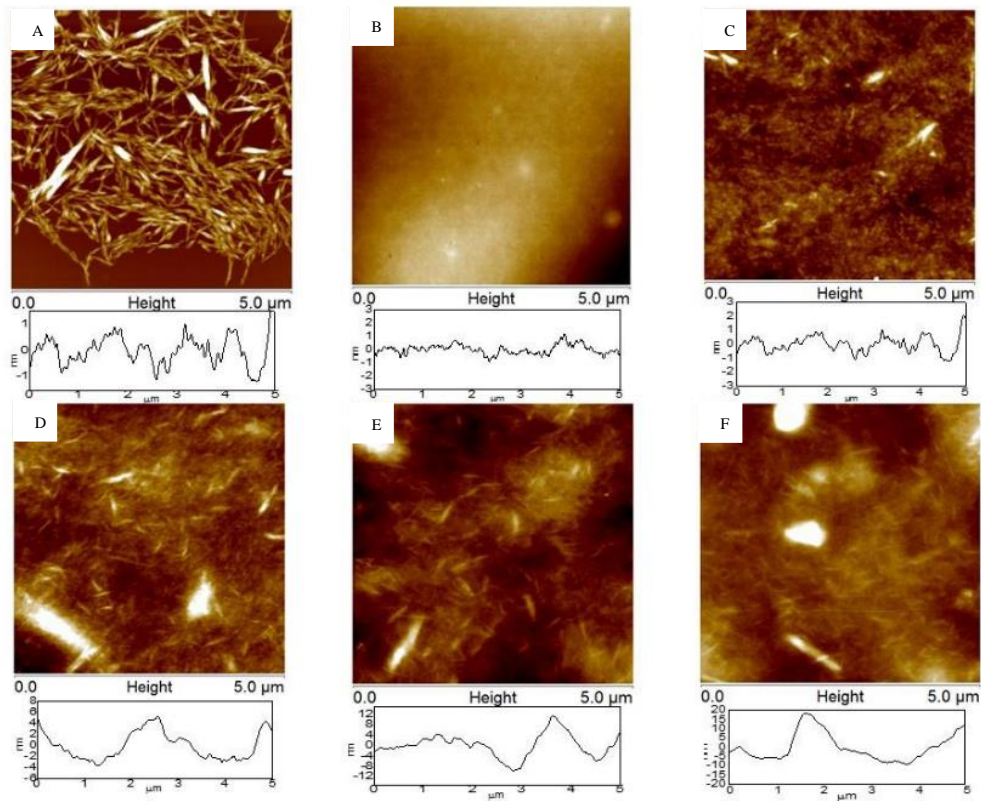
Figure 7. AFM images of A) CNCs isolated from flax fibers, B) chitosan net film, C) 5CNCs/chitosan film, D) 10CNCs/chitosan film, E) 20CNCs/chitosan film and F) 30CNCs/chitosan film [77]
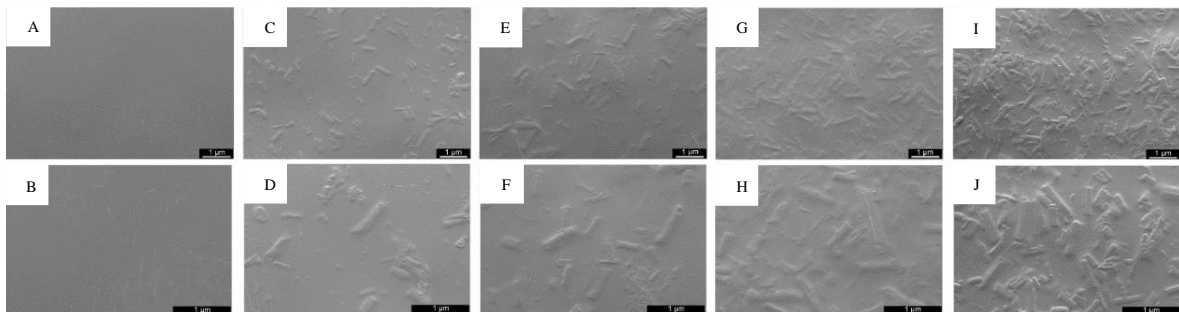


Figure 8. SEM images of (A, B) chitosan net film, (C, D) 5CNCs/chitosan film, (E, F) 10CNCs/chitosan film, (F, H) 20CNCs/chitosan film and (I, J) 30CNCs/chitosan film at two different magnifications. 500 x (up), 1000 x (down) [77]

The surface morphology results obtained in the research of Mujtaba et al. [77] are similar to those obtained in others without glycerol. The behavior observed through SEM or AFM of CNCs into the chitosan matrix is almost the same. The plasticizer probably reduces clumping since in the micrographs of Mujtaba and others [77] there are no appreciable agglomerations or could be considered insignificant. The strong interactions between cellulose and chitosan, which promote good adhesion between both polymers, are also

responsible for forming undesirable agglomerations, and plasticizers can weaken those intermolecular forces [103], [122].

Regarding the cross-linking agents, they can improve the mechanical and thermal stability of a polymeric matrix. Among the cross-linkers available for chitosan, glutaraldehyde (GA) is the most widely used [127], although sodium tripolyphosphate [6], tannic acid [116], [117], and many others have also been applied. The incorporation of these cross-linkers in a chitosan composite film reinforced with CNCs, improves the chemical adhesion between both polymers by forming a rigid cross-linked polymer network [3].

A study done by Gan et al. [3] elaborated a CNCs reinforced chitosan composite film cross-linked with glutaraldehyde through conventional heating (CH) or microwave (MC) curing. The CNCs content of the composite films was 0, 1, 2, 3, 4, and 5 wt.% (based on chitosan weight), whereas the amount of GA was 4.95 wt.% (based on chitosan weight) and, additionally, all the samples had glycerol (9.98 wt.%; based on chitosan weight). The fracture surface of non-crosslinked and cross-linked composite films was observed by FE-SEM. The micrographs of the chitosan net films with and without glutaraldehyde (Figure 9A, D, and G) exhibited a relatively smooth and uniform fracture surface. The composite films without glutaraldehyde and with 1CNCs and 5CNCs (Figure 9B, and C) displayed a rougher surface that increased depending on CNCs added. At the highest CNCs concentration, the roughness was predominant because of agglomerations of the filler. The same result was obtained for cross-linked CNCs/chitosan composites (Figure 9E, F, H, and I), although they exhibited a more uniform and compact fractured surface than the non-crosslinked composites. On the other hand, comparing both curing methods, for the MC curing the fractured surface of the composite films was smoother and more homogenous. This difference is because during the MC curing, the temperature distribution is more uniform and, as a result, the cross-linking degree is greater and homogenous, forming a more stable cross-linking network [128].
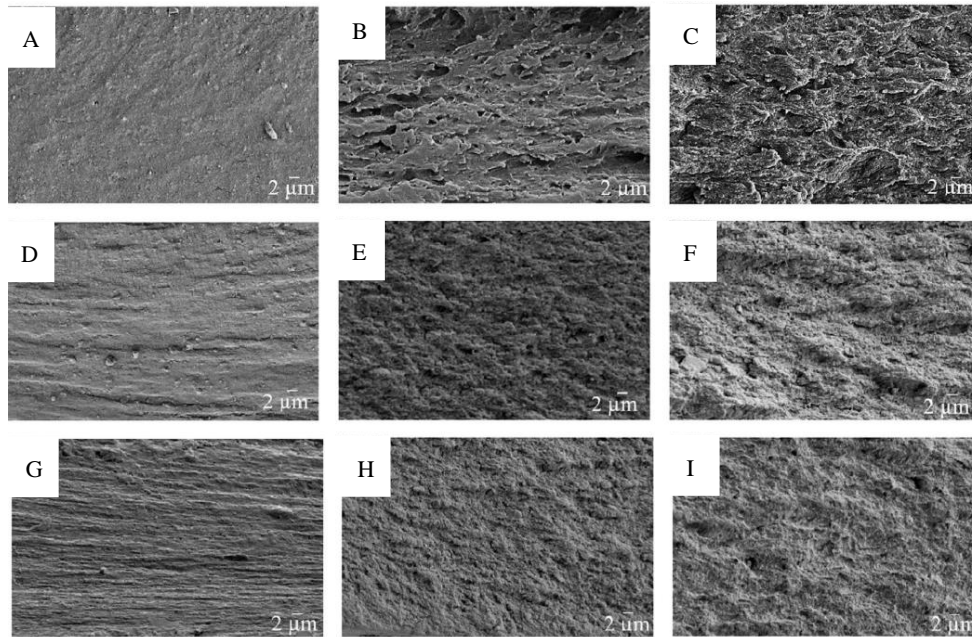
Figure 9. FESEM images of fractured surface of non-cross-linked chitosan film composites: A) chitosan film, B) 1CNCs/chitosan film, and C) 5CNCs/chitosan film; GA-cross- linked chitosan film composites: D) CH-chitosan film, E) CH-1CNCs/chitosan film, and F) CH-5CNCs/chitosan film, G) MC-chitosan film, H) MC-1CNCs/chitosan film, and I) MC-5CNCs/chitosan film at ×2000 magnification [3]

When chitosan is cross-linked with glutaraldehyde, an imine bond is formed between its amino and aldehyde group, respectively. As a consequence of the cross-linking, the interfacial adhesion between CNCs and chitosan is improved, thus obtaining a composite film with better performance [3]. As discussed, the surface morphology of CNCs/chitosan composites is almost the same for cross-linked composites since CNCs still tend to form agglomerations at high concentrations.

All the additives mentioned, such as plasticizers and cross-linking agents, are used to enhance the properties of chitosan-based films, and the same is expected when modified CNCs are used as reinforcement. Modified CNCs are subjected to different treatments to improve the compatibly with the chitosan matrix. Depending on the modifications, the surface morphology of the composite will be different. Generally modified CNCs disperse well in chitosan, and comparing with CNCs, the modified CNCs start to agglomerate at higher concentrations [111]. Furthermore, the roughness of the composites increases as the filler content is higher [9].

Among modified CNCs (see Table 1), the following have been used in chitosan matrix: cyanoethylated CNCs [9], dialdehyde CNCs [119], cationic dialdehyde CNCs [15], [118], TEMPO-oxidized CNCs [105], [108] and cationic TEMPO-CNCs [111]. Tian et al. [15]

elaborated chitosan-based composite films with cationic dialdehyde CNCs as reinforcement. SEM micrographs of fractured surfaces exhibited a smooth surface for the chitosan net film, while for the composites, the roughness increased with the addition of filler. It was described that the smoothness was kept for the composite containing 4 wt.% of the filler (based on chitosan weight). Higher amounts induced a uniform roughness surface, and when the loading was more than 12 wt.% (based on chitosan weight), the composites showed an uneven roughness that would indicate a possible phase separation. For the study of cyanoethylated CNCs, Bonardd et al. [9] incorporated this filler into chitosan matrix, obtaining blends with 10, 30, and 50 wt.% of cyanoethylated CNCs content. With AFM images, they observed a good dispersion of the cyanoethylated CNCs for all the composite samples (Figure 10). Also, the modified CNCs particles were observed and without forming notable agglomerations. As expected, the roughness of the composite films increased depending on the CNCs added, being the value 0.75, 7.19, 17.4, and 24.8 nm for the composites containing 0, 10, 30, and 50 wt.%, respectively.
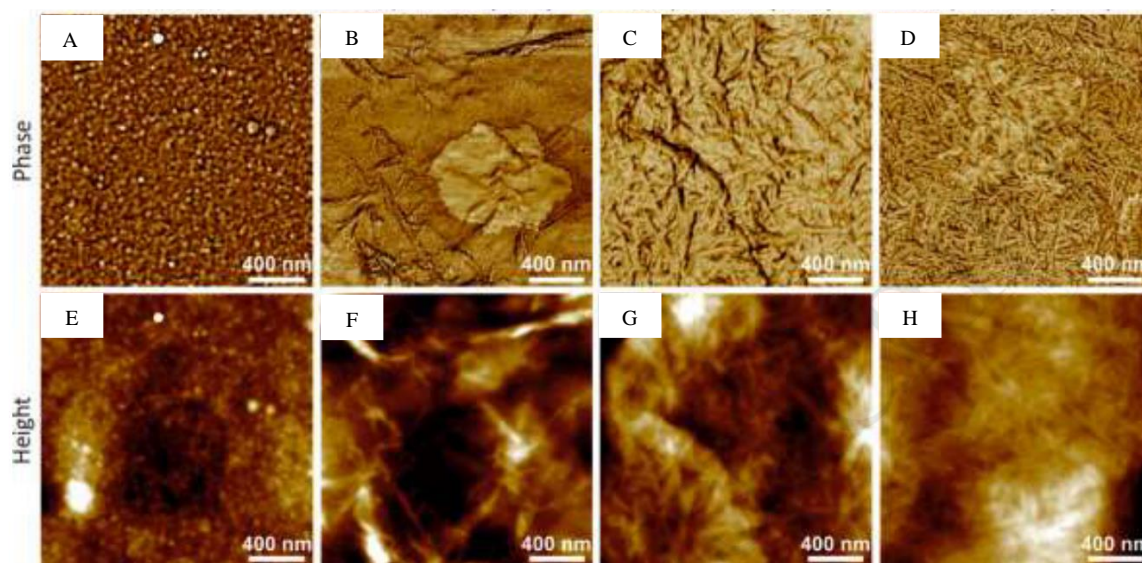


Figure 10. Phase and height AFM images of chitosan-based composite films reinforced with (A, E) 0-cyanoethylated CNCs, (B, F) 10-cyanoethylated CNCs, (C, G) 30-cyanoethylated CNCs, and (D, H) 50-cyanoethylated CNCs [9]

Modifications to the CNCs have resulted in better compatibility with chitosan. Consequently, agglomerations have been reduced [111], and chitosan-based composites have performed well with high mechanical properties [108]. Some authors have increased the negative charge of CNCs to enhance intermolecular interactions with positive chitosan, while others have tried to reduce these electrostatic interactions by obtaining cationic CNCs. However, the compatibility between CNCs and chitosan can be affected

for both cases. When a filler and a matrix consist of negative and positive charges, respectively, the composite may form agglomerations or precipitates due to strong ionic attraction. In the other case, when the filler and the matrix have the same charge, the compatibility is altered due to depletion forces, which is known as depletion flocculation [111]. Finally, the most common behavior of modified CNCs in chitosan-based films is that agglomerations are formed with higher amounts of filler than when using unmodified CNCs. This behavior indicates a better adhesion between both polymers and the obtaining of composites with sufficient stress transfer capacity [15].

Additionally, CNCs reinforced chitosan-based composite films have been studied with other components to develop or improve specific activities. It has been used curcumin/silver nanoparticles [120], essential oils (oregano, thyme) [122], [123], grape pomace extracts (Cabernet Franc and Viognier) [129] and silver nanoparticles [48]. By using curcumin/silver nanoparticles, the composite has improved its wound-healing ability [120]. In the case of incorporating essential oils, composite films have achieved better antifungal activity, in addition to having a plasticizing effect [122], [123]. By using grape pomace extracts, the antioxidant effect has increased and have also promoted a plasticizing effect [129]. Adding silver nanoparticles improved the antibacterial and antifungal activity of the composite [48].

Those active components are incorporated in low proportions to avoid influencing other properties or affect the composite film performance [130]. Salari et al. [48] used bacterial CNCs (2, 4, 6 wt.%, based on chitosan weight) and silver nanoparticles incorporating them into the chitosan matrix. The FE-SEM micrographs of the chitosan-based films containing 4BCNCs and silver nanoparticles showed a proper distribution of the filler and uniform structure (Figure 11D). This distribution indicates good interactions between the three components and as a consequence, good performance of the composite. However, with 6BCNCs (Figure 11C), the surface was rougher and exhibited remarkable agglomerations. As in the other examples, this can be attributed to a possible phase separation by the exceed of filler content.
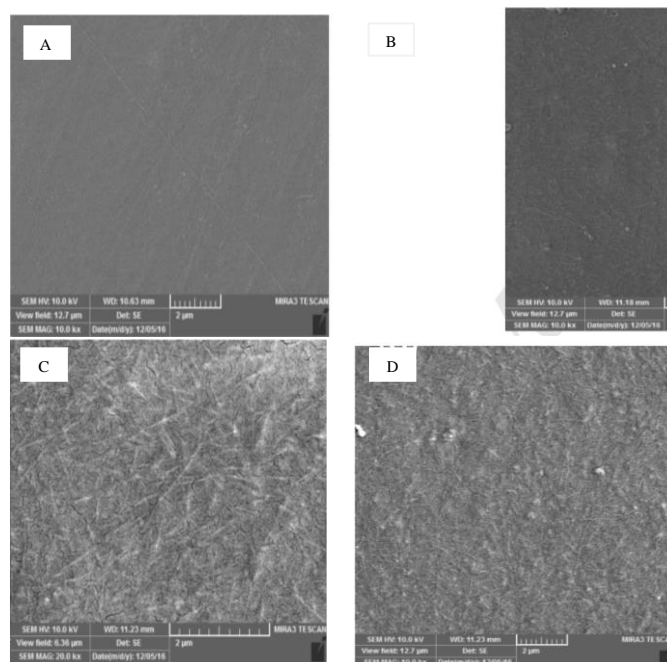
Figure 11. FE-SEM micrographs of the surface of A) chitosan film, B) 4BCNCs/chitosan film, C) 6BCNCs/chitosan film, and D) 4BCNCs/chitosan film-1 wt.% silver nanoparticles [48]

The good interfacial adhesion between chitosan and CNCs makes possible the obtention of promising composite films. However, when the amount of filler is exceeded, it starts to form agglomerations in the film matrix. These agglomerations occur mainly by two factors, the strong electrostatic interactions between the anionic group of the filler and the cationic group of chitosan [108], and the filler-filler hydrogen bonds [105], [108]. The dispersion degree of particles may be influenced by the treatments applied during the obtention of the CNCs and composite preparation. It includes bleaching and mercerization processes [107], [109]; hydrolysis time [27] and types of hydrolysis (acid [88], enzymatic[103]); mechanical stirring, ultrasonication or micro-fluidization dispersion methods [88]; crosslinking through conventional heat curing [116] or microwave curing [3]; modifications of the filler (oxidation [108], [119], cationization [15], [111], cyanoethylation [9]); and many other processes.

The presence of agglomerations in chitosan-based composite films is related to the mechanical properties of the final material since it changes the mechanical performance tendency. When CNCs are incorporated into chitosan films, the mechanical properties commonly analyzed are tensile strength (TS), Young's modulus (YM), and elongation at break (EB). The general tendency for these properties, as the CNCs content increases, is to rise in the case of the TS and YM, while the EB decreases (Table 2) [104], [110]. This

tendency continues until a threshold point is reached, that is, when the filler is in excess. The threshold point coincides with the starting formation of notable agglomerations, and additional filler loading gradually diminishes the TS and YM of the composite [110], [117]. At the same time, the EB continues to decrease or, in other cases, increases [106], [108].

Table 2. Mechanical properties of chitosan composite films reinforced with CNCs

| Reinforcement | Other components | Information | Cellulose content (wt.%) | Tensile strength (MPa) | Elongation at Break (%) | Young's modulus (MPa) | Reference |
|---|---|---|---|---|---|---|---|
| Cellulose nanocrystals | | Cross-head speed: 5 mm/min T= 25°C | 0* | 58 | 10.8 | 13.5 | [106] |
| | | | 1* | 59.1 | 7.2 | 15.2 | |
| | | | 3* | 56.1 | 9.3 | 19.9 | |
| | | | 5* | 68.2 | 13.4 | 17.8 | |
| | | | 10* | 62.7 | 13.8 | 13.8 | |
| Cellulose nanocrystals | | ASTM D638 Cross-head speed: 10 mm/min T= 24°C | 0* | 75.2 | 21.8 | 1158 | [1] |
| | | | 2* | 79.3 | 16.8 | 1607 | |
| | | | 4* | 104.7 | 9.9 | 2068 | |
| | | | 6* | 101.4 | 9.2 | 1993 | |
| | | | 8* | 99.6 | 8.9 | 1957 | |
| Cellulose nanocrystals | | Cross-head speed: 5 mm/min | 0* | 46 | 22 | 1392 | [107] |
| | | | 1* | 60 | 18 | 1625 | |
| | | | 3* | 85 | 14.5 | 1875 | |
| | | | 5* | 92 | 11 | 2506 | |
| | | | 8* | 87 | 11 | 2250 | |
| Cellulose nanocrystals | | Cross-head speed: 2 mm/min | 0 | ~35 | ~22 | ~1900 | [108] |
| | | | 2.5 | ~47 | ~7 | ~2100 | |
| | | | 5 | ~50 | ~6.5 | ~2500 | |
| | | | 10 | ~30 | ~5.5 | ~1575 | |
| Cellulose nanocrystals | | Cross-head speed: 1 mm/s | 0 | ~50 | ~11.5 | | [27] |
| | | Hydrolysis time: 1h Cross-head speed: 1 mm/s | 25 | ~70 | ~5 | | |

| Material | Treatment | | | | | Ref |
|---|---|---|---|---|---|---|
| | Hydrolysis time: 2h<br>Cross-head speed: 1 mm/s | 5 | ~50 | ~14 | | |
| | | 12.5 | ~52.5 | ~13 | | |
| | | 25 | ~69 | ~15 | | |
| | | 37.5 | ~60 | ~12 | | |
| | Hydrolysis time: 3h<br>Cross-head speed: 1 mm/s | 25 | ~73 | ~7 | | |
| Nanocrystalline cellulose I | Cellulose treatment: Hydrolysis<br>ISO 527-3<br>Cross-head speed: 10 mm/min<br>Initial force: 0.2 N | 0 | 24.7 | 41.9 | 236 | [109] |
| | | 5 | 29.2 | 23.4 | 838 | |
| | | 10 | 13.4 | 3.4 | 273 | |
| | | 20 | 11.5 | 2.3 | 359 | |
| Nanocrystalline cellulose II | Cellulose treatment: Mercerization and Hydrolysis<br>ISO 527-3<br>Cross-head speed: 10 mm/min<br>Initial force: 0.2 N | 5 | 16 | 10.4 | 667 | |
| | | 10 | 13.1 | 3 | 284 | |
| | | 20 | 15.7 | 3 | 342 | |
| Nanocrystalline cellulose I | Enzymatic Hydrolysis<br>ISO 527–3<br>Cross-head speed: 5 mm/min<br>Initial force: 0.2 N | 0 | 22.1 | 41.9 | 236 | [103] |
| | | 1 | 49 | 39.7 | 1388 | |
| | | 3 | 48.2 | 37.6 | 1104 | |
| | | 5 | 30.1 | 13.8 | 822 | |
| Nanocrystalline cellulose II | Mercerization and Enzymatic Hydrolysis<br>ISO 527–3<br>Cross-head speed: 5 mm/min<br>Initial force: 0.2 N | 1 | 33.8 | 24.9 | 1122 | |
| | | 3 | 25.7 | 18 | 819 | |
| | | 5 | 18.7 | 12.2 | 754 | |
| Cellulose nanocrystals | | 0* | 46.6 | 22.6 | 1392.6 | [104] |
| | | 1* | 63.4 | 18.1 | 1656.7 | |
| | | 3* | 87.2 | 14.4 | 1902.2 | |

| Material | Test conditions | Loading | Value 1 | Value 2 | Value 3 | Ref |
|---|---|---|---|---|---|---|
| | | 5* | 92.1 | 11.5 | 2506 | |
| | | 8* | 86.3 | 11.4 | 2232.3 | |
| Nanocrystalline cellulose I | ISO 527-3 Cross-head speed: 5 mm/min Initial force: 0.2 N | 0 | 25 | 42 | 236 | [110] |
| | | 1 | 47 | 8 | 809 | |
| | | 3 | 27 | 18 | 1253 | |
| | | 5 | 26 | 8 | 814 | |
| Nanocrystalline cellulose II | Mercerization Process ISO 527-3 Cross-head speed: 5 mm/min Initial force: 0.2 N | 1 | 80 | 36 | 3316 | |
| | | 3 | 39 | 10 | 1873 | |
| | | 5 | 22 | 10 | 958 | |
| Nanocrystalline cellulose | Load cell: 100 N T= 23 °C | 0 | 38 | | | [112] |
| | | 5 | 52.06 | | | |
| | | 7.5 | ~52.06 | | | |
| | | 10 | 42.18 | | | |
| Cellulose nanocrystals | Load cell: 100 N Cross-head speed: 10 mm/min | 0* | ~21.5 | ~7.75 | ~400 | [131] |
| | | 5* | ~22.5 | ~7 | ~425 | |
| | | 10* | ~24 | ~3 | ~500 | |
| | | 15* | ~22.5 | ~7 | ~450 | |
| | | 20* | ~17.5 | ~4 | ~700 | |
| | | 25* | ~9 | ~3.33 | ~800 | |
| Cellulose nanocrystals | Method 1 Standard GB/T 1040.3-2006 Cross-head speed: 2 mm/min | 0* | 27.2 | 34.7 | | [66] |
| | | 1* | 30.6 | 23.2 | | |
| | | 2* | 32.1 | 24.1 | | |
| | | 3* | 32.5 | 33.1 | | |
| | | 4* | 28 | 27.3 | | |
| | | 5* | 26.7 | 24.5 | | |

| Material | Additive | Method/Conditions | Content | Value 1 | Value 2 | Value 3 | Ref |
|---|---|---|---|---|---|---|---|
| | | Method 2 Standard GB/T 1040.3-2006 Cross-head speed: 2 mm/min | 0 | 38 | 26.6 | | |
| | | | 1 | 41.6 | 29.7 | | |
| | | | 2 | 42 | 33.3 | | |
| | | | 3 | 43 | 41.6 | | |
| | | | 4 | 35.6 | 44.1 | | |
| | | | 5 | 34.4 | 41.1 | | |
| Cellulose nanocrystals | Glycerol: 20 wt.% | Load cell: 250 N Cross-head speed: 5 mm/min Ambient Conditions | 0* | 5.4 | 37.16 | 21.75 | |[77] |
| | | | 5* | 5.86 | 45.29 | 23.27 | |
| | | | 10* | 5.99 | 36.32 | 26.42 | |
| | | | 20* | 6.67 | 35.34 | 52.35 | |
| | | | 30* | 6.28 | 37.49 | 40.5 | |
| Cellulose nanocrystals | Glycerol: 30 wt.% | Cross-head speed: 50 mm/min | 0 | 32 | 18.3 | 1385 | [114] |
| | | | 10 | 54 | 16.9 | 2434 | |
| | | | 15 | 56 | 13 | 2515 | |
| | | | 20 | 60 | 12.2 | 3119 | |
| | | | 30 | 60 | 11.5 | 3393 | |
| Cellulose nanocrystals | Malonic acid: 86.82 wt.% ChCl: 116.21 wt.% | Deep Eutectic Solvents (DES) ASTM D882 Cross-head speed: 5 mm/min | 0* | 11.4 | 63 | 26 | [115] |
| | | | 2* | 20.4 | 79 | 37 | |
| | | | 4* | ~18.5 | ~85 | ~35 | |
| | | | 6* | ~16.25 | 91 | ~34 | |
| Nanocrystalline cellulose | | Untreated Load cell: 500 N Cross-head speed: 1 mm/min | 0 | 36.93 | 43.1 | 721.61 | [116] |
| | | | 11.11 | ~40 | ~33.75 | 1080.1 | |
| | Tannic Acid: 20 mg | | 0 | ~42 | ~36 | ~920 | |
| | | | 11.11 | 48.32 | ~34 | 1256.5 | |
| | | Heat treatment | 0 | ~41 | ~15 | ~1000 | |

| | | | | | | | |
|---|---|---|---|---|---|---|---|
| | | Load cell: 500 N<br>Cross-head speed: 1 mm/min | 11.11 | 47.34 | ~8.75 | ~1275 | |
| | Tannic Acid: 20 mg | | 0 | ~46 | ~9.5 | ~1190 | |
| | | | 11.11 | ~42 | ~6.25 | ~1180 | |
| Cellulose nanocrystal | | ASTM D882-02<br>Cross-head speed: 1 mm/min<br>Load cell: 100 N | 0 | 33.7 | 43.6 | ~810 | [117] |
| | | | 11.11 | ~36 | ~17 | ~1060 | |
| | | | 42.86 | ~53 | ~16 | ~1625 | |
| | Tannic acid: 20 mg $_{tannic\ acid}$/ g $_{chitosan}$ | | 0 | ~40 | ~35 | ~875 | |
| | | | 11.11 | ~43 | ~14.75 | ~1125 | |
| | | | 42.86 | ~45 | ~13.75 | ~1375 | |
| | Tannic acid: 40 mg $_{tannic\ acid}$/ g $_{chitosan}$ | | 0 | 45.2 | 30.3 | ~1375 | |
| | | | 11.11 | 61.5 | 14 | ~1800 | |
| | | | 42.86 | ~46 | ~14 | ~1800 | |
| Cellulose nanocrystals | Glycerol: 9.98 wt.% | ASTM D882-A<br>Cross-head speed: 10 mm/min | 0 | 32.9 | 29.4 | ~1500 | [3] |
| | | | 1 | 37.4 | ~26 | ~2000 | |
| | | | 2 | ~42.9 | ~24.5 | ~2300 | |
| | | | 3 | ~41 | ~21 | ~2750 | |
| | | | 4 | 50.9 | ~22 | ~2500 | |
| | | | 5 | ~37.5 | 17.9 | ~3200 | |
| | Glycerol: 9.98 wt.%<br>Glutaraldehyde: 4.95 wt.% | Conventional Heat Curing<br>ASTM D882-A<br>Cross-head speed: 10 mm/min | 0 | ~45 | ~19.8 | ~2100 | |
| | | | 1 | ~49 | ~17.5 | ~3450 | |
| | | | 2 | ~54 | ~15 | ~4250 | |
| | | | 3 | ~55 | ~12.5 | ~5000 | |
| | | | 4 | ~60 | ~11 | ~5250 | |
| | | | 5 | ~50 | ~10 | ~6000 | |

| | | | | | | | |
|---|---|---|---|---|---|---|---|
| | Glycerol: 9.98 wt.% Glutaraldehyde: 4.95 wt.% | Microwave Curing ASTM D882-A Cross-head speed: 10 mm/min | 0 | ~50 | ~18 | ~2900 | |
| | | | 1 | ~56.5 | ~15.5 | ~3900 | |
| | | | 2 | ~60.5 | ~13.5 | ~5000 | |
| | | | 3 | ~65 | ~12 | ~5850 | |
| | | | 4 | ~74 | ~10 | ~6250 | |
| | | | 5 | ~59.8 | ~8 | ~6800 | |
| Cyanoethylated cellulose nanocrystals | | ASTM D1708-93 Cross-head speed: 5 mm/min | 0* | 74 | 9 | 2750 | [9] |
| | | | 10* | 80 | 4 | 3450 | |
| | | | 30* | 130 | 3 | 5000 | |
| Cationic dialdehyde cellulose nanocrystals (Modified NCC | | Standard method (GB 4456-84) Cross-head speed: 50 mm/min | 0 | 57.4 | ~19% | | [15] |
| | | | 4 | 73.1 | ~10.5 | | |
| | | | 8 | 82.4 | ~5 | | |
| | | | 12 | 90.9 | ~3.25 | | |
| | | | 16 | 84.6 | ~2.25 | | |
| | | | 20 | 82.4 | ~2.25 | | |
| TEMPO-oxidized cellulose nanocrystals | | Cross-head speed: 2 mm/min | 0 | ~35 | ~22 | ~1900 | [108] |
| | | | 2.5 | ~48 | ~9.5 | ~2000 | |
| | | | 5 | ~56 | ~4 | ~2480 | |
| | | | 10 | ~25 | ~4 | ~1800 | |
| Dialdehyde cellulose nanocrystals | | | 0 | 51.9 | ~18.5 | | [119] |
| | | | 1 | 55.7 | ~16.5 | | |
| | | | 3 | 68.4 | ~9.9 | | |
| | | | 5 | 74.7 | ~5.2 | | |
| | | | 7 | 70.6 | ~4.5 | | |
| Cationized TEMPO- | | Cross-head speed: 50 mm/min | 0 | ~26 | ~5.5 | | [111] |
| | | | 1 | ~26.5 | ~4.8 | | |

| | | | | | | | |
|---|---|---|---|---|---|---|---|
| cellulose nanocrystals | | | 2 | ~27.25 | ~4.3 | | |
| | | | 5 | ~36.25 | ~3.8 | | |
| | | | 10 | ~31.5 | ~3.3 | | |
| | | | 20 | ~28.75 | ~2.9 | | |
| TEMPO-oxidized cellulose nanocrystals | | ASTM D-882 Cross-head speed: 50 mm/min Load Cell: 50 N | 0* | 32 | 17 | 2390 | [105] |
| | | | 6.5* | 57.6 | 4.9 | 4365 | |
| | | | 14 | 76.3 | 1.3 | 8100 | |
| Cellulose nanocrystals | | Non-irradiated Load cell: 100 N | 0 | 59.67 | 29.52 | 852 | [122] |
| | | | 5 | 77.12 | 21.91 | 943.14 | |
| | Combination of oregano and thyme (1:1) essential oils | | 0 | 43.81 | 41.65 | 578.53 | |
| | | | 5 | 54.16 | 34.04 | 703.21 | |
| | | Irradiated Load cell: 100 N | 0 | 83.96 | 30.22 | 994.74 | |
| | | | 5 | 94.26 | 26.63 | 986.68 | |
| | Combination of oregano and thyme (1:1) essential oils | | 0 | 51.22 | 36.96 | 708.96 | |
| | | | 5 | 57.02 | 35.95 | 732.28 | |
| Bacterial Cellulose nanocrystals | Glycerol: 30 wt.%* | ASTM D882-91 Cross-head speed: 10 mm/min | 0* | 21.7 | 33.84 | 97.05 | [48] |
| | | | 2* | 27.03 | 29.71 | 189.67 | |
| | | | 4* | 41.32 | 23.76 | 297.41 | |
| | | | 6* | 34.75 | 25.11 | 214.19 | |
| | Glycerol: 30 wt.%* Silver nanoparticles: 1 wt.%* | | 0* | 24.35 | 32.98 | 139.51 | |
| | | | 2* | 32.94 | 25.89 | 257.4 | |
| | | | 4* | 42.89 | 22.5 | 311.88 | |
| | | | 6* | 29.23 | 27.6 | 264.85 | |

With the information in Table 2, Figures 12A, B, and C were built. These figures show the mechanical performance tendency of chitosan-based films by adding different contents of CNCs. The red line of the figures is a guideline to provide a quick idea about the tendency. The construction of these figures was carried out in percentage values, in such a way that the percentage of each parameter (TS, YM, and EB) is relative to the value obtained with the pure chitosan film tested in the article involved. For example, in the research by Yadav et al. [1], the TS of the pure chitosan film was 75.2 MPa, and with 4CNCs the TS value increased to 104.7 MPa. To calculate the TS percentage value at this filler content, 104.7 is divided to 75.2, and then the result is multiplied by 100. Doing this operation, the TS value of the composite is equal to 139.23% of the TS value of the pure chitosan film. The same process was done with selected examples of the rest of studies placed in Table 2. After that, it was calculated the media and standard deviation. All of the values of the Figures 12A, B, and C were calculated in the same way.

The selected samples were those that were tested at a cross-head speed between 1-10 mm/min (see Table 2). An interval was chosen, since a considerable number of samples analyzed under the same conditions were not available. Given this, it is considered that the error of the average values observed in the figures is produced in part by this difference in speed, although the chosen interval was as close as possible.
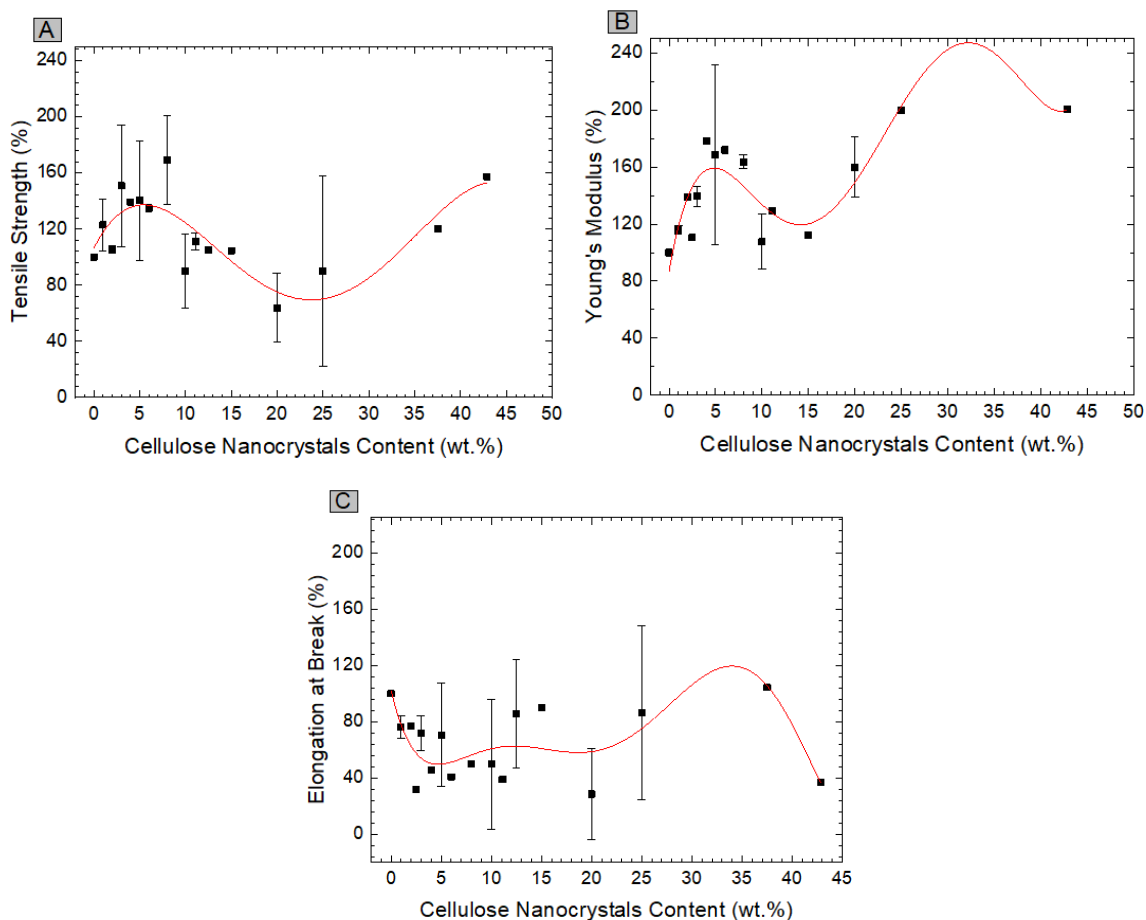
Figure 12. A) Tensile Strength, B) Young's Modulus, C) Elongation at Break of chitosan-based films varying the CNCs content

As seen in Figure 12A, the highest values of TS are obtained when chitosan-based films are optimum reinforced with 3 or 8 wt.% CNCs (based on chitosan weight). The TS values with 3CNCs and 8CNCs increase by 50.73 and 68.92%, relative to the pure chitosan film. However, if the figure is observed in detail, with the standard deviation, it can be said that the TS of the composites, is able to improve up to 96% and 100%, respectively, relative to the pure chitosan films. Thus, because of the little difference between the two composites and considering the lower amount of filler added, the composite with 3CNCs is more suitable.

Regarding the YM, as seen in Figure 12B, a good improvement is obtained when the CNCs content is 4 wt.% (based on chitosan weight). With 4CNCs, the YM increases by 78.58%, relative to the pure chitosan films. Also, it shows that higher YM values could be obtained with 5CNCs. About the EB, Figure 12C shows that by adding 2CNCs the EB may decrease by 68.19%, concerning that of the pure chitosan films.

The rigid nature of CNCs makes it possible the obtention of chitosan-based composites with high stiffness and strength [13]. The increase in TS caused by CNCs can be attributed to two factors. The first one is about intermolecular hydrogen bonds [28], and electrostatic interactions between the macromolecular chains of CNCs and chitosan, which involves their anionic groups (sulfate [104], carboxylate [105]), and cationic amino groups, respectively. The second one is due to the nano-reinforcing effect of the filler caused by the good stress transfer through the CNCs-chitosan interface [107]. This effective stress transfer is due to a mechanical percolating phenomenon that forms a stiff network of cellulose nanoparticles within the chitosan matrix [3], [122]. The decrease in this property is due to excess filler added. As the loaded filler continues to increase, the filler-filler interactions become prominent, causing agglomerations (see Figure 13) [132], [133].
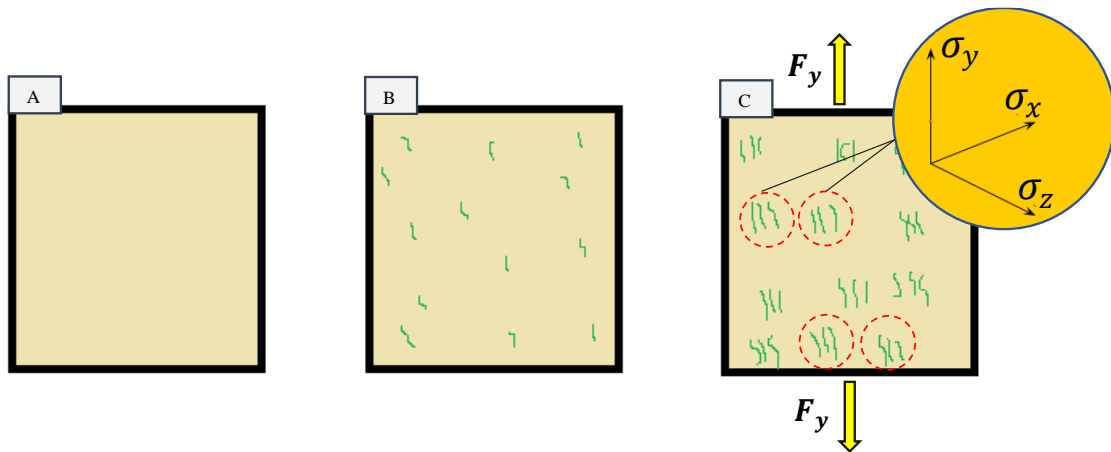


Figure 13. Behavior of Cellulose in chitosan matrix depending on the filler content. A) Pure chitosan film, B) chitosan film with low cellulose amounts, and C) chitosan film with high cellulose amounts

The Figure 13 represents the surface of a chitosan-based film when incorporating cellulose. The Figure 13A corresponds to a pure chitosan film. The Figure 13B corresponds to the same film but reinforced with a low amount of cellulose. In the Figure 13C, the amount of cellulose is excessive, forming agglomerates in the chitosan matrix. These agglomerations can be seen as clusters, reducing the possibility of stress transfer, originating a stress concentration, and in consequence, a localized stress triaxiality [15], [111].

The reasons for the YM results are the same as those described for the TS, in addition to the fact that the YM is highly influenced by the stiffness of the filler; thus, as long as it has more rigidity than chitosan chains, the YM values will increase [26]. On the other hand, the decrease of the EB also results from the rigid nature of the CNCs and the strong

interfacial interaction between both polymers, which limit the motion of the polymer matrix, reducing the ductility of the final composite film [104], [109].

Yadav et al. [1] studied the reinforcing effect of CNCs in chitosan films. The mechanical test was done at room temperature with a cross-head speed of 10 mm/min. The addition of the filler varied from 0 to 8 wt.% (based on chitosan weight), and as expected, the TS and YM increased with a low concentration of filler, while the EB was reduced. The best value of TS and YM was obtained with 4CNCs, which correspond to 104.7 and 2068 MPa. These parameters were improved by 39% and 78%, respectively, relative to the pure chitosan film. Additional filler loading (6CNCs and 8CNCs) caused an adverse effect since the TS and YM decreased gradually, although they still were better than the composite with 0CNCs. This reinforcing effect resulted from hydrogen bonds between the filler and the matrix, and the stiffness that the CNCs provided [134]. The decreasing tendency with 6CNCs and 8CNCs may be attributed to agglomerations in the matrix [135], coinciding with the results of El Achaby et al. [107]. On the other hand, the EB of the composite decreased from 21.8% to 9.9% when the filler added was increased from 0 to 4 wt.%. This tendency continued with higher CNCs addition.

As has been mentioned, the decrease in flexibility is due to the nature and addition of the filler, which prevent the motion at the interface of filler-polymer [136]. Similar results were obtained in other studies, although these would have some varieties because of the process conditions [27], [66], chitosan and CNCs source [104], characteristics of the components (molecular weight, deacetylation degree [6], [27], and purity), and many others. El Achaby et al. [107] reported that chitosan composite films with 3 wt.% CNCs exhibited increased TS and YM by 85% and 35%, respectively, and decreased EB by 34% relative to that of chitosan net film. Abou-Zeid et al. [108] observed that after forming chitosan-based composite films reinforced with 5CNCs, the TS and YM increased by 40% and 35%, respectively, and the EB diminished by 75% relative to that of pure chitosan film.

As was described and shown in Table 2, the results about the mechanical properties of chitosan composites reinforced with CNCs have the same tendency. The TS and YM increase until the optimum filler concentration is reached, while the EB keeps its deterioration as a direct effect of CNCs inclusion [110]. However, there is an exception where the addition of CNCs benefits the TS and EB parameters. Mao et al. [66] elaborated chitosan films reinforced with CNCs (0, 1, 2, 3, 4, and 5 wt.%; based on chitosan weight).

The results obtained were different from those exposed previously. The value of the TS for the samples with 0, 2, 3, 4, and 5CNCS were 38, 41.6, 42, 43, 35.6, and 34.4 MPa, respectively, while the EB values were 26.6, 29.7, 33.33, 41.6, 44.1, and 41.1%, respectively (Figure 14). The best performance was obtained with 3CNCs and 4CNCs for the TS and EB parameters, respectively. Although both properties increased, the reinforcing effect of the CNCs was not very useful since the TS only improved by 13% concerning that of the pure chitosan films, so the EB was not negatively affected. It appears that the expected rigid network formed by the crystals within the polymer matrix was not too compact or tightly bound and therefore did not limit the movement of the chains. In this regard, the electrostatic and hydrogen bonding interactions between both components were sufficient to moderately increase the TS and improve the EB by 56.4% [66].
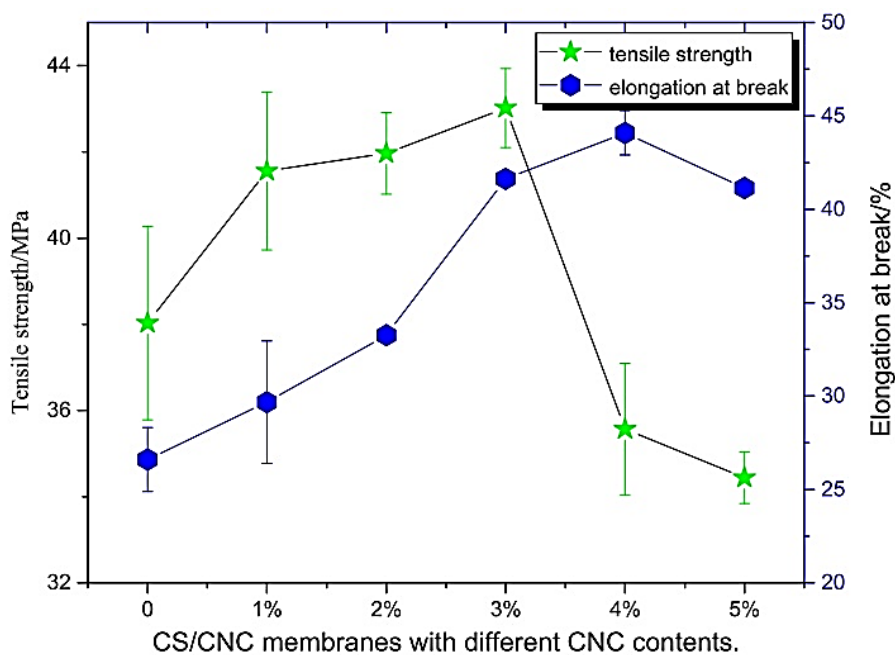


Figure 14. Effect of CNCs contents on the strength and flexibility of chitosan-based films [66]

On the other hand, the use of plasticizers, cross-linking agents, and modified CNCs have improved the mechanical properties of the composites in different ways. As described before, the plasticizers resolve the problem of decreasing flexibility [122]. The cross-linking form composites more compact, resulting in strengthener films [3]. The modified CNCs improve or develop new interactions with the chitosan matrix [108], [119].

Mujtaba et al. [77] applied glycerol (20 wt.%; based on chitosan weight) as a plasticizer of chitosan composites reinforced with CNCs (0-30 wt.%; based on chitosan weight). The mechanical test was carried out at ambient conditions and with a cross-head speed of 5 mm/min. The TS values were 5.4 (0CNCs), 5.86 (5CNCs) 5.99 (10CNCs), 6.67 (20CNCs) and 6.28 MPa (30CNCs), and the EB were 37.16, 45.29, 36.32, 35.34, and 37.49%, respectively (Figure 15). When these results are compared with samples where glycerol was not used [107], it is easy to observe that the plasticizer increased the initial EB of the films; thus the effect caused by the rigid nature of the CNCs in the composite is not so dominant. Although the TS values increased with the addition of the filler, the strength is very low. In other papers with 5CNCs (without plasticizer), the TS values have been 92 MPa [104], [107], 18.7 MPa [103], and 52.06 MPa [112].
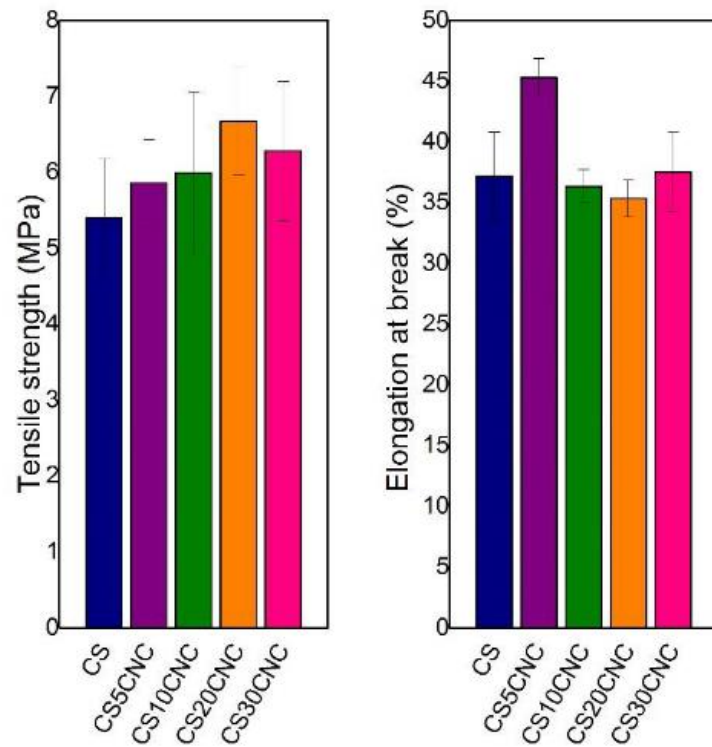


Figure 15. Mechanical properties of chitosan-based films plasticized with glycerol and reinforced with CNCs [77]

When plasticizers are added to a composite film, they increase the chain mobility of the polymer matrix by disrupting intermolecular forces between adjacent polymer chains, resulting in diminished TS, and increased EB [122]. Gan et al. [3] reported that chitosan composite films with 4CNCs and 9.98 wt.% glycerol exhibited TS and EB values of 50.9 MPa and 22%, respectively. In this case, the TS is not highly reduced by glycerol; this is because the amount added is relatively low. Thus, the strength increased by 54.7% with

4CNCs, and the EB reduced by 34%, having still higher flexibility than chitosan films without glycerol and CNCs [1]. The same paper [3] used glutaraldehyde (4.95 wt.%; based on chitosan weight) as a cross-linker to analyze its effect in the plasticized composites. Using the microwave curing method, the TS increased from 50 to 74 MPa when the loading amount of CNCs was increased from 0 to 4 wt.%. In the case of the YM, it increased from 2900 to 6250 MPa, and in the case of the EB, it decreased from 18 to 10% (Figure 16A, B, and C).

As shown in Figure 16, higher amounts of filler changed the tendency of the results. The cross-linked CNCs/chitosan composites showed lower EB and higher TS and YM values than the uncross-linked composites. The Glutaraldehyde increased the compatibility between the filler and the matrix, which is why a highly compact polymeric network with high stiffness and rigidity was formed and consequently restricts the segmental movement of polymer chains, negatively affecting the EB of the composite [137], [138].
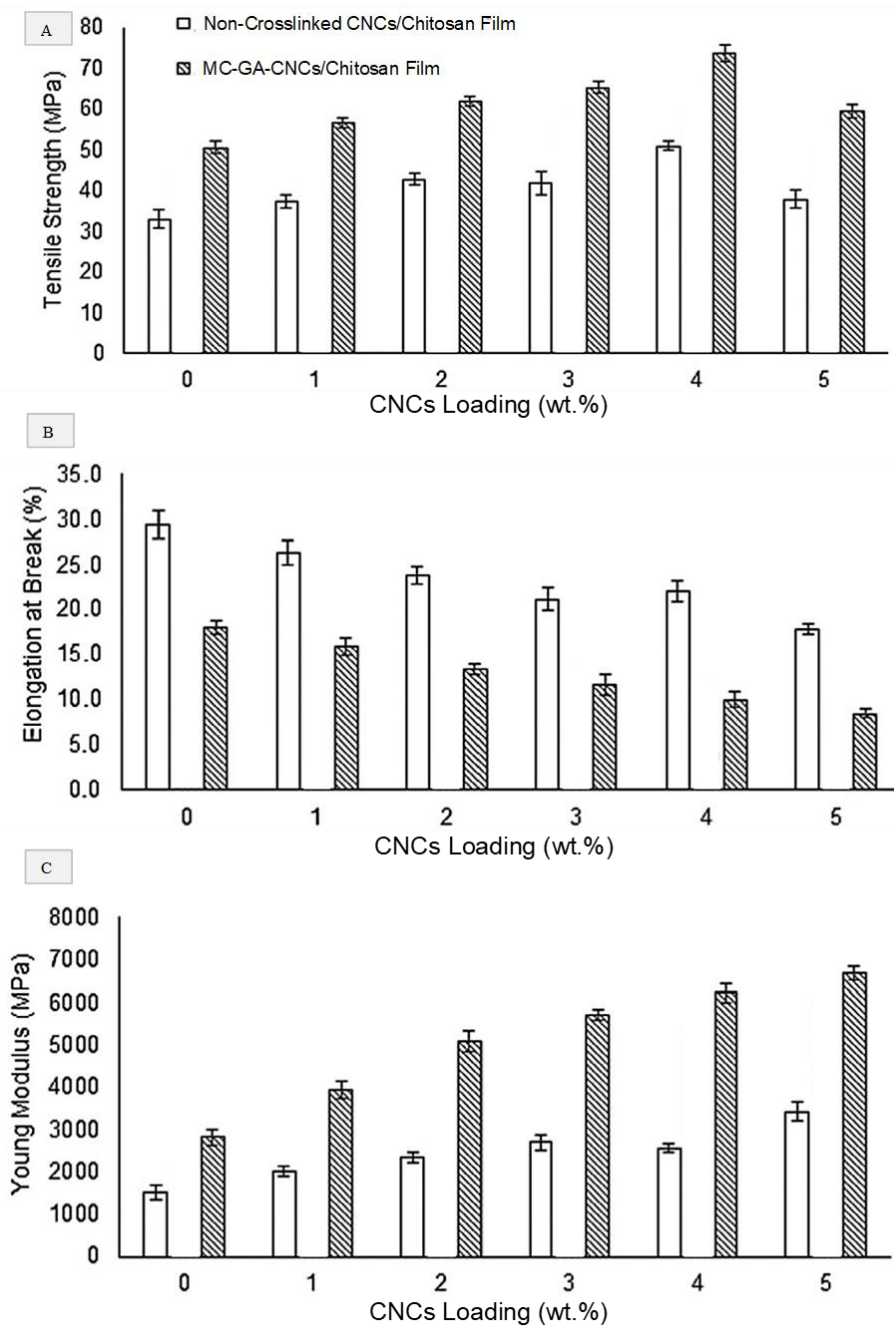
Figure 16. Mechanical properties of non-cross-linked and MC-GA-cross-linked CNCs/chitosan composite films: A) TS, B) EB, and C) YM [3]

The addition of plasticizers and cross-linking agents will depend on future applications of the composite film. If the application requires high flexibility, the plasticizer will be necessary, and if it requires stiffness, the cross-linking will be the best option. In some works, both components are used, being one in higher amounts depending on the needs [3], [117]. Regarding the use of modified CNCs, Abou-Zeid et al. [108] made a comparative study between CNCs and TEMPO-oxidized CNCs using them to reinforce

chitosan-base films. The filler content of the composite films was 0, 2.5, 5, and 10 wt.% (based on chitosan weight). The chitosan composite films with 5CNCs exhibited increased TS and YM by 40% and 35%, respectively, relative to the pure chitosan film. In the case of using TEMPO-oxidized CNCs, those properties increased by 59% and 34%, respectively (Figure 17). Additional filler loading decreased the values of TS and YM for both cases. The higher TS in the composites with the modified CNCs, is due to the stronger electrostatic interaction between the carboxylate groups of the filler and the cationic amino groups present in chitosan [105]. The decrease of these mechanical properties with a filler content above 5 wt.% could be attributed to the formation of filler agglomerations [112].

Regarding the EB, as expected, this property decreased in both cases. The composite films EB, with 2.5 and 10CNCs decreased by 66% and 75%, respectively, and with TEMPO-oxidized CNCs decreased by 56% and 82%, relative to that of the pure chitosan film [108]. This decreasing effect is because of the higher stiffness of the CNCs than the chitosan matrix and by the strong interaction between both polymers. The higher decreasing EB of the composite with the modified CNCs is because the electrostatic interactions are stronger than in the case of using CNCs, and therefore, the films are more compact and rigid, limiting more the movements of the chains [3].
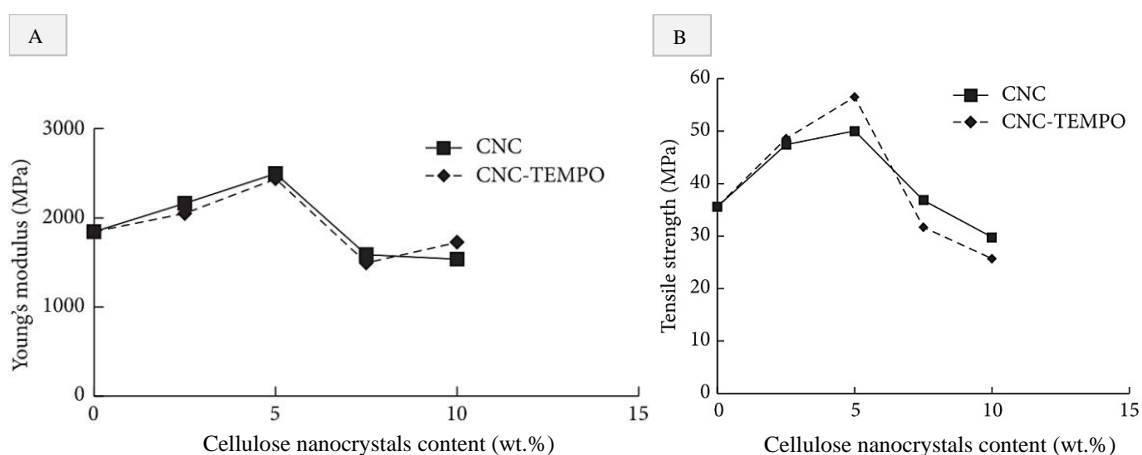


Figure 17. Mechanical properties of CNCs and TEMPO-oxidized CNCs/chitosan composite films: A) tensile strength and B) Young`s modulus [108]

On the other hand, the mechanical properties of CNCs reinforced chitosan-based composite films have also been analyzed for cases in which active agents are added. The

effects of these components do not necessarily influence the mechanical properties, although they can have certain repercussions depending on the compound. In the case of using essential oils, they cause the same effect as plasticizers [139]. Hossain et al. [122] elaborated chitosan films with a combination of oregano and thyme essential oils. The chitosan composite film with 5CNCs exhibited TS, EB, and YM values of 77.12 MPa, 21.91%, and 943.14 MPa, respectively. With the incorporation of the essential oils, the TS, EB, and YM values were 54.16 MPa, 34.04%, and 703.21 MPa, respectively. As was mentioned, this kind of active agent causes a plasticizing effect reducing TS and YM and increasing EB of composite films, although the interest in using them is to improve antimicrobial activity [139]. On the other hand, Salari et al. [48] used silver nanoparticles as the active agent, and in this case, the mechanical properties were almost equal to those without the silver.

After exposing all these examples, it is confirmed that the incorporation of CNCs into a chitosan matrix improves the TS and YM, and gradually decreases the EB. This tendency is maintained until the optimum filler concentration is reached, and a high value of strength and stiffness can be gotten with low loading filler content. Furthermore, the aspect ratio of the filler, its interaction with the polymer matrix, and its dispersion within the matrix are the main factors responsible for the reinforcing effect of CNCs [110]. Additionally, the mechanical effects of the filler could be changed using plasticizers, cross-linking agents, and modifying the CNCS. Changes that will be carried out depending on what properties are necessary to improve for a specific application.

## 4.2. Cellulose Nanofibers

As stated at the beginning, nanocellulose also includes CNFs. This filler, like its partner, has good mechanical properties and a high aspect ratio [140], with the difference that it consists of two predominant regions, one amorphous and the other crystalline [62]. Its compatibility with chitosan depends on electrostatic interactions and intermolecular hydrogen bonds, as described in section 4.1 [78]. Regarding the filler morphology, it usually has a needle-like shape [12], [18], although a spherical or irregular shape has also been observed [141] (Table 3). Table 3 shows the shape of CNFs used as reinforcement of chitosan-based films. Also, it shows that, for testing the composite films, the incorporation of CNFs in those polymeric matrices ranges from 0.5 to 60 wt.%.

Table 3. CNFs incorporated in chitosan-based films

| Reinforcement | Other components | Cellulose shape | Cellulose size | Cellulose content (wt.%) | Reference |
|---|---|---|---|---|---|
| Cellulose nanofibers | | Needle-like | D= 20 nm | 0 and 33.33 | [142] |
| Cellulose nanofibers | | | D= 5-25 nm<br>L= several micrometers | 0, 1, 3, 5, 7 and 9 | [143] |
| Nanofibrillated cellulose | | | | 0, 0.5, 1.0 and 1.5 | [140] |
| Nanofibrillar cellulose | | | | 0, 1, 3, 5, 7 and 10 | [144] |
| Cellulose nanofibers | Tween 80: 2 wt.%*<br>Glycerol: 50 wt.%* | | D= 32 nm<br>Aspect ratio= 20 | 0, 0.5, 1, 3 and 5 | [145] |
| Cellulose nanofibers | Glycerol: 25 wt.% | | | 0, 1, 3, 5 and 7 | [78] |
| Cellulose nanofibers | Polyvinylpyrrolidone: 25 wt.% | Needle-like | D= 9-11 nm<br>L= 100-200 nm | 0, 1, 3 and 5 | [146] |
| Cellulose nanofibers | Tripolyphosphate | Needle-like | D= 6-18 nm<br>L= 200-800 nm | 0 and 1 | [18] |
| Cellulose nanofibrils | Adipic Acid: 37 wt.%<br>Glycerol: 20 wt.% | | | 0, 3, 5, and 7 | [5] |
| Bacterial cellulose | Glycerol: 40, 66.93, 67.19, 67.71, 68.75 and 70.83 wt.%<br>Borate: 3.43 or 7 wt.%<br>Tripolyphosphate: 3.43 or 7 wt.% | | D=50-100 nm<br>L= 10000-20000 nm | 0, 0.39, 0.78, 1.56, 3.13 and 6.25 | [147] |
| Dialdehyde cellulose nanofibers | | | D< 20-100 nm | 0, 2, 4, 6, 8, 10, 12 | [148] |

| | | | | 0 and 50 | [22] |
|---|---|---|---|---|---|
| APS-oxidized Cellulose nanofibers | | | | 0 and 50 | [22] |
| TEMPO-oxidized cellulose nanofibers | | | | 0, 0.5, 1.0 and 1.5 * | [149] |
| APS-oxidized nanobacterial cellulose | | | | 0 and 50 | [22] |
| TEMPO-oxidized cellulose nanofibers | Sorbitol: 25, 26.32, 27.78, 29.41, 31.25 and 33.33 wt.% | Needle-like | D= 3-20 nm L= 10-100 nm | 0, 5.26, 11.11, 17.65, 25 and 33.33 | [150] |
| APS-oxidized nanocellulose I | Glycerol: 30 wt.% | Rod-like | width= 15.37 nm Particle size= 37.39 nm | 0 and 7 | [141] |
| APS-oxidized nanocellulose II | | Spherical or irregular shape | width= 12.74 nm Particle size= 35.54 nm | 0 and 7 | |
| Cellulose nanofibers | Glycerol: 0.8 mL/g Carum copticum essential oil: 5 wt.% Tween 80: 0.01 wt.% | Spherical | D= 28 nm L= 2-3 um | 0 and 4 | [151] |
| Cellulose nanofibers | Glycerol: 0.8 mL/g Carum copticum essential oil: 5 wt.% Tween 80: 0.01 wt.% | | D= 28 nm L= 2-3 um | 0 and 4 | [130] |
| Cellulose nanofibers | Ketorolac tromethamine: 10 wt.% | Needle-like | D= 46.49-59 nm L= 252.92-310.74 nm | 0, 0.25, 0.5, 0.75 and 1 | [12] |
| Cellulose nanofibril | Oregano essential oil: 2 wt.% Tween-80: 0.8 wt.% | | D= 20-50 nm L= 200 nm Aspect ratio= 50 | 0, 20, 40 and 60 | [152] |

| Nanocellulose | Glycerol: 20 wt.%<br>Grape seed extract: 21.69 wt.% | 2.89 | [153] |
| Nanobacterial cellulose | Glycerol: 30<br>Epigallocatechin-3-gallate: 0, 15 and 30 wt.% | 0, 5 and 10 | [96] |

On the other hand, when CNFs are incorporated into chitosan films, the behavior of the filler is the same as in the case of the CNCs (Figure 13). CNFs disperse well in chitosan films as long as the filler amount is small. By incorporating additional filler content, the surface of the composites shows agglomerations and a rougher surface morphology, which alter the performance of the composite film [78].

Franco et al. [140] study the influence of CNFs in chitosan-based films. The CNFs content in the composites was 0, 0.5, 1 and 1.5 wt.% (based on chitosan weight). SEM was used to analyze the surface and the cross-section of the composite films. The cross-sectional micrographs (Figure 18) showed a uniform and homogeneous structure for all the samples, confirming the good interfacial adhesion between the filler and the matrix. The surface morphology images showed almost negligible agglomerations and few rough spots. The absence of remarkable agglomerations is because the filler content is relatively low compared to other investigations, in which the agglomerations begin to be appreciable at 4-5 wt.% of the filler content [145], [146]. For example, in a research by Ghazanfari et al. [145] the SEM image of a cryo-fractured surface of the nanocomposite containing 3CNFs exhibited a uniform filler distribution with few small size agglomerates, whereas at 5CNFs the surface contains large agglomerations (Figure 19). It could be said that values higher than 3 wt.% led to agglomerated particles as occurs using CNCs (see section 4.1).
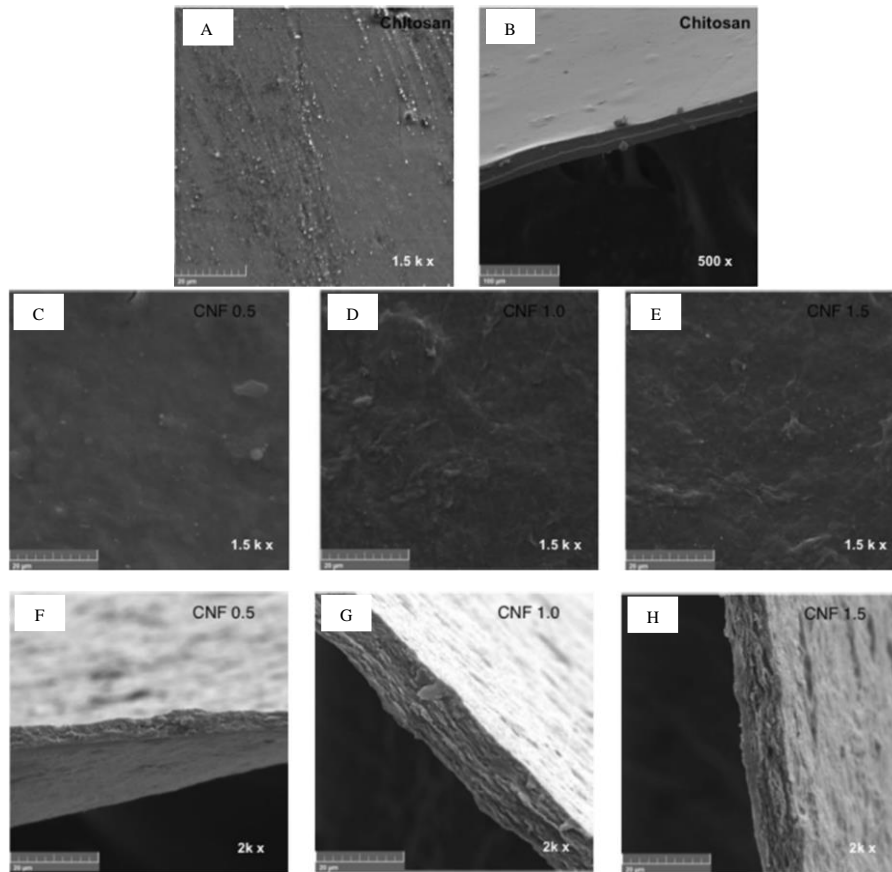
Figure 18. SEM images of surface and cross-section of (A, B) chitosan film, (C, F) 0.5CNFs/chitosan film, (D, G) 1.0CNFs/chitosan film, and (E, H) 1.5CNFs/chitosan film [140]
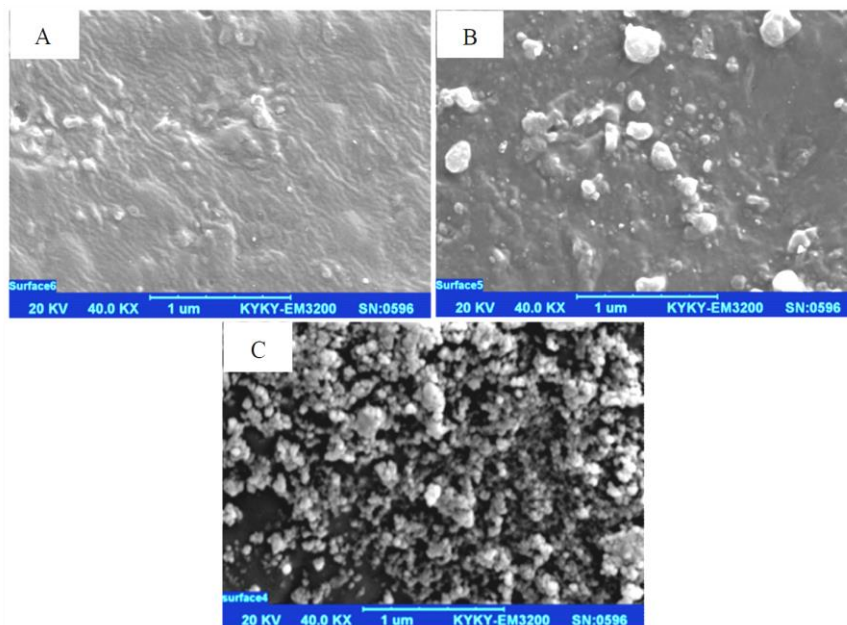


Figure 19. SEM images of a cryo-fractured surface of A) 1CNFs/chitosan film B) 3CNFs/chitosan film C) 5CNFs/chitosan film [145]

Chitosan-based composites reinforced with CNFs also have been blended with cross-linkers, plasticizers, modified CNFs replacing the CNFs, and active agents. The plasticizers used in the latest investigations have been glycerol [145], [153], and sorbitol [150]. For cross-linking, it has been applied polyvinylpyrrolidone [146], tripolyphosphate [18], [147], adipic acid [5], and borate [147]. A chitosan film elaborated by Gopi et al. [78] was reinforced with CNFs and plasticized with glycerol to enhance the physicochemical properties of the film. The filler content was 0, 1, 3, 5, and 7 wt.% (based on chitosan weight), while the glycerol amount was 25 wt.% (based on chitosan weight) for all the samples. The SEM results (Figure 20) showed that the nanofibers were well embedded in the chitosan matrix. Also, it was noticeable the formation of agglomerations and a rougher surface as the filler content increased. The good adhesion showed between the two polymers resulted from strong electrostatic interactions and hydrogen bonds [154].
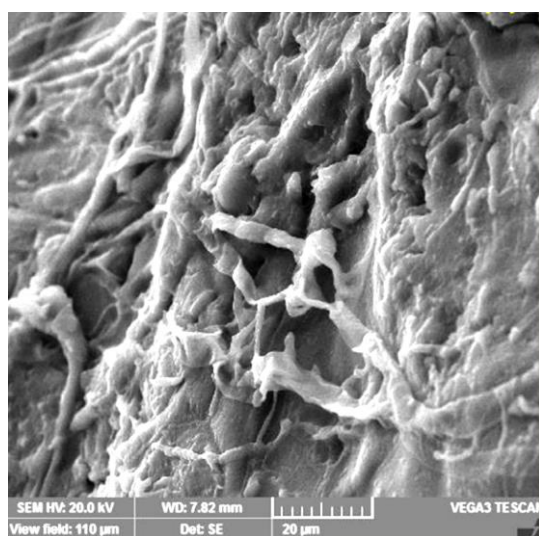


Figure 20. SEM micrographs of 5CNFs/chitosan film [78]

The addition of plasticizers and cross-linking agents to the same composite film is common practice. Liang et al. [147] elaborated chitosan-based composite films with bacterial CNFs (0, 0.39, 0.78, 1.56, 3.13, and 6.25 wt.%; based on chitosan weight), glycerol, borate, and tripolyphosphate. The cross-sectional images of the nanocomposites with 0.78BCNFs observed by SEM exhibited homogeneous and compact structures without any possible macroscopic phase separation, demonstrating excellent incorporation of all the components and compatibility between them (Figure 21). As

described in section 4.1, the glycerol function was to disrupt some inter and intramolecular hydrogen bonds to provide to the chains more movement capacity [155]. While the cross-linking agents were responsible for obtaining a compact matrix, and uniform and homogeneous composite films [156].
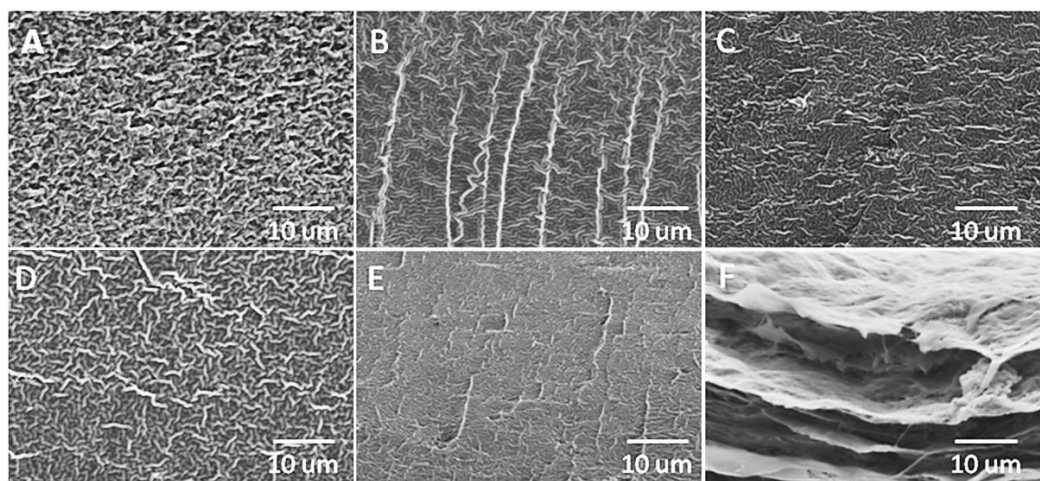


Figure 21. Fractured cross-sectional image of (A) chitosan film, (B) 0.78BCNFs/chitosan film, C) cross-linked (borate) 0.78BCNFs/chitosan film, D) cross-linked (tripolyphosphate) 0.78BCNFs/chitosan film, E) cross-linked (borate and tripolyphosphate) 0.78BCNFs/chitosan film, and F) BCNFs film imaged by SEM [147]

The addition of cross-linking agents does not prevent noticeable changes in composite surfaces when the filler content is above the threshold point. The cross-linked CNFs/chitosan composites have shown increasing roughness as filler increases [146]. On the other hand, CNFs, as was seen in the section of CNCs, are sometimes subjected to some modifications resulting in APS-oxidized CNFs [22], [141], TEMPO-oxidized CNFs [149], [150], APS-oxidized bacterial CNFs [22], and dialdehyde CNFs [148].

According to the literature, most of the CNF modifications, which will be incorporated into chitosan films, have been carried out to increase the negative character of the filler and thus enhance electrostatic interactions with chitosan [22]. When modified CNFs are incorporated into a chitosan matrix, strong intermolecular interactions make it possible to form a compact composite, although they are also responsible for agglomerations [143]. By incorporating a low filler content, the particles are well distributed. When additional filler is added, the composite film presents filler agglomerations (Figure 13) [149].

Adel et al. [141] obtained oxidized CNFs using APS, which had the function of hydrolyzing and oxidizing the cellulose fibers. The modified CNFs also had two different polymorphs, as some fibers were mercerized (CNFII) while others were not (CNFI).

These fillers were added to the chitosan matrix, and the surface morphology of the composites was observed by SEM (Figure 22). The micrographs showed a smooth and homogeneous surface for the pure chitosan. In contrast, the incorporation of CNFs resulted in a rough surface. Using APS-oxidized CNFII, the SEM images showed small dots forming agglomerations, although the particles were partially well dispersed. In the APS-oxidized CNFI, the particles tended to form more noticeable agglomerations on the surface since the dispersion was not uniform. According to the authors, the particles tended to interact with each other as greater filler amounts were added, resulting in agglomerations.
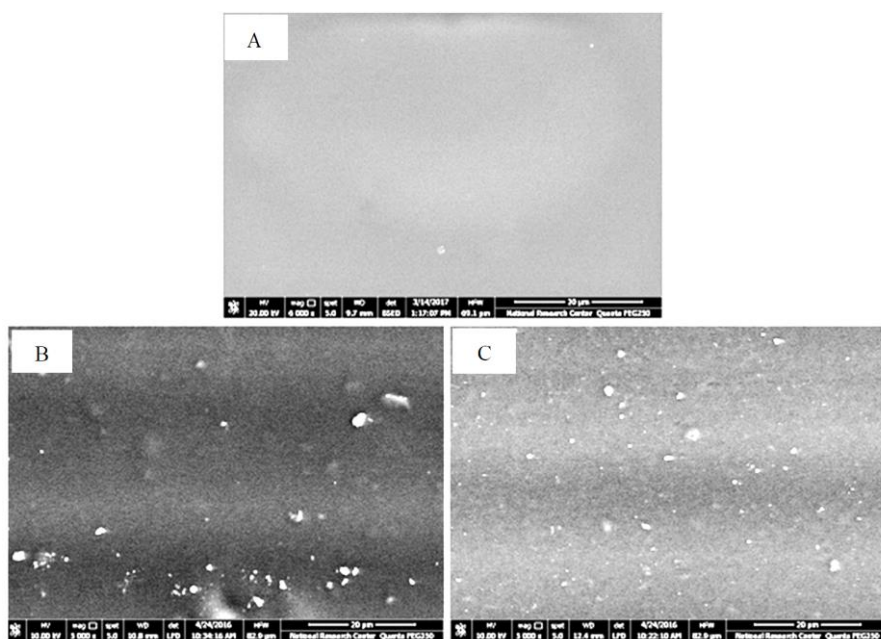


Figure 22. Surface morphology of A) chitosan film, B) 7APS-oxidized CNFI/chitosan film C) 7APS-oxidized CNFII/chitosan film [141]

The difference regarding the degree of dispersion of the particles (CNFI and CNFII) is probably due to the fact that each polymorphism has a different crystallographic structure and chain orientation. The CNFI has a parallel chain arrangement while the CNFII has an anti-parallel arrangement [157], the latter being the most effective, in terms of dispersion, in the composite developed by Adel et al. [141]. In another case, it was elaborated chitosan films reinforced with TEMPO-oxidized CNFs (0, 5.26, 11.11, 17.65, 25, and 33.33 wt.%; based on chitosan weight) and plasticized with sorbitol by Soni et al. [150]. The interesting of this work is that all the composite films did not show agglomerations. The filler was highly packed and well dispersed in the matrix, even for the films with high

reinforcement content. This scenario is caused by sorbitol, as a plasticizer it increases the intermolecular spaces and the free volume of the polymeric matrix [5].

On the other hand, active agents have also been applied in the obtention of chitosan composites reinforced with CNFs. As mentioned before, these components are applied depending on the use given to the composite film. It has been used essential oils (carum copticum [151], origanum vulgare ssp. gracile [130], oregano [152]), drugs (ketorolac tromethamine [12]), and grape seed extracts [153]. In all cases, the CNFs serve as carriers of the active agent and act as release controllers. The releasing of the active agents results in a better antibacterial, antifungal, and antioxidant activity for the cases of the essential oils and grape seed extracts [130], [153]. By using a drug, the film acquires properties depending on the loaded agent; in the case of using Ketorolac tromethamine, the film serves as an analgesic [12].

The surface morphology of chitosan composites with the active agents is almost the same as those that only are reinforced with CNFs. In composite films with ketorolac tromethamine (10 wt.%; based on chitosan weight), the cross-sectional images exhibited a rougher surface as the CNFs content increased, being the film with 1CNFs the roughest (Figure 23E). Whit little CNFs loading (0.25 wt.%; based on chitosan weight) in the chitosan matrix, the presence of the filler was negligible, and the surface maintained its smoothness [12].
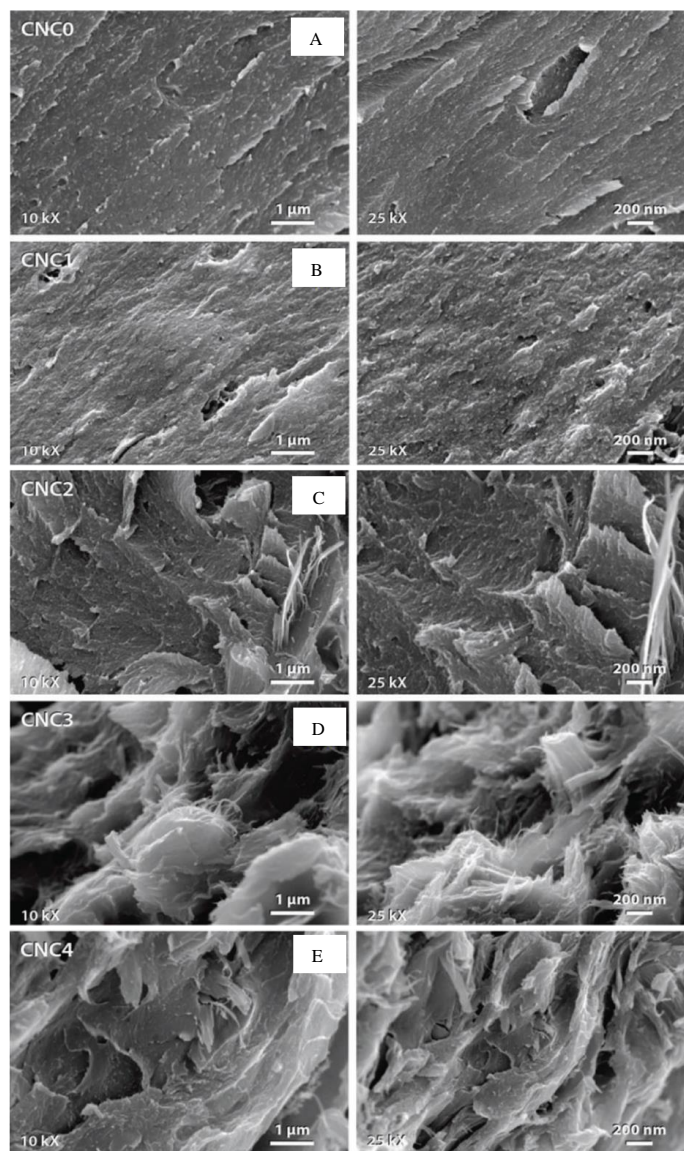
Figure 23. SEM micrographs of chitosan films with ketorolac tromethamine and reinforced with A) 0CNFs, B) 0.25CNFs, C) 0.5CNFs, D) 0.75CNFs, and E) 1CNFs at low and high magnification [12]

In another example of chitosan-based composite films, in which was used CNFs and Carum copticum essential oil [151], the addition of 4CFNs (based on chitosan weight ) formed agglomerations, and the surface became rougher, as shown the SEM images (Figure 24A, B, and C). Also, the composites were analyzed through AFM, which were taken two and three-dimensional images and phase traces of the films (Figure 24D, E, and F). The two-dimensional images exhibited a uniform and homogeneous structure for the chitosan net. The addition of the essential oil improved the surface structure of the film since it showed fewer irregular holes, although the roughness was increased. For the composite reinforced with cellulose nanofibers and the essential oil, the surface displayed

some irregular holes. The phase trace histograms exhibited well distribution of the essential oils, but with the addition of the CNFs small agglomerations were formed.
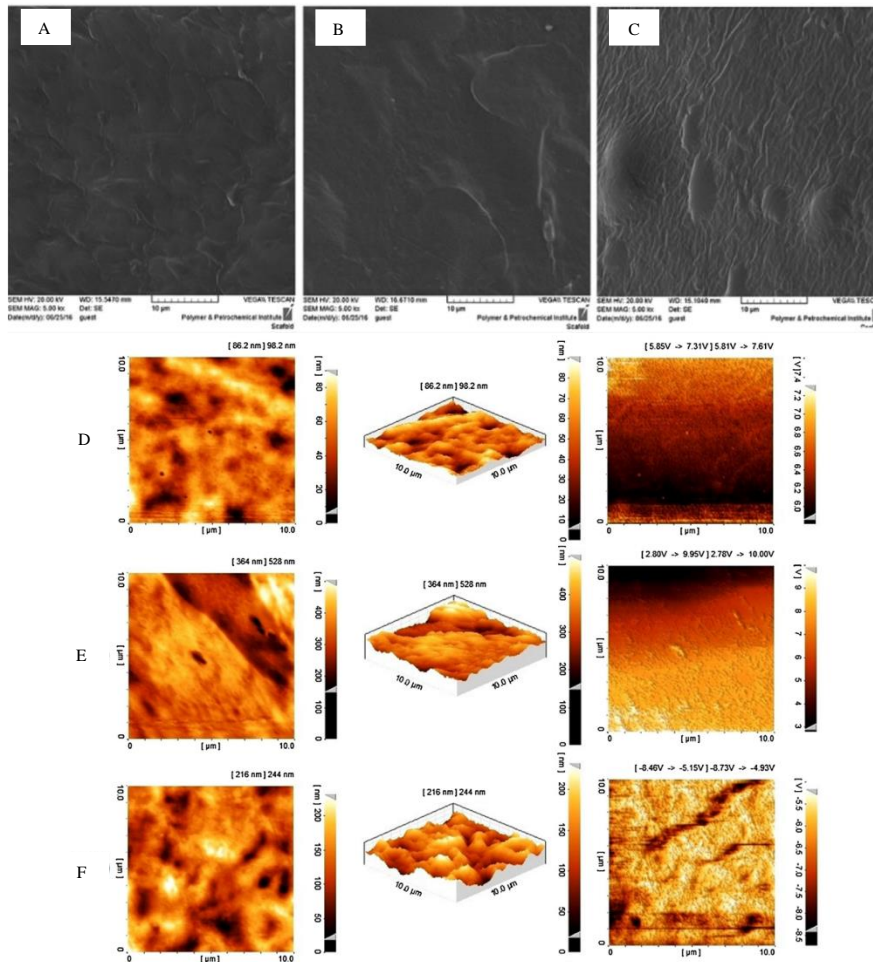


Figure 24. Scanning electron micrographs of A) chitosan film, B) chitosan film-essential oil, and C) 4CNFs/chitosan film-essential oil (surface images of films); AFM topographic images of D) chitosan film, E) chitosan film-essential oil, and F) 4CNFs/chitosan film-essential oil [151]

The agglomerations of CNFs were appreciable in most of the examples exposed in this section. This feature occurred when the amount of filler added was not appropriate and even happened with plasticizers, cross-linking and active agents, or modified CNFs. On the other hand, regarding the mechanical properties of CNFs reinforced chitosan composite films, the effects are the same as those in which CNCs are the filler. In most cases, TS and YM increase as CNFs loading amount increases, while EB decreases, as shown in Table 4. However the tendency has a dose-dependent behavior, an amount of filler greater than the threshold point causes a negative effect, reducing TS and YM [12], [143].

Table 4. Mechanical properties of chitosan composite films reinforced with CNFs

| Reinforcement | Other components | Information | Cellulose content (wt.%) | Tensile strength (MPa) | Elongation at Break (%) | Young`s Modulus (MPa) | Reference |
|---|---|---|---|---|---|---|---|
| Cellulose nanofibers | | Load cell: 100 N Cross-head speed: 1.5 mm/min | 0 | 60 | 2 | 4700 | [142] |
| | | | 33.33 | 69 | 2.6 | 5200 | |
| Cellulose nanofibers | | Cross-head speed: 1 mm/s | 0 | ~79 | | | [143] |
| | | | 1 | ~40 | | | |
| | | | 3 | ~25 | | | |
| | | | 5 | ~15 | | | |
| | | | 7 | ~8 | | | |
| | | | 9 | ~4 | | | |
| Nanofibrillated cellulose | | ASTM D882-02 Cross-head speed: 5 mm/min T= 25 °C | 0 | 17.49 | 17.99 | 407.63 | [140] |
| | | | 0.5 | 47.45 | 5.43 | 1931.87 | |
| | | | 1 | 52.24 | 3.73 | 1979.21 | |
| | | | 1.5 | 56.59 | 1.67 | 5384.05 | |
| Cellulose nanofibers | Tween 80: 2 wt.%* Glycerol: 50 wt.%* | Direct addition ASTM D882-97 Cross-head speed: 50 mm/min | 0 | 0.50 | 15 | | [145] |
| | | | 0.5 | 0.6 | 16.1 | | |
| | | | 1 | 1.1 | 18.6 | | |
| | | | 3 | 1.6 | 24.1 | | |
| | | | 5 | 1.2 | 18.7 | | |
| | | Direct addition ASTM D882-97 Cross-head speed: 50 mm/min | 0 | 0.41 | 15 | | |
| | | | 3 | 0.51 | 16.32 | | |

| Material | Additive | Test conditions | | | | | Ref |
|---|---|---|---|---|---|---|---|
| | | Direct addition and ultrasonic bath treatment ASTM D882-97 Cross-head speed: 50 mm/min | 3 | 0.568 | 24.12 | | |
| | | Indirect addition ASTM D882-97 Cross-head speed: 50 mm/min | 3 | 1.162 | 36.68 | | |
| | | Indirect addition and ultrasonic bath treatment ASTM D882-97 Cross-head speed: 50 mm/min | 3 | 1.68 | 9.42 | | |
| Cellulose nanofibers | Glycerol: 25 wt.% | ASTM D412 –2002 Load cell: 1000 N Cross-head speed: 500 mm/min T= 27 °C | 0 | 5.68 | 28.87 | 50.97 | [78] |
| | | | 1 | 6.24 | 26.43 | 54.36 | |
| | | | 3 | 6.94 | 23.64 | 58.12 | |
| | | | 5 | 7.44 | 20.77 | 59.94 | |
| | | | 7 | 7.08 | 22.56 | 57.88 | |
| Cellulose nanofibers | Polyvinyl pyrrolidone: 25 wt.% | Cross-head speed: 1 mm/s Room temperature | 0 | 23.42 | | 1188 | [146] |
| | | | 1 | ~28.3 | | ~1550 | |
| | | | 3 | ~30 | | ~1690 | |
| | | | 5 | 32.44 | | 2139 | |
| Cellulose nanofibers | | Cross-head speed: 10 mm/min Room temperature | 0 | 48.45 | 8.11 | 3183 | [5] |
| | Glycerol: 20 wt.% | | 0 | 25.69 | 31.03 | 381 | |
| | | | 3 | 38.18 | 24.73 | 728 | |
| | | | 5 | 45.66 | 21.4 | 983 | |
| | | | 7 | 40.03 | 17.89 | 1027 | |
| | Adipic Acid: 37 wt.% | Conventional Heat Curing treatment | 0 | 103.25 | 4.37 | 5434 | |

| | | | | | | | |
|---|---|---|---|---|---|---|---|
| | Adipic Acid: 37 wt.%<br>Glycerol: 20 wt.% | ASTM D882<br>Cross-head speed: 10 mm/min<br>Room temperature | 0 | 81.57 | 13.98 | 2297 | |
| | | | 3 | 113.41 | 12.55 | 3004 | |
| | | | 5 | 127.81 | 11.93 | 4715 | |
| | | | 7 | 109.37 | 8.51 | 4082 | |
| Bacterial cellulose | Glycerol: 40 wt.% | Standard GB/T 1040-2006<br>Cross-head speed: 100 mm/min | 0 | 20.4 | 64.8 | | [147] |
| | Glycerol: 66.93 wt.% | | 0.39 | ~28.2 | ~59.5 | | |
| | Glycerol: 67.19 wt.% | | 0.78 | ~30 | ~59 | | |
| | Glycerol: 67.71 wt.% | | 1.56 | ~25 | ~58 | | |
| | Glycerol: 68.75 wt.% | | 3.13 | ~17.5 | ~40 | | |
| | Glycerol: 70.83 wt.% | | 6.25 | ~16.87 | ~25 | | |
| | Glycerol: 67.19 wt.%<br>Borate: 7 wt.% | | 0.78 | ~32.5 | 62.50% | | |
| | Glycerol: 67.19 wt.%<br>Tripolyphosphate: 7 wt.% | | 0.78 | 30 | 77.40% | | |
| | Glycerol: 67.19 wt.%<br>Borate: 3.43 wt.%<br>Tripolyphosphate: 3.43 wt.% | | 0.78 | 39 | 72.5% | | |
| Dialdehyde cellulose nanofibers | | Cross-head speed: 1 mm/min | 0 | 34.8 | | | [148] |
| | | | 2 | 56.3 | | | |
| | | | 4 | ~56.3 | | | |
| | | | 6 | ~58 | | | |
| | | | 8 | ~56.3 | | | |
| | | | 10 | ~68 | | | |
| | | | 12 | 76.8 | | | |

| | | | | | | | |
|---|---|---|---|---|---|---|---|
| APS-oxidized cellulose nanofibers | | ISO 1924-1 Cross-head speed: 25 mm/min | 0 | ~38 | ~0.975 | | [22] |
| | | | 50 | ~10 | ~1.4 | | |
| TEMPO-oxidized cellulose nanofibers | | Cross-head speed: 5 mm/min | 0* | ~27.5 | ~25% | | [149] |
| | | | 0.5* | ~26.5 | ~24% | | |
| | | | 1* | ~23 | ~30% | | |
| | | | 1.5* | ~21 | ~7% | | |
| APS-oxidized bacterial cellulose | | Cross-head speed: 25 mm/min | 0 | ~38 | ~0.975 | | [22] |
| | | | 50 | 76 | ~0.85 | | |
| TEMPO-oxidized cellulose nanofibers | Sorbitol: 25 wt.% | ASTM D882−12 Load cell: 50 N Cross-head speed: 5 mm/min | 0 | 10.7 | ~27 | ~275 | [150] |
| | Sorbitol: 26.32 wt.% | | 5.26 | ~13 | ~22.5 | ~350 | |
| | Sorbitol: 27.78 wt.% | | 11.11 | ~11 | ~18.75 | ~450 | |
| | Sorbitol: 29.41 wt.% | | 17.65 | ~16.5 | ~17 | ~520 | |
| | Sorbitol: 31.25 wt.% | | 25 | 17.5 | ~12.5 | 545 | |
| | Sorbitol: 33.33 wt.% | | 33.33 | 18.7 | ~9 | 652 | |
| APS-Oxidized nanocellulose I | Glycerol: 30% wt.% | Bleaching process Cross-head speed: 10 mm/min | 0 | 16.74 | 50.81 | 113.65 | [141] |
| | | | 7 | 31.7 | 52.65 | 413.28 | |
| APS-Oxidized nanocellulose II | | Mercerization process Cross-head speed: 10 mm/min | 7 | 24.93 | 49.23 | 273.26 | |
| Cellulose nanofibers | Glycerol: 0.8 mL/g | ASTM D 882-10 Cross-head speed: 400 mm/min | 0 | 21.56 | 52.2 | | [151] |
| | Glycerol: 0.8 mL/g Carum copticum essential oil: 5 wt.% Tween 80: 0.01 wt.% | | 0 | 25.15 | 47.6 | | |
| | | | 4 | 27.28 | 46 | | |
| Cellulose nanofibers | Glycerol: 0.8 mL/g | Cross-head speed: 40 mm/min Room temperature | 0 | 21.56 | 52.2 | 720.27 | [130] |

| | | | | | | | |
|---|---|---|---|---|---|---|---|
| | Glycerol: 0.8 mL/g | | 0 | 20.94 | 53.2 | 712.96 | |
| | Carum copticum essential oil: 5 wt.% Tween 80: 0.01 wt.% | | 4 | 31.94 | 48.5 | 979.18 | |
| Cellulose nanofibers | ketorolac tromethamine: 10 wt.% | Cross-head speed: 5 mm/min | 0 | 37.8 | 16.8 | 107 | [12] |
| | | | 0.25 | 42.5 | 8.13 | 242.1 | |
| | | | 0.5 | 50.4 | 5.33 | 575.5 | |
| | | | 0.75 | 54.5 | 4.97 | 720.9 | |
| | | | 1 | 55.9 | 4.5 | 920.7 | |
| Cellulose nanofibril | Oregano essential oil: 2 wt.% Tween-80: 0.8 wt.% | Cross-head speed: 10 mm/min | 0 | 7.71 | 31.31 | | [152] |
| | | | 20 | 10.24 | 5.14 | | |
| | | | 40 | 13.79 | 5.63 | | |
| | | | 60 | 16.8 | 4.48 | | |
| Nano-bacterial cellulose | Glycerol: 30 wt.% | Cross-head speed.: 50 mm/ min | 0 | 42.38 | 32.99 | | [96] |
| | | | 5 | 49.55 | ~13 | | |
| | | | 10 | 33.34 | 9.11 | | |
| | Glycerol: 30 wt.% Epigallocatechin-3-gallate: 15 wt.% | | 0 | ~30 | ~2.5 | | |
| | | | 5 | ~47 | ~7.5 | | |
| | | | 10 | ~41 | ~5 | | |
| | Glycerol: 30 wt.% Epigallocatechin-3-gallate: 30 wt.% | | 0 | ~18.5 | ~2 | | |
| | | | 5 | ~44.5 | ~3.75 | | |
| | | | 10 | ~29 | ~2.5 | | |

The tendency about the mechanical performance is better observed in Figures 25A, B, and C. These figures were built with selected information from Table 4. The mechanical parameter values (TS, YM, and EB) are in percentage and were calculated in the same way as in section 4.1, with the difference that the selected samples were those that were tested at a cross-head speed between 1.5-5 mm/min. As shown in Figures 25A, and B, the highest TS and YM values are obtained with 1.5CNFs since they improve by 223.56% and 1220.82%, respectively, relative to the pure chitosan films. If the loaded filler continues to increases, the strength and stiffness of the composite reduce.
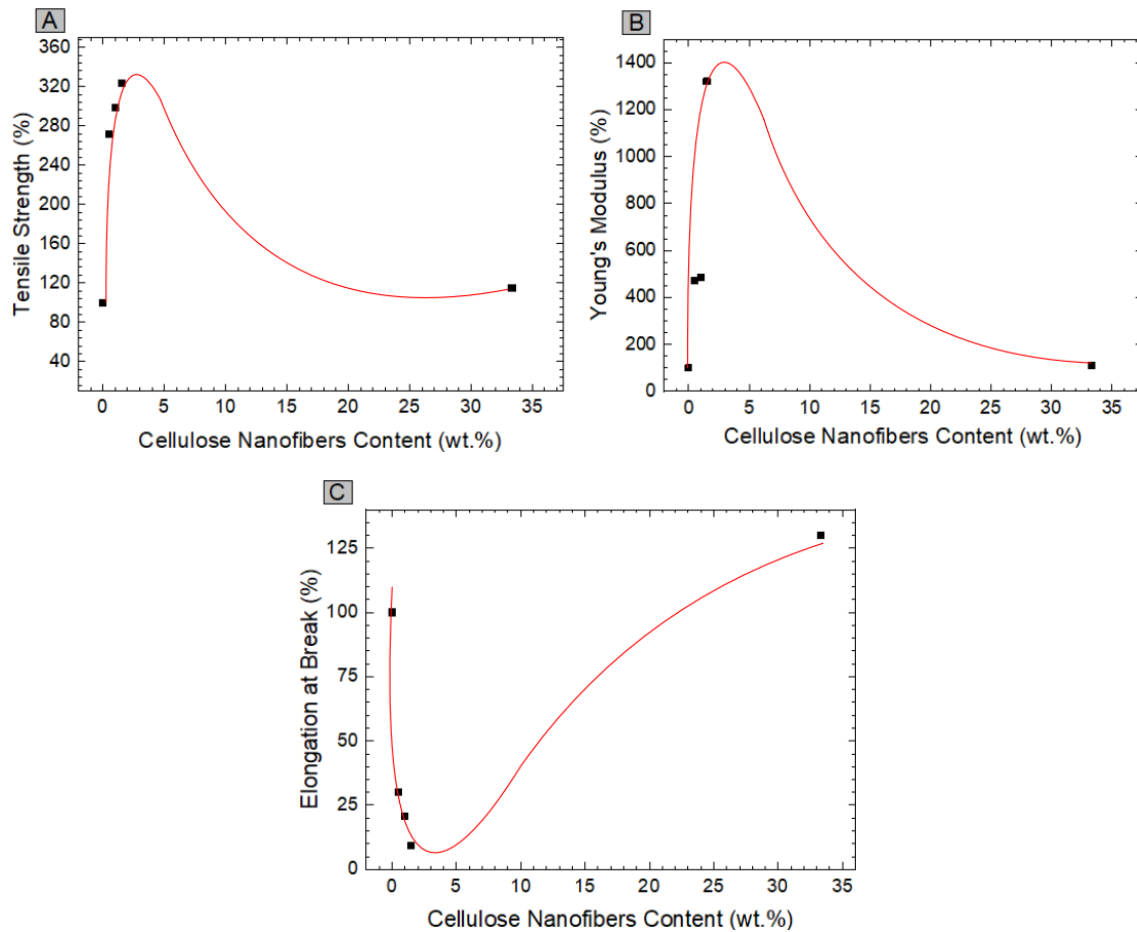


Figure 25. A) Tensile Strength, B) Young`s Modulus, C) Elongation at Break of chitosan-based films varying the CNFs content

Regarding the EB, Figure 25C shows that by adding 1.5CNFs the EB reduces by 90.82%. Additional filler loading may enhance this property. The reasons for these results are the same described in section 4.1. The strong interactions between the filler and the matrix, and the rigid nature of the filler are responsible for the improved TS and YM, and decreased EB [140], [152]. In contrast, the tendency changes are due to the formation of agglomerates resulting from an excess filler content [158].

On the other hand, when the figures of the mechanical performance of the CNCs/chitosan composite films (Figures 12A, B, and C) and CNFs/chitosan composite films (Figures 25A, B, and C) are compared, it is observed that, with low filler content, in both cases good improvements are obtained in TS and YM. However, by using CNFs, the increase of these parameters is greater with less filler content. In this regard, it could be said that in terms of strength and stiffness, the CNFs are better reinforcements. Regarding the EB, both fillers reduce the flexibility, although by using CNFs, this effect is more noticeable.

Franco et al. [140] elaborated chitosan films reinforced with CNFs at different proportions. The content of this filler varied from 0 to 1.5 wt.% (based on chitosan weight). The mechanical results showed that TS and YM increased from 17.49 to 56.59 MPa and 407.63 to 5384.04 MPa, respectively, and EB decreased from 17.99 to 1.67% (Figure 26). These values mean that TS and YM improved by 223% and 1300%, respectively, and EB decreased by 90.72%, relative to the pure chitosan film. These results corroborate the idea exposed before since they are a consequence of the strong interactions between the filler and the matrix, effective stress transfer, and the restricted mobility caused by the filler rigidity [158].
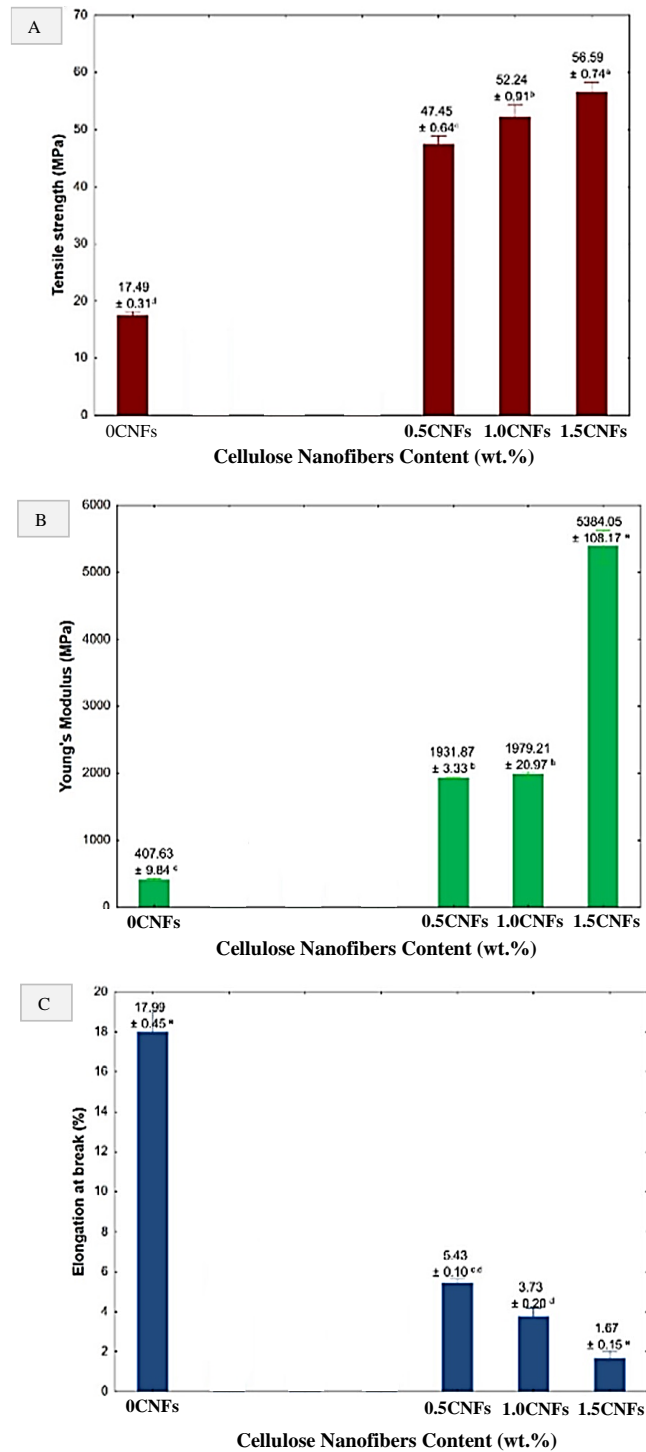
Figure 26. Mechanical properties of CNFs/chitosan composite films: A) tensile strength, B) elongation at break, and C) Young's modulus [140]

The brittle characteristics obtained when chitosan films are reinforced with CNFs can be overcome with the addition of plasticizers [159]. Falamarzpour et al. [5] formed chitosan films reinforced with CNFs (0, 3, 5, and 7 wt.%; based on chitosan weight) and plasticized with glycerol (20 wt.%; based on chitosan weight). The mechanical test showed that TS, EB, and YM of the pure chitosan film were 48.45 MPa, 8.11%, and 3183

MPa. With the addition of glycerol, these values were 25.69 MPa, 31.03%, and 381 MPa, respectively. As expected, the TS and YM diminished, and the EB increased due to the plasticizer. With the addition of 5CNFs (with glycerol), TS and YM increased to 45.66 and 983 MPa, respectively, and the EB decreased to 21.4%. However, when these final results are compared with the mechanical properties of the pure chitosan film, it is observed that TS and YM decreased by 5.76% and 69.10%, respectively, and EB increased by 163.87%. In this regard, it could be said that incorporating CNFs and glycerol into a chitosan-based film is an excellent option to increase flexibility without significantly affecting the tensile strength, although the stiffness gradually deteriorates.

Continuing with the example described recently, the authors cross-linked the chitosan films with adipic acid through heat curing [5]. The cross-linked composite film with 5CNFs and 20 wt.% glycerol exhibited TS, EB, and YM values of 127.81 MPa, 11.93%, and 4715 MPa, respectively. When these results are compared with those obtained with the pure chitosan film, it is concluded that all of the mechanical parameters were improved. The TS, EB, and YM increased by 163.80%, 47.28%, and 48.13%, respectively, concerning the pure chitosan film.

As demonstrated, the use of plasticizers leads to an increase in the flexibility and a decrease in the strength and rigidity of the films, while the cross-linking agents improve the last two characteristics [126], [147]. Thus, by combining both components in chitosan films reinforced with cellulose, it is possible to obtain excellent and balanced mechanical properties.

On the other hand, when modified fibers are used as reinforcement, the changes in mechanical properties have the same tendency as those obtained with CNFs. Soni et al. [150] studied the incorporation of TEMPO-oxidized CNFs (33.33 wt%) in chitosan films, obtaining values of enhanced TS and YM by 74.77% and 137.09%, respectively, and reduced EB by 66.67%, concerning that of the pure chitosan film (Figure 27). These results, as when using CNFs, are due to the high aspect ratio and good mechanical strength of the filler. Adel et al. [141] reported that chitosan composite films with 7 wt.% APS-oxidized nanocellulose and 30 wt.% glycerol exhibited increased TS and YM by 48.92% and 140.44%, respectively, and reduced EB by 3.21%. With these types of modifications, strong electrostatic interactions occur between the anionic carbonyl groups and the cationic amino groups of the filler and chitosan, respectively, which would be the reason for the significant improvement the strength and stiffness of the films [22], [150].
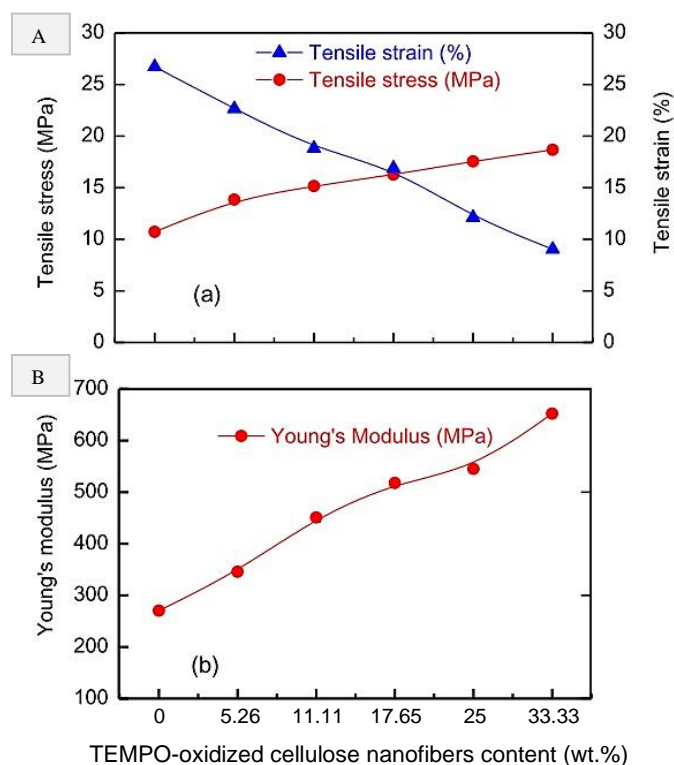
Figure 27. Mechanical properties of TEMPO-oxidized CNFs/chitosan composite films: A) tensile strength and tensile strain, and B) Young's modulus [150]

In addition to those modifications, Zheng et al. [148] observed that after forming chitosan-based composite films reinforced with 12 wt.% dialdehyde CNFs the TS improved by 120.69%, relative to that of the pure chitosan film. For this modification, the interactions with the chitosan matrix are based on hydrogen bonding and the crosslinking effect of the filler. The aldehyde groups react covalently with the amino groups of the chitosan chains, forming a Schiff base structure. The load can be efficiently transferred through all the networks by forming a covalent bond, thus obtaining composites films that support stress effectively.

With the addition of the active agents, the tendency of the mechanical properties remains the same or negligible changes occur. Sarkar et al. [12] found that the TS of the chitosan composite films loaded with ketorolac tromethamine increased from 37.8 to 55.9 MPa, and EB reduced from 16.8 to 4.5%, with an increase of CNFs content from 0 to 1 wt.%. As can be seen, the drug did not affect the reinforcing effect of the CNFs since TS and YM increased, and EB decreased with the addition of the filler (Figure 28).
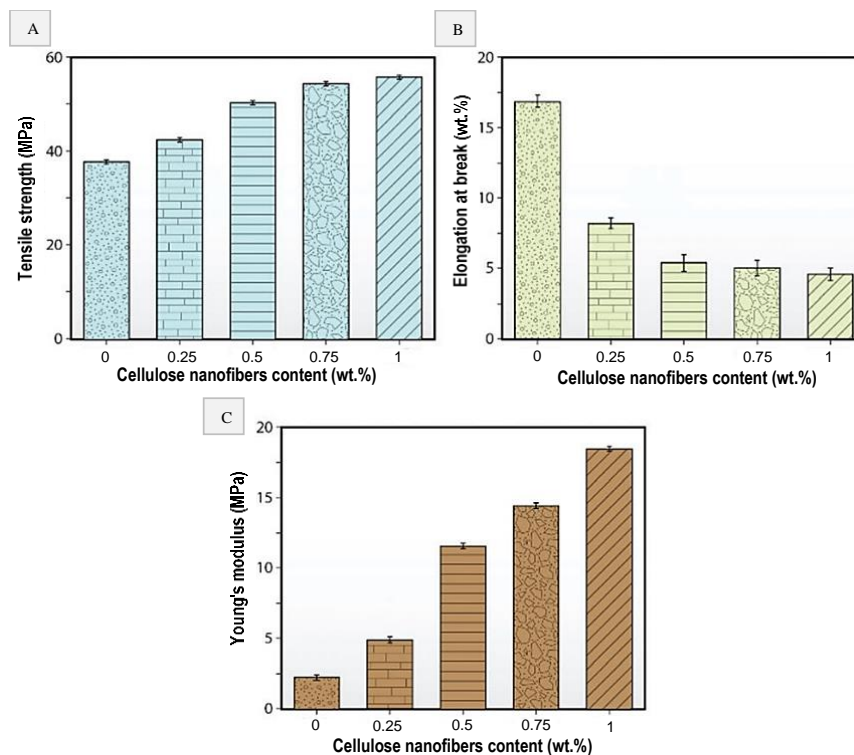
Figure 28. Mechanical properties of CNFs/chitosan composite films loaded with ketorolac tromethamine: A) tensile strength, B) elongation at break, and C) Young's modulus [12]

In the case of incorporating essential oils, it is well known that they could act as plasticizers in addition to their antimicrobial and antioxidant effects [152]. However, they are added in low proportions, making insignificant that last one consequence. Jahed et al. [130] used glycerol, Carum copticum essential oil (5 wt.%; based on chitosan weight), and CNFs (4 wt.%; based on chitosan weight) to elaborate chitosan-based composite films. They reported that the chitosan film with glycerol showed TS, EB, and YM values of 21.56 MPa, 52.2%, and 720.27 MPa. The film with glycerol and the essential oil exhibited TS, EB and YM values of 20.94 MPa, 53.2% and 712.96 MPa, respectively. Finally, the film with glycerol, the essential oil and the CNFs showed TS, EB, and YM values of 31.94 MPa, 48.95%, and 919.18 MPa, respectively. The relatively high value of EB and moderate values of TS and YM of the initial film is because the presence of glycerol. Furthermore, as observed, the addition of the active agent kept the flexibility, strength and stiffness of the film almost unchanged, and with the incorporation of the filler as expected, the mechanical strength of the composite film was improved.

In brief, by incorporating a low content of CNFs in a chitosan matrix, it is possible to obtain composites with a good distribution of the nanoparticles. As has been explained,

the appropriate distribution plays an important role in the stress transfer capacity of the film. Furthermore, with the low content of CNFs, the composites can have an excellent mechanical performance because of the high aspect ratio of the filler and the strong interactions formed with the matrix (electrostatic and hydrogen bond). Finally, the mechanical properties of the composites may vary depending on the blending methods (direct or indirect addition [143], [145]), dispersion methods (ultrasonic bath [145]), filler obtaining processes [22], [147] and treatments (bleaching and mercerization [141]), chitosan characteristics, and the plasticizers, cross-linking and active agents used. With the results of the analyzed articles, it can be summarized that the tendency when adding CNFs in chitosan films is that TS and YM increase, and EB decreases.

### 4.3. Microfibrillated Cellulose

Microcellulose, as its name said, involves micrometer size particles. This term, like nanocellulose, can be classified into two types: micro-fibrillated cellulose (MFC) and microcrystalline cellulose (MCC). Both being cellulose fibers with the difference that the second one has a high degree of crystallinity [61], [132]. MFC is characterized by being a rigid filler that can provide strength and stiffness to a composite material [124]. When it is blended with chitosan, the primary interaction is through hydrogen bonds between the hydroxyl groups of cellulose, and the hydroxyl and amino groups of chitosan, although it could change by modifying the filler [28], [61]. The shape of MFC depends on the treatments applied during its isolation and source [105], although it is common for it to has an irregular shape (Table 5). When incorporated into the chitosan matrix, it would form agglomerations, since the irregularities of its shape also represent filler agglomerations [124].

Table 5. MFC incorporated in chitosan-based films

| Reinforcement | Other components | Cellulose shape | Cellulose size | Cellulose content (wt.%) | Reference |
|---|---|---|---|---|---|
| Cellulose | | | | 11.11 and 42.86 | [49] |
| Cellulose | | | | 14.29 and 33.33 | [26] |
| Cellulose | | Irregular | | 0, 5.26, 11.11, 17.65 and 25 | [124] |
| Cellulose | | | Particle size= 5-15 µm | 0, 10, 30, and 50 | [28] |
| Carboxymethyl cellulose | | | | 0, 0.5, 1.0 and 1.5 | [140] |
| Methyl cellulose | Modified or unmodified TiO2: 2.5 or 1.25 wt.% | | | 12.5 | [160] |
| Carboxymethyl cellulose | Aluminum | | | 0, 1, 5, 10 and 50 | [10] |
| Methyl cellulose | NH4SCN salt: 0, 14.29, 28.57, 42.86 and 57.14 wt.% | | | 42.86 | [17] |

Table 5 shows study cases in which MFC has been used as a reinforcement of chitosan-based films. Wong et al. studied the influence of bleaching treatment by hydrogen peroxide on cellulose fibers from durian husk to be added in chitosan [124]. The SEM results showed that the cellulose particles had an irregular shape (Figure 29). According to the authors, this irregularity is accompanied by a low aspect ratio, which in terms of stress transfer from the matrix to the filler, is inefficient and provides poor matrix-filler interfacial adhesion. In the bleached fibers, the interaction with the matrix was improved because the MFC surface was rougher, developing a better interlocking mechanism with the chitosan matrix.
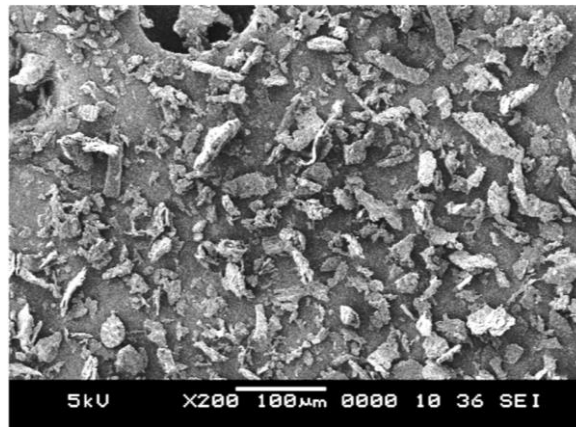


Figure 29. SEM micrograph of cellulose fibers [124]

In another example, cellulose was isolated from oil palm empty fruit to incorporate it into a chitosan matrix and study its water treatment ability [28]. Figure 30 represents the SEM results obtained in the microstructure analysis. Figure 30A, corresponding to chitosan film, exhibited a smooth surface. Figure 30B, corresponding to MFC, confirms the micrometric size of the particles since it was about 5-15 $\mu m$. Figure 30C, corresponding to the composite film, showed that the MFC particles were well incorporated in the chitosan matrix, even they cannot be distinguished. The composite film was homogenous, although the surface roughness increased with the addition of the filler. The results indicate a good adhesion between the filler and the matrix, making possible the obtention of a compact composite film with good performance [140].
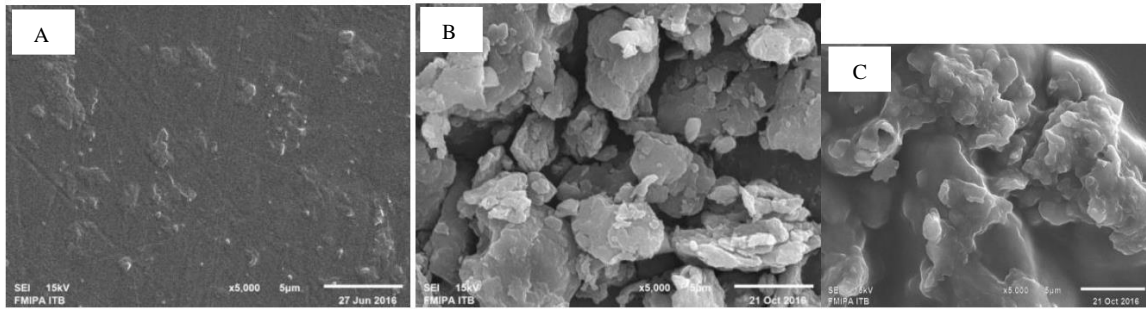
Figure 30. SEM micrographs of A) chitosan film B) cellulose particles and (c) MFC/chitosan film [28]

On the other hand, MFC has been modified to improve or develop interactions that it would have with chitosan. The last MFC modifications used in the chitosan matrix have been methylcellulose [160] and carboxymethyl cellulose [140]. Furthermore, in other experiments, active agents such as $TiO_2$ particles [160] and aluminum [10] have also been added. Franco et al. [140] compared characteristics of chitosan composites reinforced with carboxymethyl cellulose and CNFs. SEM results (Figure 31) showed that with the addition of carboxymethyl cellulose (0.5, 1, and 1.5 wt.%; based on chitosan weight) the roughness of the composite films increased affecting the surface homogeneity. Also, the cross-section images confirmed the agglomerations formed by the filler, which are seen like larger clusters as the content increases. The morphological images of the composites with CNFs showed a better dispersion of particles since the agglomerations were less noticeable and almost negligible (Figure 18). This information indicates that the adhesion between the modified cellulose and the matrix was not proper [161]. The remarkable agglomerations would be a result of hydrogen bonds between the filler particles [162]. Agglomerations that, as described in section 4.1, could act as stress concentrators in case of subjecting the composite films to stress, affecting the performance [124].
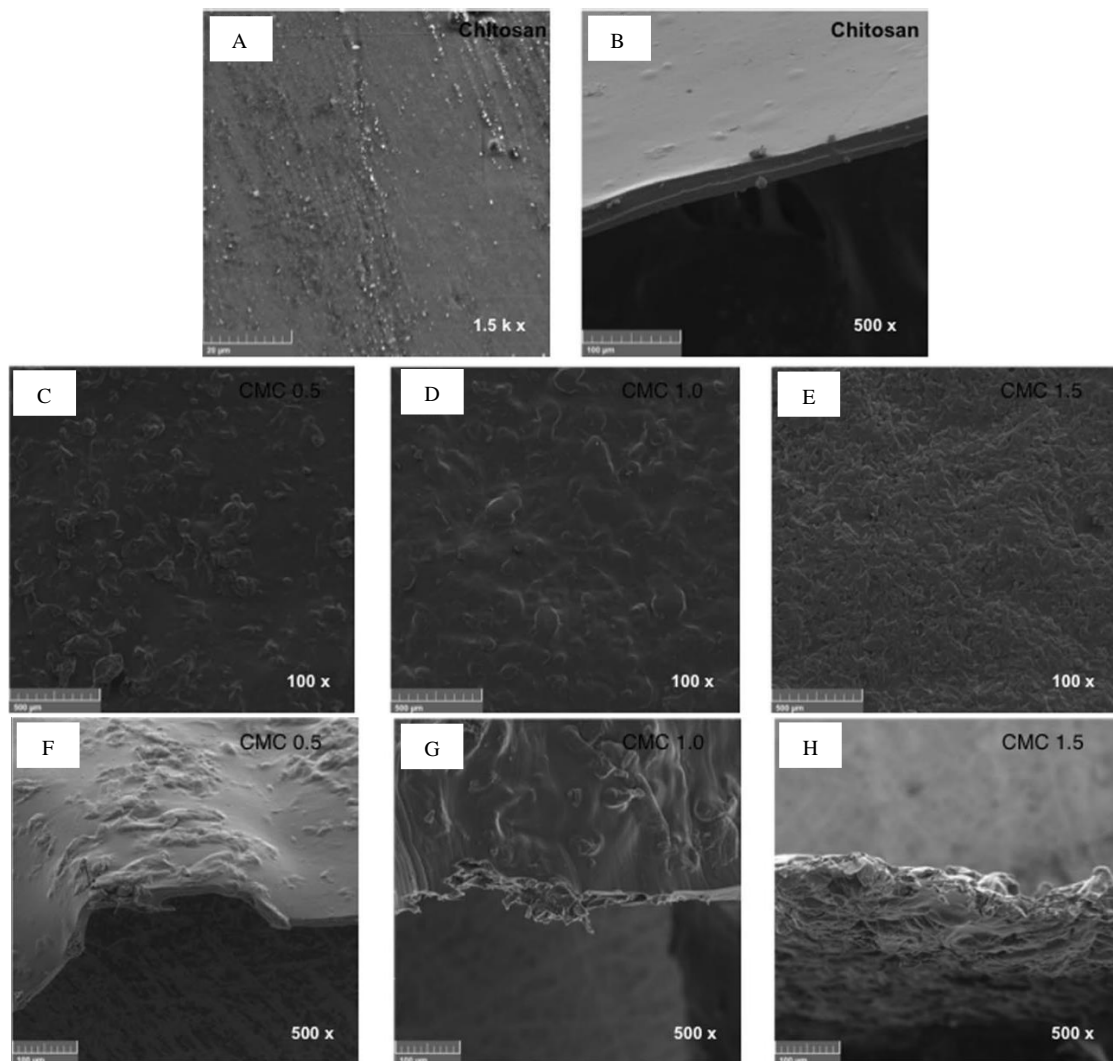
Figure 31. Surface and cross-section images of (A, B) chitosan film, (C, F) 0.5 carboxymethyl cellulose/chitosan film, (D, G) 1 carboxymethyl cellulose/chitosan film, and (E, H) 1.5 carboxymethyl cellulose/chitosan [140]

As was described, it seems that MFC tends to form agglomerations like the nanoparticles, with the difference that by adding the same amount of filler content, the microparticles agglomerate easier; this fact was demonstrated by Franco et al. [140]. In contrast, nanocellulose forms agglomerations at a higher dose in the film matrix [143]. In the case of incorporating active agents, the tendency was the same, although the composite improved other properties. $TiO_2$ particles were well incorporated in a chitosan composite reinforced with carboxymethyl cellulose. The SEM results showed good adhesion between the three components resulting in good mechanical performance [160].

Regarding the mechanical properties, when chitosan composite films are loaded with MFC due to its intrinsic rigid nature [124] and its possibility to form strong hydrogen bonds with chitosan [49], what would be expected is that TS and YM improve and EB

decrease. However, as shown in Table 6, it is complex to define a general tendency since the composites have behaved differently. When microcellulose is used, the treatments applied during its isolation and post-obtaining highly influence the final properties of the composites. There are a wide variety of possible treatments (alkaline treatment, bleaching treatment, esterification, and anhydride treatment) and whatever is used, the filler is still considered microcellulose [163].

Table 6. Mechanical properties of chitosan composite films reinforced with MFC

| Reinforcement | Other components | Information | Cellulose content (wt.%) | Tensile strength (MPa) | Elongation at Break (%) | Young`s Modulus (MPa) | Reference |
|---|---|---|---|---|---|---|---|
| Cellulose | | ISO527-3-1995 (E) Cross-head speed: 2 mm/min | 11.11 | 48 | 2.5 | 3518.7 | [49] |
| | | | 42.86 | 58 | 7 | 4015.0 | |
| Cellulose | | ASTM D882–88 T= 35 ℃ | 0 | 28.5 | 1 | 4700 | [26] |
| | | | 14.29 | 39 | 1.7 | 4200 | |
| | | | 33.33 | 45.4 | 2.8 | 3900 | |
| Cellulose | | Un-bleaching ASTM D882 Cross-head speed: 15 mm/min Load cell: 5 kN T: 25°C | 0 | ~45 | ~12 | ~2750 | [124] |
| | | | 5.26 | ~37.5 | ~10 | ~2850 | |
| | | | 11.11 | ~35 | ~8 | ~3075 | |
| | | | 17.65 | ~33 | ~6 | ~3180 | |
| | | | 25 | ~30 | ~4.9 | ~3275 | |
| | | Bleaching ASTM D882 Cross-head speed: 15 mm/min Load cell: 5 kN T: 25°C | 5.26 | ~46.5 | ~8 | ~3000 | |
| | | | 11.11 | ~41 | ~7 | ~3200 | |
| | | | 17.65 | ~36 | ~4.7 | ~3250 | |
| | | | 25 | ~33 | ~3.7 | ~3600 | |
| Microcellulose | | | 0 | 120.62 | | | [28] |
| | | | 10 | 188.287 | | | |
| | | | 30 | 148.08 | | | |
| | | | 50 | 108.85 | | | |
| Carboxymethyl cellulose | | ASTM D882-02 Cross-head speed: 5 mm/min T= 25 ℃ | 0 | 17.49 | 17.99 | 407.63 | [140] |
| | | | 0.5 | 15.09 | 7.58 | 468.63 | |
| | | | 1 | 7.91 | 5.74 | 446.23 | |
| | | | 1.5 | 6.32 | 5.17 | 428.39 | |

| Methyl cellulose | | Cross-head speed: 2 mm/s Load Cell: 5 kg | 12.5 | 15 | [160] |
|---|---|---|---|---|---|
| | Unmodified TiO2: 1.25 wt.% | | 12.5 | 16 | |
| | Unmodified TiO2: 2.5 wt.% | | 12.5 | 18 | |
| | Modified TiO2: 1.25 wt.% | | 12.5 | 20 | |
| | Modified TiO2: 2.5 wt.% | | 12.5 | 23 | |

According to the examples of Table 6, with the optimal MFC content, TS and YM of chitosan-based films improve in 80 and 70% of the examples, respectively. While the EB has a double tendency since it increases in 50% of the examples and decreases in the others. To have a better idea about the mechanical performance tendency of the composites, with the information in Table 6 the following figures were constructed in the same way as in the previous sections (see section 4.1), with the difference that the selected samples were those that were tested at a cross-head speed between 1-15 mm/min.
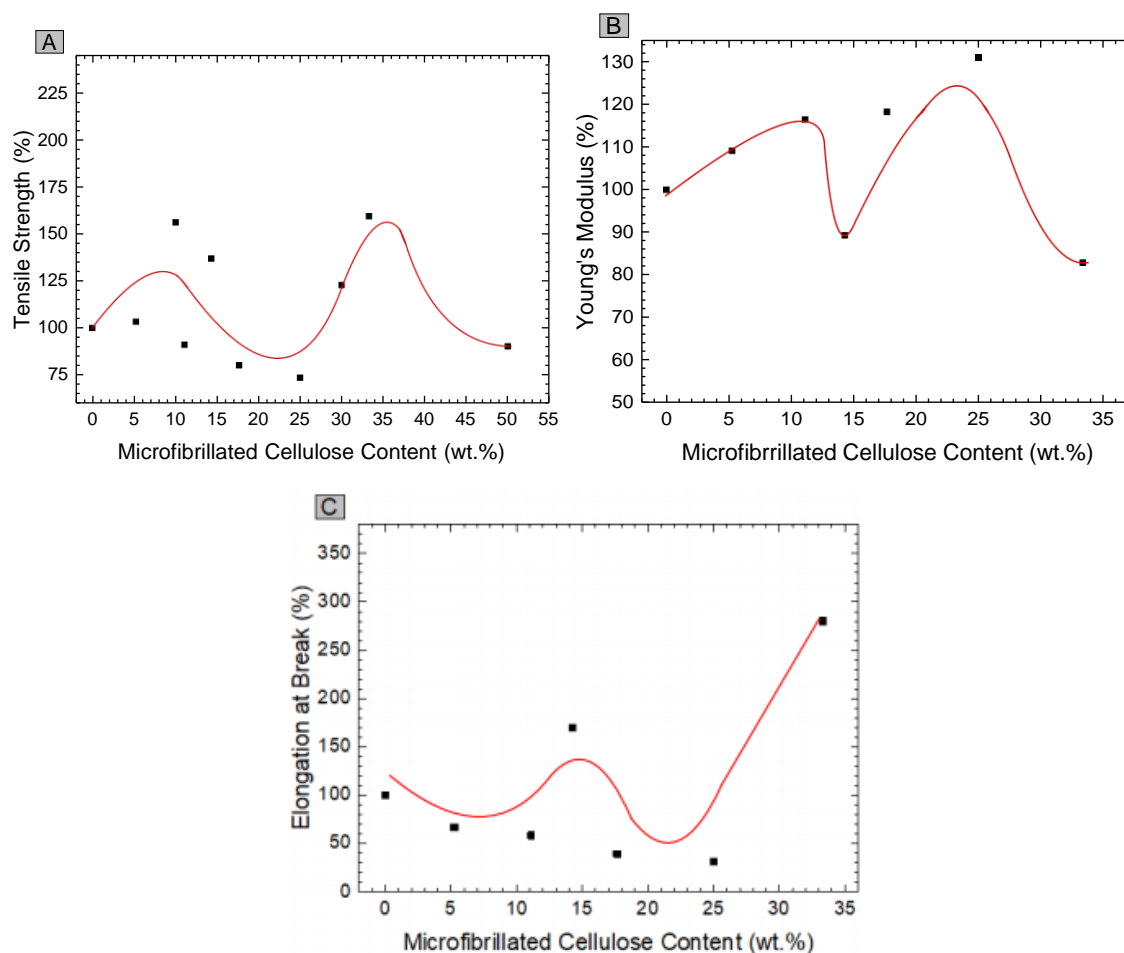


Figure 32. A) Tensile Strength, B) Young's Modulus, C) Elongation at Break of chitosan-based films varying the MFC content

As shown in Figure 32A, the TS values of the chitosan-based films with 10MFC and 33.33MFC increase by 56.10 and 59.30%, respectively, relative to the pure chitosan films. Again, due to the slight difference between both, the composite with 10MFC would be considered better. Figure 32B shows that the best YM value is obtained when the loaded filler is 25 wt.% since it improves by 30.91%, relative to the pure chitosan film. Also,

moderate YM values can be obtained with 10CFM, increasing by 16.36%. As in the other sections, these two parameters reach their maximum values as the filler content increases, and then they fall. This cycle repeats several times.

Regarding the EB, Figure 32C shows that by adding 11MFC, the EB reduced by 57.33% relative to the pure chitosan films. With higher filler addition, the reduction could be more. In contrast to the other two properties, EB decreases, and then at specific points, it increases.

By comparing these figures about the mechanical performance of MFC/chitosan composite films with the Figures 12A, B, and C and Figures 25A, B, and C, it could be said that better results were obtained with the nanometric particles. Using CNCs or CNFs with lower filler amounts were obtained similar and even better TS and YM values. For EB, as this parameter decreased by using any of the three reinforcements, none is considered better, although the EB decreased less with MFC.

Zhang et al. [26] made films of chitosan mixed with cellulose by co-dissolving the polysaccharides simultaneously in an alkali/urea solvent. The TS of the composite films increased from 28.5 to 45.5 MPa when the filler content increased from 0 to 33.33 wt.% (based on chitosan weight). This behavior is probably because strong hydrogen bonds formed between the hydroxyl groups of cellulose and the hydroxyl and amino groups of chitosan [49]. About the EB, this improved from 1 to 2.8%, and YM decreased from 4700 to 3900 MPa. These last two properties, as described before, are related to the rigid nature of the filler so that in cases where the chitosan chain is stronger than that of cellulose in stiffness, the YM deteriorates [23].

On the other hand, Wong et al. [124] prepared chitosan films using unbleached and bleached cellulose fibers. They observed that after forming chitosan films with 5.26 wt.% of unbleached or bleached cellulose, the TS reduced or increased by 16.67% or 3.33%, respectively, concerning that of the pure chitosan film (Figure 33A). For unbleached fibers, the TS decreased because the fibers were in irregular shape (filler agglomerations) with a low aspect ratio. These agglomerations acted as stress concentrators, and with the low aspect ratio, stress transfer from matrix to filler and matrix-filler adhesion were weak. Using the bleached fibers, the authors corroborated through a quantitative model that the interfacial interaction between filler and matrix was better than using untreated fibers; thus, the TS increased.

Regarding EB, it decreased for both cases [124]. With 25 wt.% of unbleached or bleached fibers, the EB decreased by 59.19% or 69.16%, respectively, concerning the pure chitosan film (Figure 33B). This decreasing EB was due to the stiffness of the filler, reducing the ductility of the chitosan-based film. Also, the addition of cellulose prevents the movement of each molecule in the composite, which affects the flexibility negatively [28]. The composites with the treated fibers had lower EB due to better adhesion between both polymers, which increases the rigidity of the composites. About the YM, with 25 wt.% of unbleached or bleached cellulose, this increased by 19.09% or 30%, respectively (Figure 33C). Again, the reason for this was the high stiffness of the filler [23]. Furthermore, the higher YM increase when bleached cellulose was used is due to the better interfacial adhesion, and the bleaching process increases the percentage of crystallinity of the fibers, resulting in higher strength and stiffness [19].
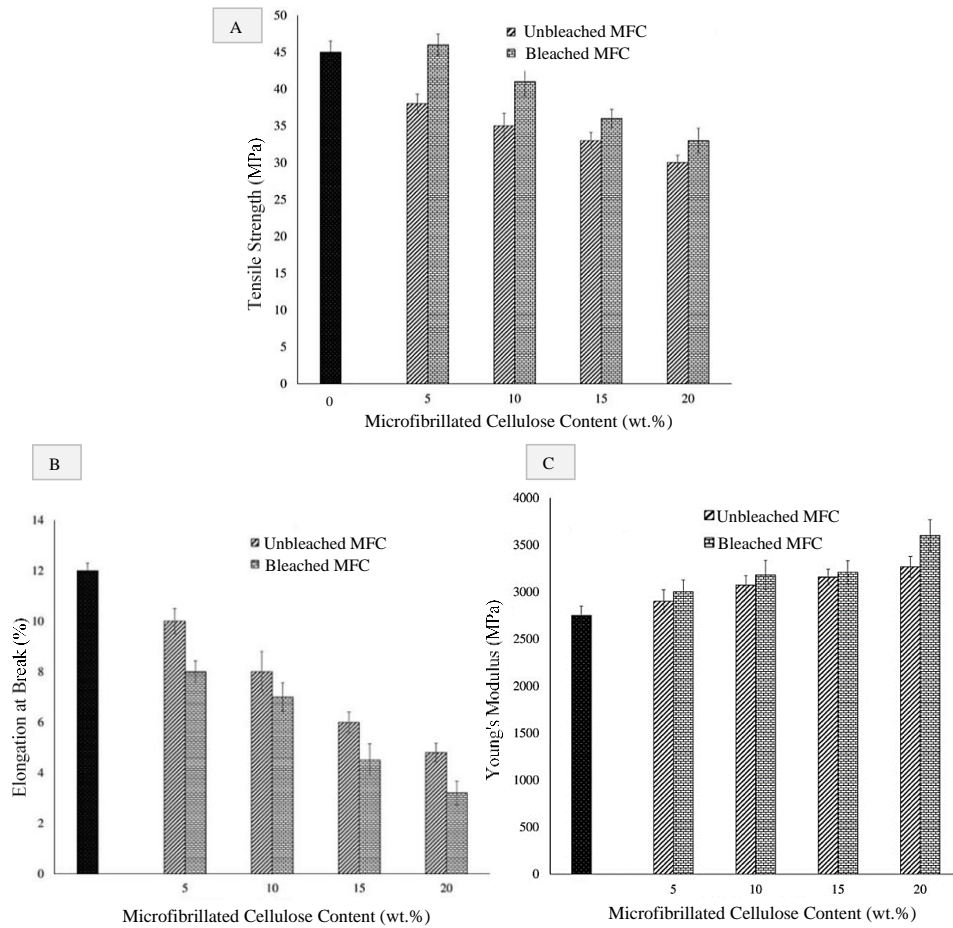


Figure 33. Mechanical properties of unbleached MFC/chitosan composite films and bleached MFC/chitosan composite films: A) tensile strength, B) elongation at break, and C) Young's modulus [124]

With the example shown, it is confirmed that the treatments applied to cellulose influence the final characteristics of the chitosan-based composite films. In this regard, MFC is also subjected to chemical modifications to improve its adhesion with the matrix and mechanical properties of composites [163]. Franco et al. [140] used carboxymethyl cellulose (0, 0.5, 1, and 1.5 wt.%; based on chitosan weight) to reinforce chitosan to evaluate the performance of the composite films obtained. Unexpectedly, they observed that TS and EB decreased by 63.89 and 71.96%, respectively, when the loaded filler was increased from 0 to 1.5 wt.%. While the YM increased by 14.96% when the added filler was increased from 0 to 0.5 wt.%, and the additional filler loading caused a decreasing effect (Figure 34). As can be seen, the addition of the modified MFC did not improve any mechanical parameters of the composite films; it even deteriorated them. According to the authors, TS decreased due to poor filler-matrix interactions, and strong filler-filler interactions. It is well known that the reinforcement effect of cellulose is attributed to the adhesion strength between both polymers since in its absence, there is ineffective stress transfer resulting in low TS [164]. About EB, although there were no strong interactions between both polymers, the addition of the filler restricted the motion of the matrix by its high intrinsic stiffness and filler agglomerations [140].
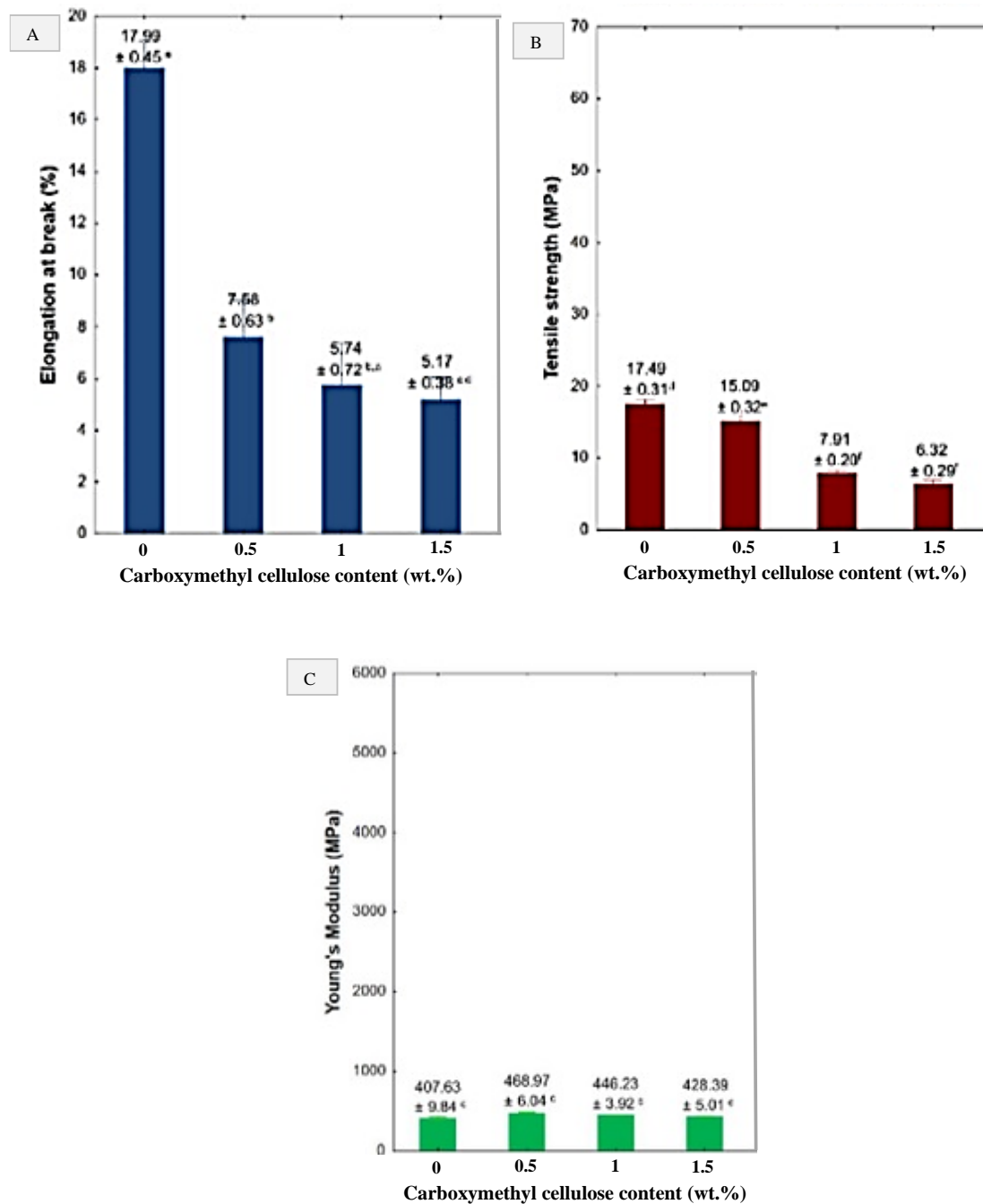
Figure 34. Mechanical properties of carboxymethyl cellulose/chitosan composite films: A) tensile strength, B) elongation at break and C) Young's modulus [140]

In summary, MFC can form good interactions with the chitosan matrix. However, it depends significantly on the process applied during its obtention. Furthermore, it is easy to form agglomerations at being incorporated in the chitosan matrix, especially when the filler is in exceed. Regarding the mechanical properties, it is necessary high amounts of loading filler to obtain moderate TS values or achieve the distribution of particles throughout the film matrix. Simultaneously, it would lead to the formation of

agglomerates since with more significant amounts of filler the agglomerations are easily formed. Also, YM increases in most cases as long as the rigidity of the cellulose chains is greater than that of chitosan. On the contrary, EB decreases significantly when the filler has a considerable stiffness that limits the movement of the polymer.

### 4.4. Microcrystalline Cellulose

Microcrystalline cellulose is a filler that results from the hydrolysis of the amorphous region of cellulose fibers [61]. MCC has a high degree of crystallinity, and the crystals have a regular stiffness which offers strength when incorporated into a polymer matrix [165]. The most common morphology of this filler is a rod-like shape [166], although it has also shown a spherical, cuboid [167], and irregular shape [168], [169] (Figure 35 and Tale 7); remembering that it depends on the processes applied during its isolation and production.
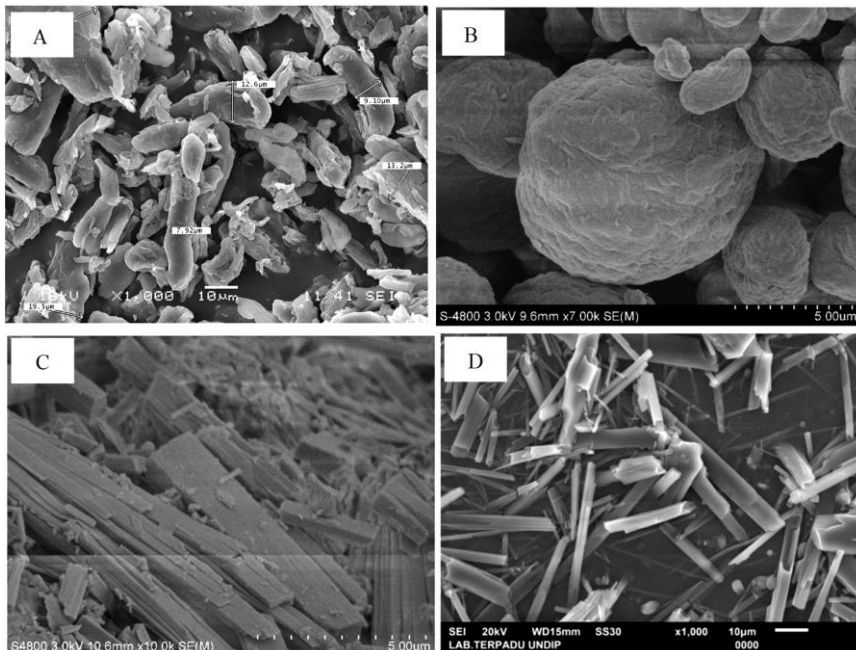


Figure 35. SEM micrographs of microcrystalline cellulose with A) irregular shape, B) spherical shape, C) cuboid shape, and D) rod shape

Table 7 shows different examples where MCC has been applied as a reinforcement of chitosan-based films. Also, it exhibits the dimensions, shape, and amount of the added filler.

Table 7. MCC incorporated in chitosan-based films

| Reinforcement | Other components | Cellulose shape | Cellulose size | Cellulose content (wt.%) | Reference |
|---|---|---|---|---|---|
| Microcrystalline cellulose | | Irregular | | 0, 10, 20 and 30 | [168] |
| Microcrystalline cellulose | Glycerol: 20 wt.% | | Particle size= 20-100 µm | 0, 1, 2, and 5 | [132] |
| Carrot fiber cellulose (cellulose 33.17% and lignin 4.68%) | Glycerol: 20 wt.% | Irregular | D= 108.6 µm | 0, 1, 2, and 5 | |
| Microcrystalline cellulose | Glycerol: 25, 27.5 and 30 wt.% | | | 0, 10 and 20 | [170] |
| Microcrystalline cellulose | Glycerol: 30 wt.% | Spheres | D= 2-10 µm | 0, 2, 4 and 6 | [167] |
| Urea-modified microcrystalline cellulose | | | Size= 50 um | 0, 1, 3, 5, 7, 9 and 11* | [171] |
| Cellulose microcrystals | Curcumin: 36 wt.% | | | 0, 10, 20 and 30 | [172] |
| Cellulose microcrystals | Curcumin: 0.0495, 0.054 and 0.0585 wt.% | | | 0, 10, 20 and 30 | [165] |

When MCC is incorporated into chitosan matrix films, it disperses well; even when the filler content increases moderately, interfacial interactions between filler and matrix become prominent. It is well known that the successful interactions between both polymers help in stress transfer resulting in promising composites [165]. However, as in the other sections, there is a point in which the addition of MCC causes adverse effects and appreciable agglomerations that are ineffective in terms of performance (see Figure 13) [132], [168].

Bajpai et al. [168] elaborated chitosan films loaded with MCC by vapor-induced phase inversion, making an aqueous suspension of MCC in chitosan and exposing it to ammonium vapor. The filler content of the composites was 10, 20, and 30 wt.% (based on chitosan weight), and the samples were observed by SEM and AFM. The surface and cross-sectional images provided by SEM (Figure 36) showed that the chitosan net film was almost smooth, while the composite with 20MCC was denser, and the particles were well distributed in the matrix. Also, it was very noticeable that the addition of the filler increased the roughness of the composites, and the shape of the crystals was irregular. Furthermore, the authors indicated that a closer look at the SEM images exhibited few agglomerations at some points within the matrix. However, these results using ammonium vapor were satisfactory since in other work carried out by themselves [168], the composites with 20MCC showed large agglomerations. The AFM images (Figure 36E and F) corroborated the SEM results; the good distribution of the filler in the matrix was observed again. This distribution confirms that the vapor-induced phase inversion technique prevented the formation of agglomerations.
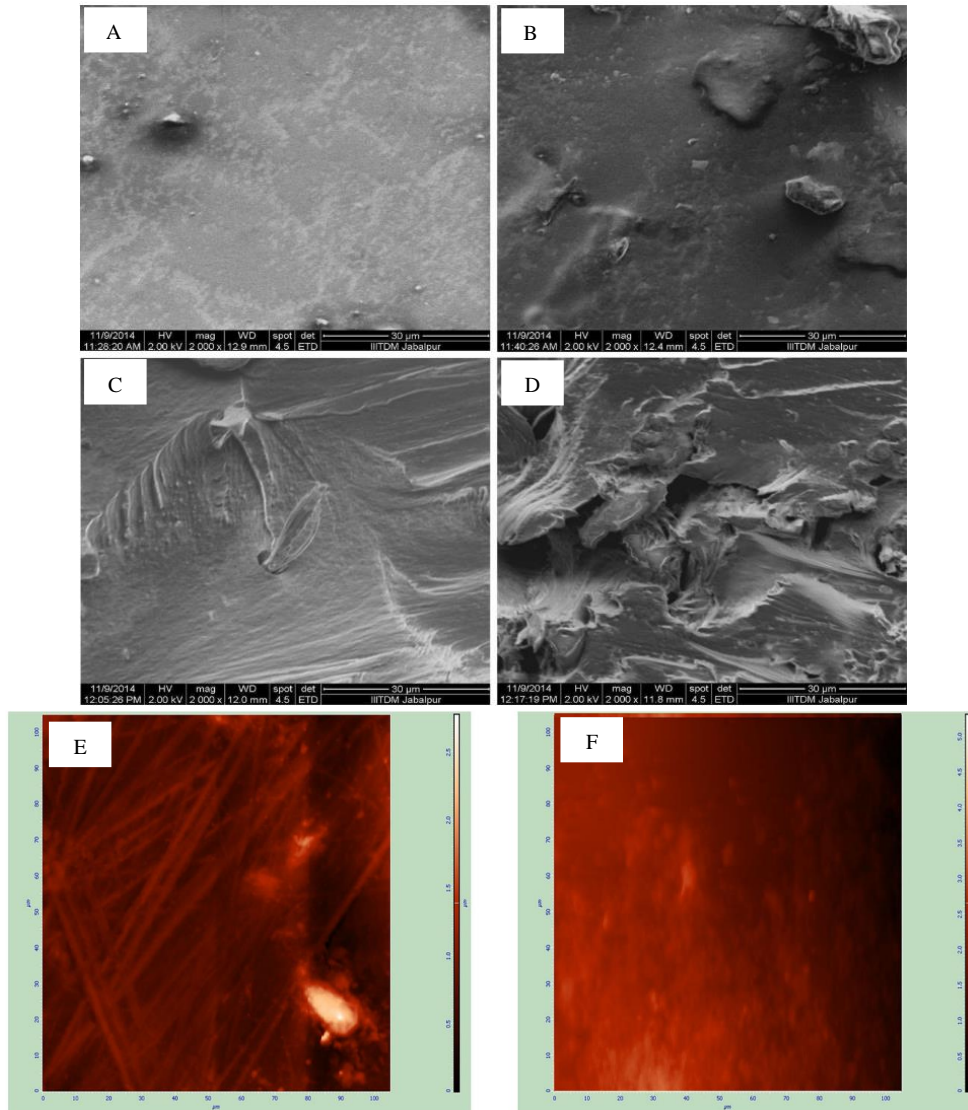
Figure 36. Surface and cross-sectional SEM images of (A, C) chitosan film, (B, D) 20MCC/chitosan film; AFM images of E) chitosan film, and F) 20MCC/chitosan film [168]

The chitosan-based composites reinforced with MCC have also been blended with plasticizers, being glycerol widely used [132], [170]. Coelho et al. [170] used glycerol as a plasticizer and applied moderate electric fields (MEF) or ultrasonic bath (UB) to the composite films. The filler content in the composites was 0, 10, and 20 wt.% (based on chitosan weight), while the glycerol content was 25, 27.5, and 30 wt.% (based on chitosan weight), respectively. The SEM results (Figure 37) showed that the pure chitosan film had a homogeneous surface, while the composites reinforced with cellulose exhibited a heterogeneous surface that increased with the addition of the filler. These results were obtained in the case of applying MEF or UB. As expected, the surface became rougher; however, no remarkable agglomerates were seen, and this is due to the applied techniques. UB is known as a successful tool for dispersing MCC within a film matrix [173]. While

MEF have improved some final properties of edible films [174]. Furthermore, as explained in section 4.1, glycerol also influenced the moderate dispersibility of the filler since plasticizers are capable of breaking intra and inter hydrogen bonds, which are sometimes the cause of cellulose crystal agglomerations [5], [140].
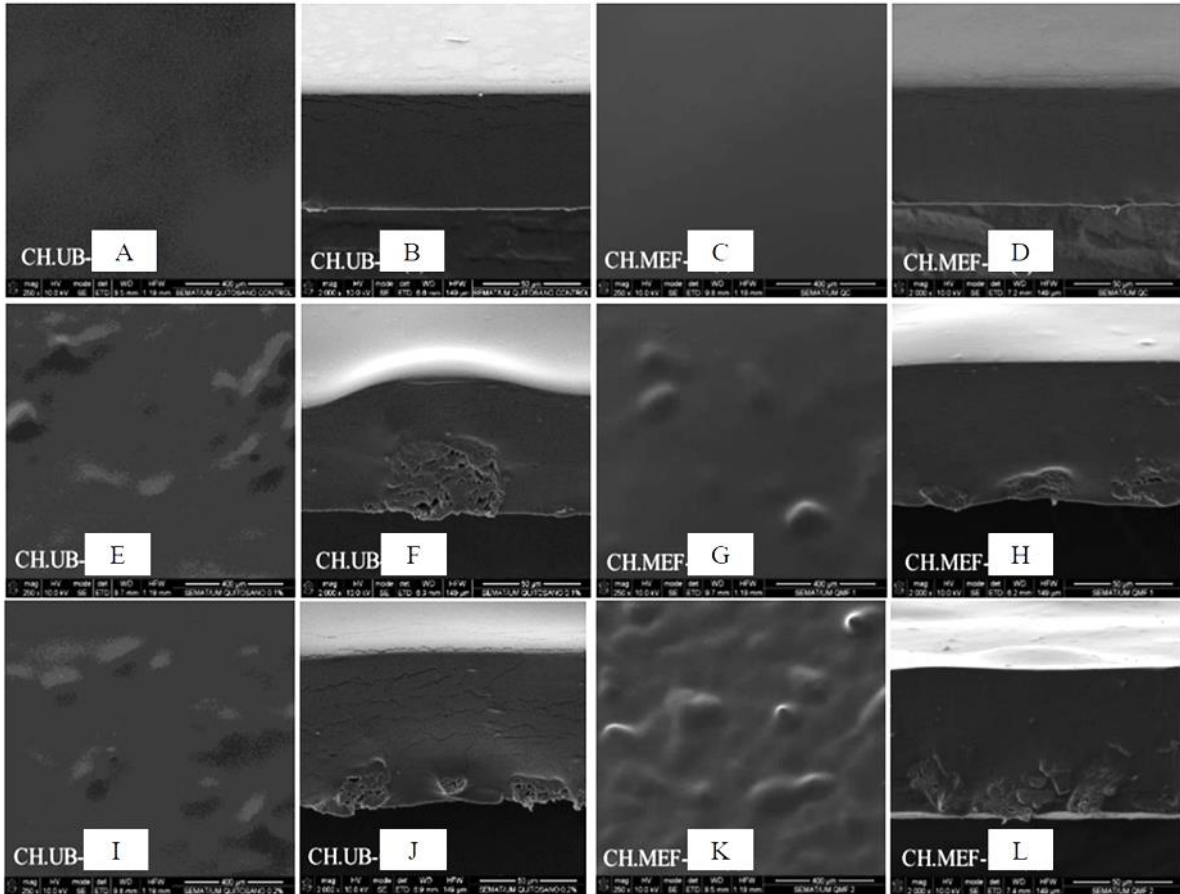


Figure 37. Surface and cross-sectional images of (A, B) chitosan film-UB, (C, D) chitosan film-MEF, (E, F) 10MCC/chitosan film-UB, (G, H) 10MCC/chitosan film-MEF, (I, J) 20MCC/chitosan film-UB, (K, L) 20MCC/chitosan film-MEF [170]

MCC has also undergone modifications. The large particle size of MCC has been found to sometimes disrupt its proper distribution in composite materials, limiting its reinforcing effect. Therefore, the fillers are modified, hoping to improve compatibility with the desired matrix [171]. The modified MCCs incorporated in chitosan-based films in the last years are dialdehyde-modified MCC [167] and urea-modified MCC [171].

When dialdehyde-modified MCC is used, this filler, as the dialdehyde CNFs, also acts as a cross-linker forming a covalent bond with chitosan. The aldehyde groups of the filler form Schiff base structures (C=N double bonds) with the amino groups of the chitosan, resulting in composites with good final properties [15], [167]. A study carried out by Ma

et al. [167] prepared chitosan composite films reinforced with dialdehyde-modified MCC (0, 2, 4 and 6 wt.%, based on chitosan weight) and plasticized with glycerol (30 wt.%, based on chitosan weight). The MCC was treated with citric acid to maintain its spherical shape and, the oxidation was carried out with sodium periodate. Figure 38A presents the SEM image of the chitosan composite with 6MCC, while Figures 38B and C show the composite films with 6-dialdehyde MCC for an oxidation reaction time of 1 and 3 hours, respectively. The composites with modified MCC showed uniform dispersion of the particles. Also, the filler was well embedded in the matrix and did not form significant agglomerations. According to the authors, the aldehyde samples had better distribution in the chitosan matrix than the MCC due to the Schiff base structure formation, which improved the interaction between both polymers.
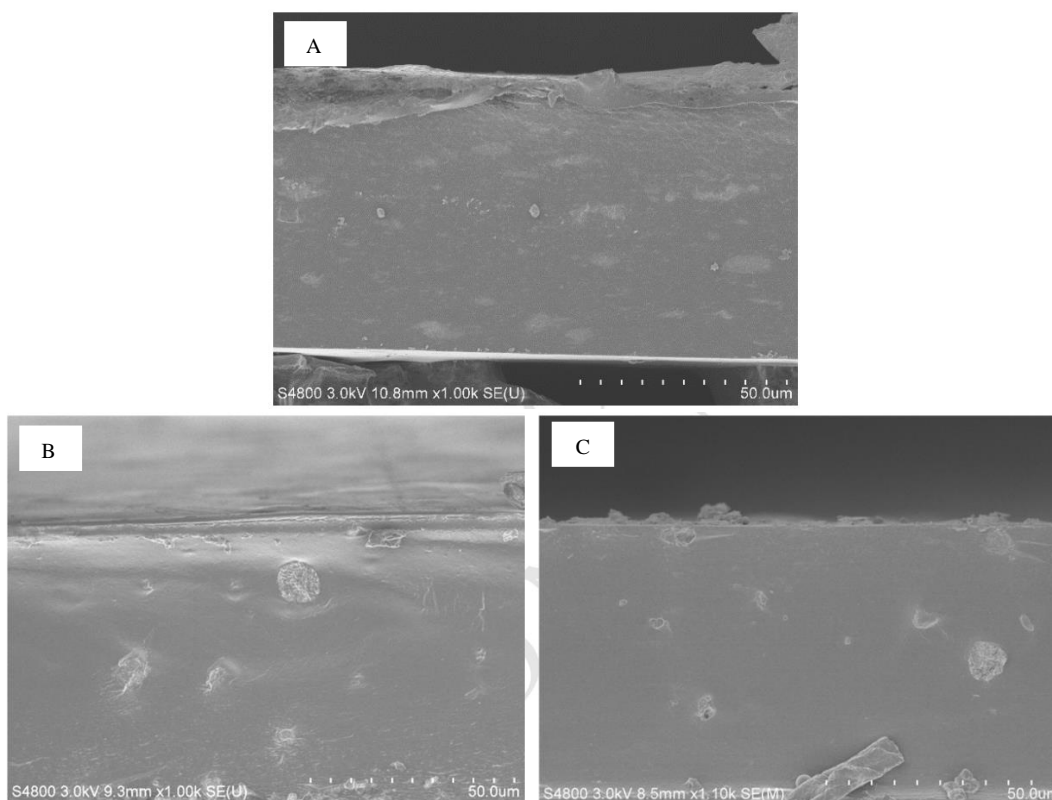


Figure 38. SEM micrographs of A) 6MCC/chitosan, (B) 6-dialdehyde MCC (1h)/chitosan film, and (C) 6-dialdehyde MCC (3h)/chitosan film [167]

In another study, urea-modified MCC was used as the filler of chitosan films [171]. The SEM results (Figure 39) of the composite films showed the surface morphologies with gray particles in the matrix which were attributed to the presence of the filler. When the filler content was less than 7 wt.%, the grey particles were more or less distributed through the film. As the addition of the filler increased, the gray particles were bigger. Thus, the

composite with 11 wt.% showed more agglomerations, which would lead to macroscopic phase separation if the amount of filler continues to increase. As observed in this example, the tendency was to form agglomerates, especially when the filler was excessive. The overload of the filler would lead to more contact between filler-filler and less contact between polymer chains and the filler. This fact deteriorates the reinforcement effect, which would result in composite films less strength than that of the pure polymer [175]
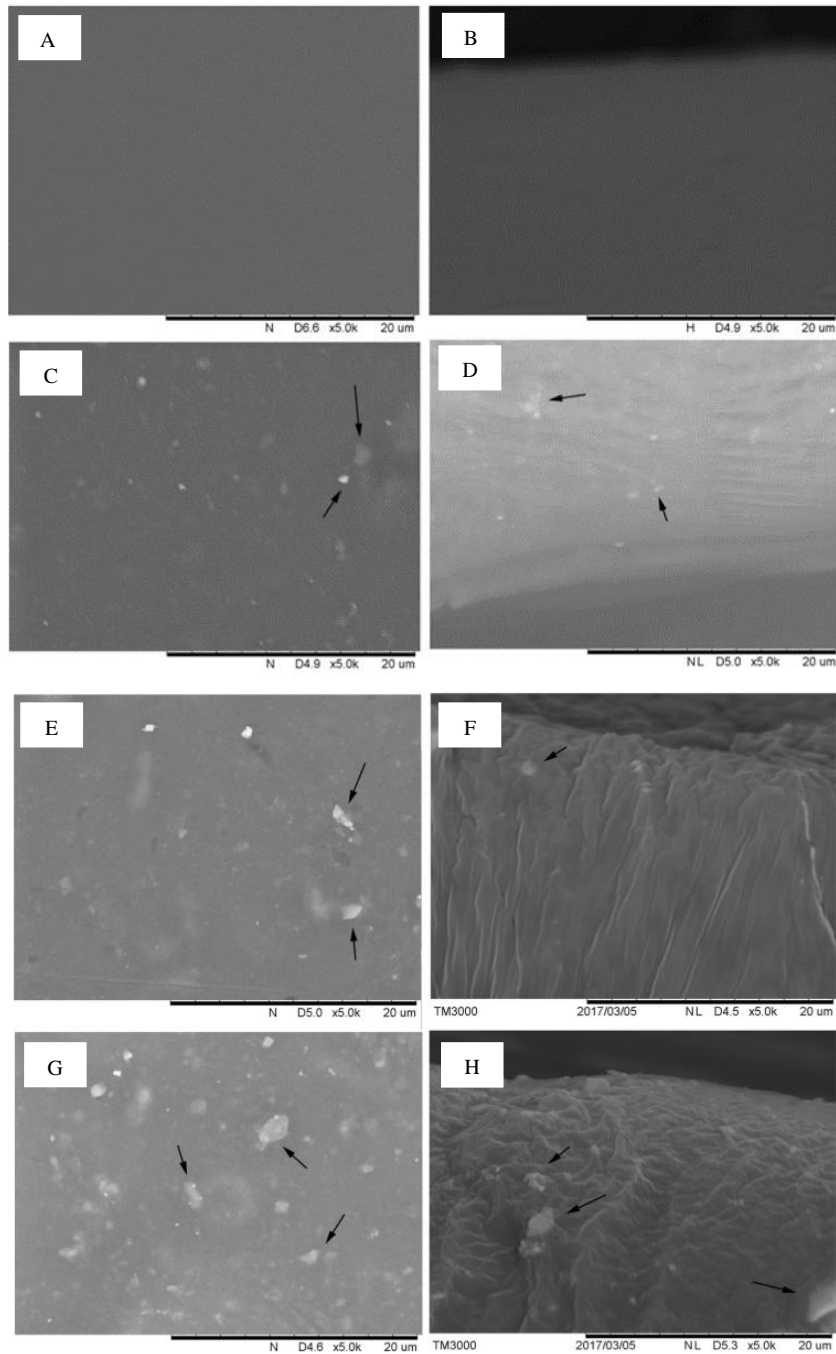


Figure 39. SEM micrographs of the surfaces and cross-sections of (A, B) chitosan film, (C, D) 3-urea MCC/chitosan film, (E, F) 7-urea MCC/chitosan film, and (G, H) 11-urea MCC/chitosan film [171].

On the other hand, the composite film activity has also been influenced by the addition of active agents like curcumin [165], [172]. This agent is characterized by its wound healing, antibacterial, antioxidant, anti-inflammatory, and anticancer activity [176]. A research made by Bajpai et al. [165] studied the release of curcumin from chitosan films reinforced with MCC. The amount of MCC was 0, 10, 20, and 30 wt.% (based on chitosan weight) for the composite films, while the curcumin addition was constant with a value of 450 per gram of film. The SEM results showed by the authors are about the composites with 20MCC, and with and without the active agent. The surface morphology of the composite without the active agent (Figure 40A and C), exhibited a quite roughness due to the presence of the filler. In general terms, the MCCs were well distributed throughout the film matrix although the surface exhibited few spots with small agglomerations. For the case of the composite loaded with curcumin the surface was smother (Figure 40B and D). It was indicated that the active agent appeared to have overlapped the cellulose crystals, and the presence of particles was less noticeable. It appeared that a layer had formed on the crystals with the addition of curcumin. With these results it was clear that the addition of the active agent did not affect the adhesion of the composite nor compatibility between the components. It has been shown that for these types of cases the composite serves as the carrier of the active agent and that cellulose is responsible for slowing the release rate [172].
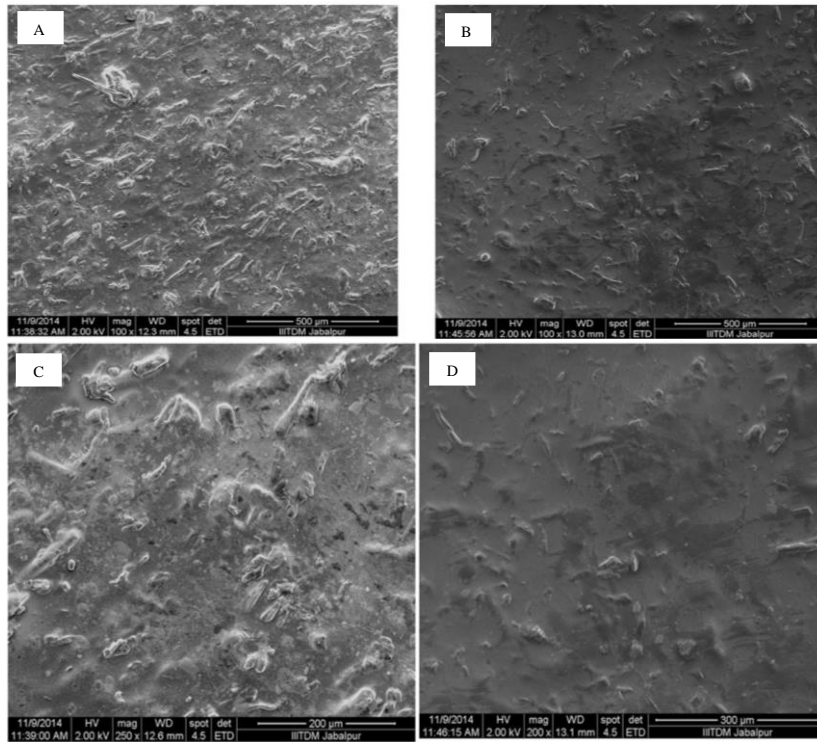
Figure 40. Surface morphology at 100x and 200x magnifications of (A-C) 20MCC/chitosan film, and (B-D) 20MCC/chitosan film with curcumin [165]

Regarding the mechanical properties, Table 8 shows the compilation of the studies published the last five years.

Table 8. Mechanical properties of chitosan composite films reinforced with MCC

| Reinforcement | Other components | Information | Cellulose content (wt.%) | Tensile strength (MPa) | Elongation at Break (%) | Young`s Modulus (MPa) | Reference |
|---|---|---|---|---|---|---|---|
| Microcrystalline cellulose | Glycerol: 20 wt.% | ASTM D882 Cross-head speed: 50 mm/min | 0 | 10.86 | 18.23 | 624.3 | [132] |
| | | | 1 | 14.46 | 17.51 | 1108.3 | |
| | | | 2 | 14.59 | 16.12 | 1127.8 | |
| | | | 5 | 10.72 | 18.01 | 690.3 | |
| Carrot fiber cellulose (cellulose 33.17% and lignin 4.68%) | Glycerol: 20 wt.% | | 1 | 11.44 | 15.73 | 816.2 | |
| | | | 2 | 12.98 | 15.57 | 947 | |
| | | | 5 | 16.91 | 14.54 | 1057.2 | |
| Microcrystalline cellulose | Glycerol: 25 wt.% Glycerol: 27.5 wt.% Glycerol: 30 wt.% | Ultrasonic Bath Treatment ASTM D882-02 (2010) Cross-head speed: 5 mm/min Load cell: 5 kg | 0 | 3.5 | 108.21 | 0.02 | [170] |
| | | | 10 | 4.4 | 112.55 | 0.04 | |
| | | | 20 | 4.95 | 64.4 | 0.09 | |
| | Glycerol: 25 wt.% Glycerol: 27.5 wt.% Glycerol: 30 wt.% | Moderate Electric Fields Treatment ASTM D 882-02 (2010) Cross-head speed: 5 mm/min Load cell: 5 kg | 0 | 7.36 | 106.78 | 0.05 | |
| | | | 10 | 5.55 | 63.94 | 0.08 | |
| | | | 20 | 6.77 | 72.19 | 0.1 | |
| Citric acid modified cellulose spheres | Glycerol: 30 wt.% | Cross-head speed: 50 mm/min | 0 | 26.8 | 50.9 | | [167] |
| | | | 2 | ~44 | ~45 | | |
| | | | 4 | ~55 | ~43 | | |
| | | | 6 | 58.2 | 41.8 | | |
| Dialdehyde citric acid modified cellulose spheres | Glycerol: 30 wt.% | Reaction time with sodium periodate: 1 h Cross-head speed: 50 mm/min | 2 | ~47 | ~39 | | |
| | | | 4 | ~58 | ~30 | | |
| | | | 6 | 62.7 | ~23 | | |

| | | | | | | | |
|---|---|---|---|---|---|---|---|
| Dialdehyde citric acid modified cellulose spheres | Glycerol: 30 wt.% | Time reaction with sodium periodate: 3 h<br>Cross-head speed: 50 mm/min | 2 | ~62 | ~30 | | |
| | | | 4 | ~72 | ~20 | | |
| | | | 6 | 75.9 | ~15 | | |
| Dialdehyde modified cellulose spheres | Glycerol: 30 wt.% | | 2 | ~51 | ~36 | | |
| | | | 4 | ~64 | ~25 | | |
| | | | 6 | 68.8 | ~17.5 | | |
| Urea-modified microcrystalline cellulose | | Cross-head speed: 3 mm/min | 0* | 29.9 | 5.32 | 9.68 | [171] |
| | | | 1* | 34.6 | 5.72 | 11.8 | |
| | | | 3* | 34.6 | 7.86 | 8.07 | |
| | | | 5* | 46.8 | 9.3 | 13.4 | |
| | | | 7* | 59.1 | 11.5 | 23.4 | |
| | | | 9* | 30.5 | 10.5 | 15.8 | |
| | | | 11* | 30.2 | 11 | 8.88 | |
| Cellulose microcrystals | Curcumin: 0.045 wt.% | Cross-head speed: 200 mm/min | 0 | 5.78 | ~29 | | [165] |
| | Curcumin: 0.0495 wt.% | | 10 | ~8.2 | ~20 | | |
| | Curcumin: 0.054 wt.% | | 20 | 13.8 | ~15 | | |
| | Curcumin: 0.0585 wt.% | | 30 | 8.1 | ~5 | | |

According to Table 8, it can be said that the general tendency is for TS and YM to increase and EB to decrease due to the addition of MCC in the chitosan matrix. TS and YM reach their maximum value and then decrease if the filler addition continues [132]. Before reaching the threshold point concentration, the addition of MCC promotes the interfacial interaction between the cellulose and chitosan chains. After the threshold point, filler-filler interactions become prominent, leading to agglomerations and changes in the tendency of the mechanical results [132], [133].
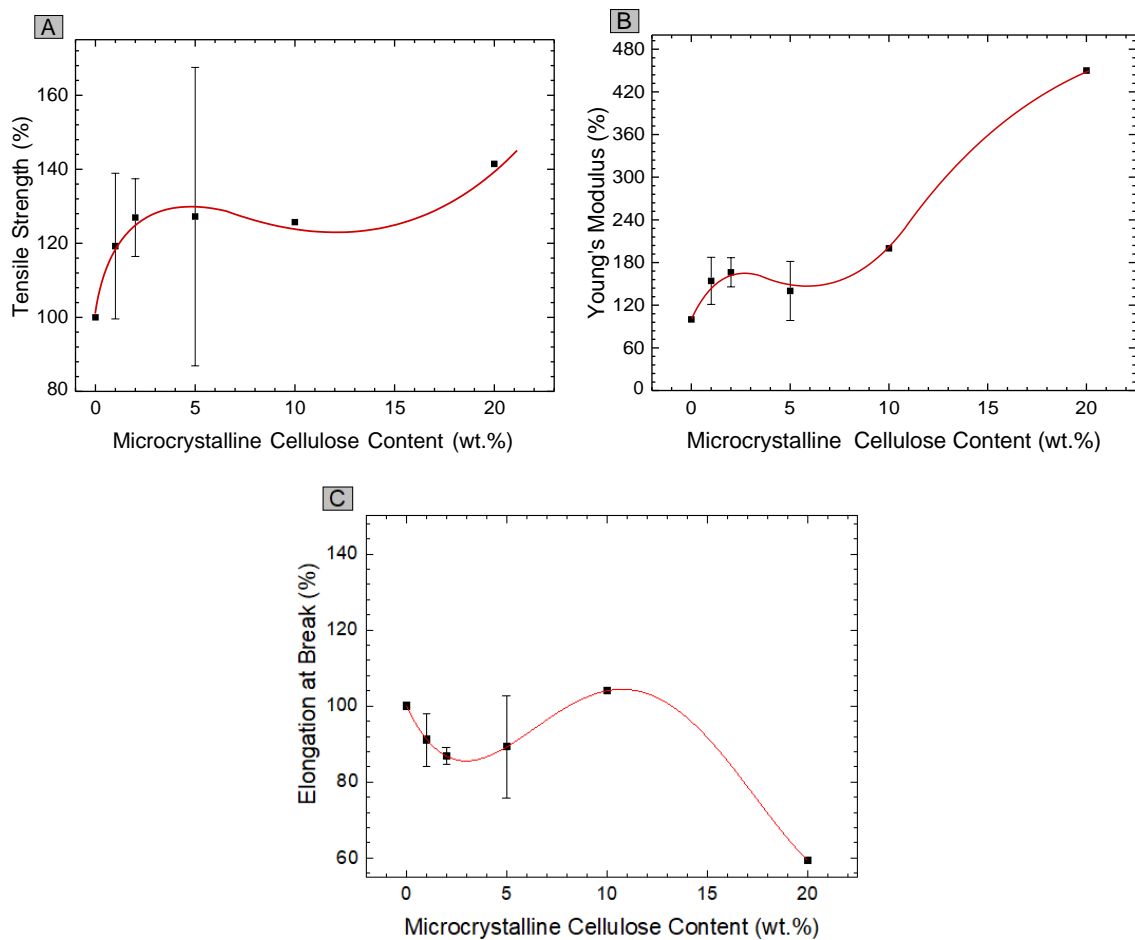


Figure 41. A) Tensile Strength, B) Young's Modulus, C) Elongation at Break of chitosan-based films varying the MCC content

With the information of Table 8, it was built Figures 41A, B, and C that correspond to the mechanical performance of chitosan-based films reinforced with MCC (see section 4.1). Due to the available information, the selected samples were those that were tested at a cross-head speed between 1-50 mm/min and plasticized with glycerol. Figure 41A shows that the best value is obtained with 20MCC since the TS increases by 41.43% relative to

the pure chitosan films. However, it also shows that with lower filler amounts, moderate TS values can be reached. For example, with 2MCC the TS improves by 26.93%, and with 5MCC the TS increases by 27.21% and may even improve by up to 68%. Figure 41B exhibits that with 2MCC the YM enhances by 66.17%, in relation to the pure chitosan films. With 10MCC or 20MCC higher values are obtained, although it implies more filler amounts. Regarding the EB, the Figure 41C shows that with 5MCC this parameter decreases by 10.72%, relative to the pure chitosan films. With higher amounts (20MCC) the decrease can be higher too.

When comparing these figures with those presented in the previous sections (Figures 12, 25, and 32), the idea described in the last section is maintained since the highest values in terms of strength and stiffness were reach with the nanometric fillers. Suitable values of TS were obtained with 3CNCs, 1.5CNF, 10MFC or 5MCC, while for YM values were with 4CNCs, 1.5CNFs, 25MFC or 2MCC. About the EB, as expected, the composites reinforced with the fillers that showed the best YM and TS values were those that obtained the worst EB values. Therefore, the microparticles reduced the EB of the chitosan composites to a lesser extent. Also, the filler concentration in which the elongation at break of the composites was very low is the same as the tensile strength and Young's modulus increased considerably.

Sogut et al. [132] elaborated chitosan films reinforced with MCC (0, 1, 2, and 5 wt.%; based on chitosan weight) and plasticized with glycerol (20 wt.%; based on chitosan weight). The mechanical results exhibited increased TS and YM by 34.35 and 80.65%, respectively, and decreased EB by 11.57%, when the filler addition varied from 0 to 2 wt.%. The additional filler loading (5 wt.%) caused a decrease in TS and YM, and increased EB. As described in previous sections, the increase in TS and YM resulted from good interfacial adhesion between both polymers, while the adverse effects at 5 wt.% were because the filler formed agglomerates [110], [167]. Regarding the EB, according to the authors, the strong interactions between the filler and the matrix restricted the mobility of the polymer chains, in addition to which it could also be attributed to the regular stiffness of the crystal [165]. In the same study, the mechanical properties of chitosan composite films were evaluated using carrot fibers (33.17% cellulose and 4.68% lignin) as reinforcement instead of MCC [132]. The tendency results were similar to those obtained with the MCC, although the mechanical parameters changed in different proportions with the addition of the filler. Incorporating 2 wt.% carrot fibers, TS and YM

increased by 19.52 and 51.69%, respectively, and EB decreased by 14.59%. TS and YM improvements were less than when MCC was used. Although better mechanical parameters were obtained with 5 wt.% carrot fibers, they were still worse than those obtained with MCC (2 wt.%), except for the TS, which with 5 wt.% carrot fibers increased by 55.71%, relative to the pure chitosan film.

In the example described recently, the tendency proposed at the beginning of the section is observed since TS and YM increased while EB decreased with the filler addition. However, sometimes this tendency changes, especially when using specific treatments or modifications to cellulose. Coelho et al. [170] applied moderate electric fields to chitosan-based composites reinforced with MCC, and unexpectedly, the TS decreased by 8.02% when the loaded filler increased from 0 to 20 wt.%. In another study, Huang et al. [171] reported that after forming chitosan-based composite films reinforced with 7 wt.% urea modified MCC, the TS, EB, and YM values increased to 59.1 MPa, 11.5%, and 23.4 MPa, respectively, corresponding to an improvement of 97.66, 116.16 and 141.74%, respectively, when the loaded filler varied from 0 to 7 wt.%. With a filler content of 7 wt.%, the composites had the best results since higher amounts of filler negatively affected the tested properties. The good results in this example are due to favorable interactions between the surface-modified MCC and chitosan. The FTIR results indicated the formation of new hydrogen bonds, which would correspond to the interaction between -$CONH_2$ groups of the surface-modified filler and the surrounding chitosan chains [177], [178]. Furthermore, the morphological results showed a good dispersion of the microparticles in the matrix. Therefore, the absence of agglomerations and good filler-matrix interactions made the composite ideal for effective stress transfer [140].

On the other hand, in Table 8, curcumin as an active agent in chitosan films reinforced with cellulose does not change the proposed tendency for mechanical properties. Bajpai et al. [165] reported that TS increased from 5.78 to 13.8 MPa, and EB decreased from 29 to 15%, when the filler content varied from 0 to 20 wt.% (Figure 42). With the information provided by the authors, it was not possible to know if the initial mechanical properties of chitosan were affected by the addition of curcumin. However, these agents are usually applied in proportions that do not negatively affect the integrity of the film [130].
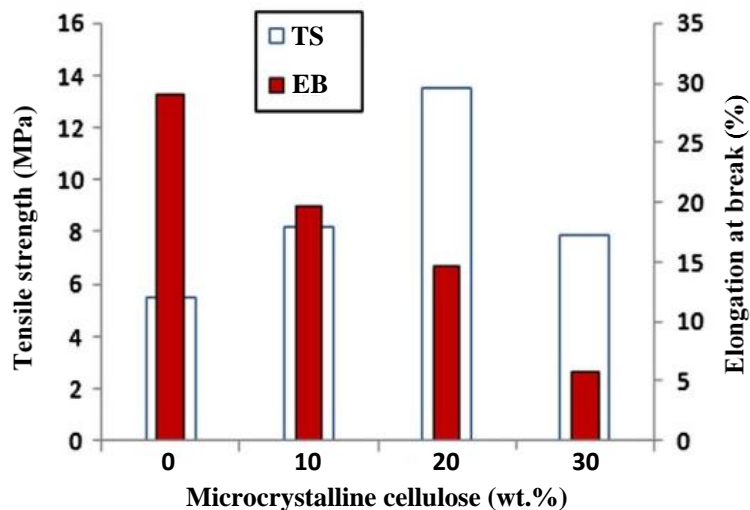
Figure 42. Mechanical properties of MCC/chitosan composite films loaded with curcumin [165]

In summary, the addition of MCC into chitosan films has resulted in composites with a compact adhesion. The tendency for all cases has been a good dispersion of the filler throughout the chitosan matrix as the filler amount is lower than the threshold point. However, the degree of filler dispersion depends on many variables like size, shape, degree of crystallinity and purity [124], [132], [167], treatments applied, and many others. Many possible methods were reviewed for improving the distribution of the microcrystalline particles like vapor induced phase inversion [168], [172], moderate electric fields, ultrasonic bath [148], [170], bleaching treatments [124], and modifications of cellulose [167], [171]. The same methods were used to improve the mechanical properties of the composites, and, in most cases, the mechanical performance tendency was maintained for TS and YM to increase, whereas EB tends to decrease due to the inclusion of the MCC.

On the other hand, the reason why better results regarding the TS and YM, were obtained with the nanometric fillers is due to their size. "For smaller particles with higher total surface area, the mechanism of stress transfer is more efficient" [110]. The use of nanoparticles, instead of microparticles, increases the amount of hydrogen bonds between the filler and the matrix, interactions that play an important role in the stress transfer [132]. In addition, with low amounts of filler, the nanoparticles are well distributed throughout the matrix, allowing the reinforcing effect of the filler to occur earlier while preventing agglomerations [1], [140]. Regarding the EB, the highest decreasing effect when using nanoparticles is because they can form stronger filler-matrix interactions as

an effect of their high aspect ratio, obtaining more compact composites with less movement capacity [140].

It could be said that the effects of cellulose, at being incorporated into chitosan-based films, are to increase the stiffness and strength, and reduce the flexibility of the composites. However, to say which reinforcement is better, depends on the final application of the composite film. For example, in the case of using the film for structural applications, where the poor elongation will not be classified as a failure, CNFs/chitosan composite films become promising materials since the TS and YM can be improved by 223.56% and 1220.83%, respectively, with 1.5CNFS in the chitosan films [140]. In the case of using the film for food packaging purposes where moderate mechanical strength and flexibility are required to withstand external stresses and maintain its integrity, CNCs/chitosan composites films could be the best choice, as the flexibility of the films is not significantly reduced by incorporating the filler, and the TS is increased [1], [179].

Therefore, if the goal is to prepare chitosan-based composite films for applications where the required mechanical strength and stiffness are high and flexibility does not play an important role, the best fillers may be the CNFs.

## CHAPTER V:

## Conclusion

### 5.1. Conclusion

In this review the surface morphology and mechanical performance of chitosan-based composite films reinforced with cellulose were analyzed. It was shown that by incorporating MFC, MCC, CNFs, or CNCs in chitosan-based films, the particles were well dispersed throughout all the matrix. However, the degree of dispersion highly depended on the interactions between both polymers, the size of the particles, and the loaded filler. Hydrogen bonds and electrostatic interactions governed the matrix-filler interactions. Also, the nanometric fillers showed better distribution than the micrometric since the first ones have a high aspect ratio, promoting their good interfacial adhesion with the matrix. Regarding the amount of filler, at high filler concentrations, the filler-filler interactions became prominent, forming agglomeration on the surface composites, while the filler-matrix interactions became poor.

About the mechanical performance of the composite films, the tendency was the same for all the fillers reviewed (MFC, MCC, CNFs, or CNCs). The TS and YM increased, while the EB decreased. The mechanical performance mainly depended on the interactions between both polymers and consequently the degree of distributions of the fillers. The formation of agglomerates acted as stress concentrators, causing adverse effects and changing the tendency results. Furthermore, the performance of the composites was highly influenced by the inherent characteristics of the components. These characteristics, like flexibility, rigidity, and stiffness of the polymers depended on the source, isolation, and preparation method.

The highest values of the mechanical properties, considering that in all cases, cellulose improved the strength and stiffness, and reduced the flexibility of the chitosan-based films, were obtained with the CNFs. By incorporating only 1.5 wt.% of these nanofibers

in the matrix, the TS and YM improved by 224 and 1221%, respectively, while the EB was reduced by 91%. These results do not imply that CNFs are the best filler for chitosan. Determining the best filler would require establishing the final application for the film. A film that requires a high flexibility could be obtained using 2MCC given that the TS and YM are enhanced by 27 and 66%, respectively, while the EB is reduced by 13%. While a film that requires higher levels of mechanical strength would benefit of using 3CNCs as a filler, given a resulting TS and YM increase of 51 and 40%, respectively, while a EB decrease of 28%. Or 10MFC, that offers a TS and YM improvement of 56 and 16%, respectively, while a EB reduction of 58%. It is important to keep present that these values are relative to the pure chitosan films and were chosen because at that filler concentration the mechanical strength figures reached the first maximum value.

Furthermore, the further incorporation of other components or additives would solve or balance the mechanical results. By adding plasticizers, the composites will have better flexibility; in the case of using cross-linking agents, the strength is improved by forming a more compact matrix; and in the case of modifying the filler, new favorable interactions would be developed between the filler and the matrix, resulting in interesting mechanical properties.

# References

[1]    M. Yadav, K. Behera, Y. Chang, and F. Chiu, "Cellulose Nanocrystal Reinforced Chitosan Based UV Barrier Composite Films for Sustainable Packaging," 2020, [Online]. Available: apa: Yadav, M., Behera, K., Chang, Y.-H., & Chiu, F.-C. (2020). Cellulose Nanocrystal Reinforced Chitosan Based UV Barrier Composite Films for Sustainable Packaging. Polymers, 12(1), 202. doi: 10.3390/polym12010202.

[2]    M. Mujtaba, R. E. Morsi, G. Kerch, and Z. Maher, "Current advancements in chitosan-based film production for food technology," *Int. J. Biol. Macromol.*, p. #pagerange#, 2018, doi: 10.1016/j.ijbiomac.2018.10.109.

[3]    P. G. Gan, S. T. Sam, M. F. Abdullah, M. F. Omar, and W. K. Tan, "Comparative study on the properties of cross-linked cellulose nanocrystals/chitosan film composites with conventional heating and microwave curing," *J. Appl. Polym. Sci.*, vol. 137, no. 48, pp. 1–14, 2020, doi: 10.1002/app.49578.

[4]    J. Yang, G. J. Kwon, K. Hwang, and D. Y. Kim, "Cellulose-chitosan antibacterial composite films prepared from LiBr solution," *Polymers (Basel).*, vol. 10, no. 10, pp. 1–7, 2018, doi: 10.3390/polym10101058.

[5]    P. Falamarzpour, T. Behzad, and A. Zamani, "Preparation of nanocellulose reinforced chitosan films, cross-linked by adipic acid," *Int. J. Mol. Sci.*, vol. 18, no. 2, 2017, doi: 10.3390/ijms18020396.

[6]    E. Y. Wardhono *et al.*, "Cellulose nanocrystals to improve stability and functional properties of emulsified film based on chitosan nanoparticles and beeswax," *Nanomaterials*, vol. 9, no. 12, pp. 1–17, 2019, doi: 10.3390/nano9121707.

[7]    X. Liu, Y. Zhu, J. Ren, H. Xuan, J. Zhang, and L. Ge, "Multilayer Edible Fresh – keeping Films ' Characterization and Their Preservation Effect," pp. 3607–3611, 2016, doi: 10.1002/slct.201600694.

[8]    "SFly - PRODUCER OF CHITIN, CHITOSAN - BLACK SOLDIER FLY." http://sflyproteins.com/ (accessed Nov. 09, 2020).

[9]    S. Bonardd, E. Robles, I. Barandiaran, C. Saldías, Á. Leiva, and G. Kortaberria,

"Biocomposites with increased dielectric constant based on chitosan and nitrile-modified cellulose nanocrystals," *Carbohydr. Polym.*, vol. 199, pp. 20–30, 2018, doi: 10.1016/j.carbpol.2018.06.088.

[10] T. I. Nasution, M. Balyan, and I. Nainggolan, "Improved lifetime of chitosan film in converting water vapor to electrical power by adding carboxymethyl cellulose," *IOP Conf. Ser. Mater. Sci. Eng.*, vol. 309, no. 1, 2018, doi: 10.1088/1757-899X/309/1/012092.

[11] S. Chaudhary, S. Kumar, V. Kumar, and R. Sharma, "Chitosan nanoemulsions as advanced edible coatings for fruits and vegetables: Composition, fabrication and developments in last decade," *Int. J. Biol. Macromol.*, vol. 152, pp. 154–170, 2020, doi: 10.1016/j.ijbiomac.2020.02.276.

[12] G. Sarkar *et al.*, "Cellulose nanofibrils/chitosan based transdermal drug delivery vehicle for controlled release of ketorolac tromethamine," *New J. Chem.*, vol. 41, no. 24, pp. 15312–15319, 2017, doi: 10.1039/c7nj02539d.

[13] Y. Tang, X. Zhang, R. Zhao, D. Guo, and J. Zhang, "Preparation and properties of chitosan/guar gum/ nanocrystalline cellulose nanocomposite films," *Carbohydr. Polym.*, vol. 197, no. January, pp. 128–136, 2018, doi: 10.1016/j.carbpol.2018.05.073.

[14] P. Cazón and M. Vázquez, "Mechanical and barrier properties of chitosan combined with other components as food packaging film," *Environ. Chem. Lett.*, vol. 18, no. 2, pp. 257–267, 2020, doi: 10.1007/s10311-019-00936-3.

[15] X. Tian, D. Yan, Q. Lu, and X. Jiang, "Cationic surface modification of nanocrystalline cellulose as reinforcements for preparation of the chitosan-based nanocomposite films," *Cellulose*, vol. 24, no. 1, pp. 163–174, 2017, doi: 10.1007/s10570-016-1119-3.

[16] D. Hu, H. Wang, and L. Wang, "Physical properties and antibacterial activity of quaternized chitosan/carboxymethyl cellulose blend films," *LWT - Food Sci. Technol.*, vol. 65, pp. 398–405, 2016, doi: 10.1016/j.lwt.2015.08.033.

[17] S. B. Aziz, M. H. Hamsan, R. M. Abdullah, and M. F. Z. Kadir, "A promising polymer blend electrolytes based on chitosan: Methyl cellulose for EDLC application with high specific capacitance and energy density," *Molecules*, vol. 24,

no. 13, 2019, doi: 10.3390/molecules24132503.

[18] R. S. S. Zanette *et al.*, "Cotton cellulose nanofiber/chitosan nanocomposite: characterization and evaluation of cytocompatibility," *J. Biomater. Sci. Polym. Ed.*, vol. 30, no. 16, pp. 1489–1504, 2019, doi: 10.1080/09205063.2019.1646627.

[19] N. A. Rosli, I. Ahmad, and I. Abdullah, "Isolation and characterization of cellulose nanocrystals from agave angustifolia fibre," *BioResources*, vol. 8, no. 2, pp. 1893–1908, 2013, doi: 10.15376/biores.8.2.1893-1908.

[20] M. Bilal, K. Niazi, Z. Jahan, S. S. Berg, and Ø. W. Gregersen, "Mechanical , thermal and swelling properties of phosphorylated Nanocellulose fibrils / PVA nanocomposite membranes," *Carbohydr. Polym.*, 2017, doi: 10.1016/j.carbpol.2017.08.125.

[21] S. Khattak *et al.*, "Applications of cellulose and chitin/chitosan derivatives and composites as antibacterial materials: current state and perspectives," *Appl. Microbiol. Biotechnol.*, vol. 103, no. 5, pp. 1989–2006, 2019, doi: 10.1007/s00253-018-09602-0.

[22] L. Vecbiskena and L. Rozenberga, "Nanocelluloses obtained by ammonium persulfate (APS) oxidation of bleached kraft pulp (BKP) and bacterial cellulose (BC) and their application in biocomposite films together with chitosan," *Holzforschung*, vol. 71, no. 7–8, pp. 659–666, 2017, doi: 10.1515/hf-2016-0187.

[23] H. P. S. Abdul Khalil *et al.*, "A review on chitosan-cellulose blends and nanocellulose reinforced chitosan biocomposites: Properties and their applications," *Carbohydr. Polym.*, vol. 150, pp. 216–226, 2016, doi: 10.1016/j.carbpol.2016.05.028.

[24] Y. Wu, S. Yu, F. Mi, C. Wu, and S. Shyu, "Preparation and characterization on mechanical and antibacterial properties of chitsoan / cellulose blends," vol. 57, pp. 435–440, 2004, doi: 10.1016/j.carbpol.2004.05.013.

[25] T. B. Taketa *et al.*, "Tracking Sulfonated Polystyrene Diffusion in a Chitosan/Carboxymethyl Cellulose Layer-by-Layer Film: Exploring the Internal Architecture of Nanocoatings," *Langmuir*, vol. 36, no. 18, pp. 4985–4994, 2020, doi: 10.1021/acs.langmuir.0c00544.

[26] R. Zhang *et al.*, "Self-assembly of chitosan and cellulose chains into a 3D porous polysaccharide alloy films: Co-dissolving, structure and biological properties," *Appl. Surf. Sci.*, vol. 493, no. April, pp. 1032–1041, 2019, doi: 10.1016/j.apsusc.2019.06.193.

[27] D. A. Marín-Silva, S. Rivero, and A. Pinotti, "Chitosan-based nanocomposite matrices: Development and characterization," *Int. J. Biol. Macromol.*, vol. 123, pp. 189–200, 2019, doi: 10.1016/j.ijbiomac.2018.11.035.

[28] Rahmi, Lelifajri, Julinawati, and Shabrina, "Preparation of chitosan composite film reinforced with cellulose isolated from oil palm empty fruit bunch and application in cadmium ions removal from aqueous solutions," *Carbohydr. Polym.*, vol. 170, pp. 226–233, 2017, doi: 10.1016/j.carbpol.2017.04.084.

[29] "Chitosan | Heppe Medical Chitosan." https://www.gmp-chitosan.com/en/products-services/chitosan.html (accessed Nov. 14, 2020).

[30] T. K. Varun, S. Senani, N. Jayapal, J. Chikkerur, S. Roy, and V. B. Tekulapally, "Extraction of chitosan and its oligomers from shrimp shell waste , their characterization and antimicrobial effect," vol. 10, 2017, doi: 10.14202/vetworld.2017.170-175.

[31] P. S. Bakshia, D. Selvakumara, K. Kadirvelub, and N. S. Kumara, "CHITOSAN AS AN ENVIRONMENT FRIENDLY BIOMATERIAL – A REVIEW ON RECENT MODIFICATIONS AND APPLICATIONS," *Int. J. Biol. Macromol.*, 2019, doi: 10.1016/j.ijbiomac.2019.10.113.

[32] I. Younes and M. Rinaudo, "Chitin and Chitosan Preparation from Marine Sources. Structure, Properties and Applications," pp. 1133–1174, 2015, doi: 10.3390/md13031133.

[33] F. Khoushab and M. Yamabhai, "Chitin Research Revisited," pp. 1988–2012, 2012, doi: 10.3390/md8071988.

[34] A. Muxika, A. Etxabide, J. Uranga, P. Guerrero, and K. De Caba, "Chitosan as a bioactive polymer : Processing , properties and applications," *Int. J. Biol. Macromol.*, vol. 105, pp. 1358–1368, 2017, doi: 10.1016/j.ijbiomac.2017.07.087.

[35] A. Percot, C. Viton, and A. Domard, "Optimization of Chitin Extraction from

Shrimp Shells," pp. 12–18, 2003.

[36] S. Islam, M. A. R. Bhuiyan, and M. N. Islam, "Chitin and Chitosan: Structure, Properties and Applications in Biomedical Engineering," *J. Polym. Environ.*, vol. 25, no. 3, pp. 854–866, 2017, doi: 10.1007/s10924-016-0865-5.

[37] H. El Knidri, R. Belaabed, A. Addaou, A. Laajeb, and A. Lahsini, "Extraction, chemical modification and characterization of chitin and chitosan," *Int. J. Biol. Macromol.*, vol. 120, pp. 1181–1189, 2018, doi: 10.1016/j.ijbiomac.2018.08.139.

[38] R. Priyadarshi and J. W. Rhim, "Chitosan-based biodegradable functional films for food packaging applications," *Innov. Food Sci. Emerg. Technol.*, vol. 62, no. December 2019, p. 102346, 2020, doi: 10.1016/j.ifset.2020.102346.

[39] R. M. Silva, G. A. Silva, O. P. Coutinho, J. F. Mano, and R. L. Reis, "Preparation and characterisation in simulated body conditions of glutaraldehyde crosslinked chitosan membranes," *J. Mater. Sci. Mater. Med.*, vol. 15, no. 10, pp. 1105–1112, 2004, doi: 10.1023/B:JMSM.0000046392.44911.46.

[40] C. Chatelet, O. Damour, and A. Domard, "Influence of the degree of acetylation on some biological properties of chitosan films," vol. 22, pp. 261–268, 2001.

[41] Y. Wang, E. Wang, Z. Wu, H. Li, Z. Zhu, and X. Zhu, "Synthesis of chitosan molecularly imprinted polymers for solid-phase extraction of methandrostenolone," *Carbohydr. Polym.*, vol. 101, pp. 517–523, 2014, doi: 10.1016/j.carbpol.2013.09.078.

[42] M. Hosseinnejad and S. M. Jafari, "Evaluation of different factors affecting antimicrobial properties of chitosan," *Int. J. Biol. Macromol.*, 2016, doi: 10.1016/j.ijbiomac.2016.01.022.

[43] J. Sundaram, J. Pant, M. J. Goudie, S. Mani, and H. Handa, "Antimicrobial and Physicochemical Characterization of Biodegradable , Nitric Oxide-Releasing Nanocellulose-Chitosan Packaging Membranes University of Georgia University of Georgia," 2016, doi: 10.1021/acs.jafc.6b01936.

[44] I. Leceta, P. Guerrero, I. Ibarburu, M. T. Dueñas, and K. De Caba, "Characterization and antimicrobial analysis of chitosan-based films," *J. Food Eng.*, vol. 116, no. 4, pp. 889–899, 2013, doi: 10.1016/j.jfoodeng.2013.01.022.

[45]  G. L. Dotto, M. L. G. Vieira, and L. A. A. Pinto, "Use of chitosan solutions for the microbiological shelf life extension of papaya fruits during storage at room temperature," *LWT - Food Sci. Technol.*, vol. 64, no. 1, pp. 126–130, 2015, doi: 10.1016/j.lwt.2015.05.042.

[46]  X. Sun, Z. Wang, H. Kadouh, and K. Zhou, "The antimicrobial , mechanical , physical and structural properties of chitosan-gallic acid films," *LWT - Food Sci. Technol.*, vol. 57, no. 1, pp. 83–89, 2014, doi: 10.1016/j.lwt.2013.11.037.

[47]  Z. Zhong, R. Xing, S. Liu, and L. Wang, "Synthesis of acyl thiourea derivatives of chitosan and their antimicrobial activities in vitro," vol. 343, pp. 566–570, 2008, doi: 10.1016/j.carres.2007.11.024.

[48]  M. Salari, M. Sowti Khiabani, R. Rezaei Mokarram, B. Ghanbarzadeh, and H. Samadi Kafil, "Development and evaluation of chitosan based active nanocomposite films containing bacterial cellulose nanocrystals and silver nanoparticles," *Food Hydrocoll.*, vol. 84, pp. 414–423, 2018, doi: 10.1016/j.foodhyd.2018.05.037.

[49]  M. He *et al.*, "Construction of novel cellulose/chitosan composite hydrogels and films and their applications," *Cellulose*, vol. 25, no. 3, pp. 1987–1996, 2018, doi: 10.1007/s10570-018-1683-9.

[50]  L. Zheng and J. Zhu, "Study on antimicrobial activity of chitosan with different molecular weights," vol. 54, pp. 527–530, 2003, doi: 10.1016/j.carbpol.2003.07.009.

[51]  T. Murphy, M. Morris, E. Cummins, and J. P. Kerry, "Antimicrobial activity of chitosan, organic acids and nano-sized solubilisates for potential use in smart antimicrobially-active packaging for potential food applications," *Food Control*, 2013, doi: 10.1016/j.foodcont.2013.04.042.

[52]  R. C. Goy, S. T. B. Morais, and O. B. G. Assis, "Evaluation of the antimicrobial activity of chitosan and its quaternized derivative on E. coli and S. aureus growth," *Rev. Bras. Farmacogn.*, 2015, doi: 10.1016/j.bjp.2015.09.010.

[53]  S. Lim and S. M. Hudson, "Synthesis and antimicrobial activity of a water-soluble chitosan derivative with a fiber-reactive group," vol. 339, pp. 313–319, 2004, doi: 10.1016/j.carres.2003.10.024.

[54] C. Qin, H. Li, Q. Xiao, Y. Liu, J. Zhu, and Y. Du, "Water-solubility of chitosan and its antimicrobial activity," vol. 63, pp. 367–374, 2006, doi: 10.1016/j.carbpol.2005.09.023.

[55] H. Wang, J. Qian, and F. Ding, "Emerging Chitosan-Based Films for Food Packaging Applications," *J. Agric. Food Chem.*, vol. 66, no. 2, pp. 395–413, 2018, doi: 10.1021/acs.jafc.7b04528.

[56] P. Kumari, K. Barman, V. B. Patel, M. W. Siddiqui, and B. Kole, "Reducing postharvest pericarp browning and preserving health promoting compounds of litchi fruit by combination treatment of salicylic acid and chitosan," *Sci. Hortic. (Amsterdam).*, 2015, doi: 10.1016/j.scienta.2015.10.017.

[57] A. Díez-Pascual and A. Díez-Vicente, "Antimicrobial and sustainable food packaging based on poly(butylene adipate-co-terephthalate) and electrospun chitosan nanofibers," pp. 93095–93107, 2015, doi: 10.1039/C5RA14359D.

[58] E. Latou, S. F. Mexis, A. V Badeka, S. Kontakos, and M. G. Kontominas, "Combined effect of chitosan and modified atmosphere packaging for shelf life extension of chicken breast fillets.," *LWT - Food Sci. Technol.*, vol. 55, no. 1, pp. 263–268, 2014, doi: 10.1016/j.lwt.2013.09.010.

[59] X. Shao, B. Cao, F. Xu, S. Xie, D. Yu, and H. Wang, "Effect of postharvest application of chitosan combined with clove oil against citrus green mold," *Postharvest Biol. Technol.*, vol. 99, pp. 37–43, 2015, doi: 10.1016/j.postharvbio.2014.07.014.

[60] A. M. Youssef, H. Abou-yousef, S. M. El-sayed, and S. Kamel, "Mechanical and antibacterial properties of novel high performance chitosan/nanocomposite films," *Int. J. Biol. Macromol.*, vol. 76, pp. 25–32, 2015, doi: 10.1016/j.ijbiomac.2015.02.016.

[61] T. Heinze, "Cellulose: Structure and Properties," 2015, doi: 10.1007/12.

[62] R. J. Moon, A. Martini, J. Nairn, J. Simonsen, and J. Youngblood, *Cellulose nanomaterials review: structure , properties and nanocomposites.* 2011.

[63] M. Moniri *et al.*, "Production and Status of Bacterial Cellulose in Biomedical Engineering," pp. 1–26, 2017, doi: 10.3390/nano7090257.

[64] Y. Habibi, L. A. Lucia, and O. J. Rojas, "Cellulose Nanocrystals: Chemistry , Self-Assembly , and Applications," vol. d, pp. 3479–3500, 2010.

[65] M. A. Azizi Samir, F. Alloin, and A. Dufresne, "Review of Recent Research into Cellulosic Whiskers, Their Properties and Their Application in Nanocomposite Field," pp. 612–626, 2005.

[66] H. Mao, C. Wei, Y. Gong, S. Wang, and W. Ding, "Mechanical and Water-Resistant Properties of Eco-Friendly Chitosan Membrane Reinforced with Cellulose Nanocrystals," 2019, doi: 10.3390/polym11010166.

[67] S. P. Rowland and E. J. Roberts, "The Nature of Accessible Surfaces in the Microstructure of Cotton Cellulose," vol. 10, pp. 2447–2461, 1972.

[68] S. Thapa *et al.*, "Microbial cellulolytic enzymes: diversity and biotechnology with reference to lignocellulosic biomass degradation," *Rev. Environ. Sci. Bio/Technology*, vol. 0123456789, 2020, doi: 10.1007/s11157-020-09536-y.

[69] H. Yamamoto and F. Horii, "CPMAS carbon-13 NMR analysis of the crystal transformation induced for Valonia cellulose by annealing at high temperatures," pp. 1313–1317, 1993.

[70] D. O. Carlsson, J. Lindh, M. Strømme, and A. Mihranyan, "Susceptibility of I$\alpha$- and I$\beta$-Dominated Cellulose to TEMPO-Mediated Oxidation," 2015, doi: 10.1021/acs.biomac.5b00274.

[71] S. F. Tanner, N. Cartier, and H. Chanzy, "High-Resolution Solid-state 13C Nuclear Magnetic Resonance Spectroscopy of Tunicin, an Animal Cellulose," vol. 1617, no. 4, pp. 1615–1617, 1989.

[72] S. M. Hudson and J. A. Cuculo, "The Solubility of Cellulose in Liquid Ammonia / Salt Solutions," vol. 18, pp. 3469–3481, 1980.

[73] K. H. Attori, E. A. Be, T. Y. Oshida, and J. A. C. U. Ã, "New Solvents for Cellulose . II . Ethylenediamine / Thiocyanate Salt System," vol. 36, no. 2, pp. 123–130, 2004.

[74] D. Klemm, B. Heublein, H. Fink, and A. Bohn, "Cellulose : Fascinating Biopolymer and Sustainable Raw Material," pp. 3358–3393, 2005, doi: 10.1002/anie.200460587.

[75] J. Marett, A. Aning, and E. J. Foster, "The isolation of cellulose nanocrystals from pistachio shells via acid hydrolysis," *Ind. Crop. Prod.*, vol. 109, no. September, pp. 869–874, 2017, doi: 10.1016/j.indcrop.2017.09.039.

[76] S. Kampangkaew, C. Thongpin, and O. Santawtee, "The synthesis of cellulose nanofibers from Sesbania Javanica for filler in thermoplastic starch," *Energy Procedia*, vol. 56, no. C, pp. 318–325, 2014, doi: 10.1016/j.egypro.2014.07.163.

[77] M. Mujtaba, A. M. Salaberria, M. A. Andres, M. Kaya, A. Gunyakti, and J. Labidi, "Utilization of flax (Linum usitatissimum) cellulose nanocrystals as reinforcing material for chitosan films," *Int. J. Biol. Macromol.*, vol. 104, pp. 944–952, 2017, doi: 10.1016/j.ijbiomac.2017.06.127.

[78] S. Gopi, A. Amalraj, S. Jude, S. Thomas, and Q. Guo, "Bionanocomposite films based on potato, tapioca starch and chitosan reinforced with cellulose nanofiber isolated from turmeric spent," *J. Taiwan Inst. Chem. Eng.*, vol. 96, pp. 664–671, 2019, doi: 10.1016/j.jtice.2019.01.003.

[79] J. C. C. S, N. George, and S. K. Narayanankutty, "Isolation and Characterization of Cellulose Nanofibrils From Arecanut Husk Fibre," *Carbohydr. Polym.*, 2016, doi: 10.1016/j.carbpol.2016.01.015.

[80] C. E. Maepa, J. Jayaramudu, J. O. Okonkwo, S. S. Ray, and E. R. Sadiku, "Extraction and Characterization of Natural Cellulose Fibers from Maize Tassel Extraction and Characterization of Natural Cellulose Fibers from Maize Tassel," *GPAC*, vol. 20, no. 2, pp. 99–109, 2015, doi: 10.1080/1023666X.2014.961118.

[81] K. O. Reddy *et al.*, "Extraction and Characterization of Cellulose Single Fibers from Native African Napier Grass," *Carbohydr. Polym.*, 2018, doi: 10.1016/j.carbpol.2018.01.110.

[82] K. O. Reddy, C. U. Maheswari, M. Dhlamini, and V. P. Kommula, "An Exploration on the Characteristics of Cellulose Microfibers From Palmyra Palm Fruits," vol. 5341, no. February, 2016, doi: 10.1080/1023666X.2016.1147799.

[83] R. D. Kale, P. Shobha, and B. Vikrant, "Extraction of Microcrystalline Cellulose from Cotton Sliver and Its Comparison with Commercial Microcrystalline Cellulose," *J. Polym. Environ.*, vol. 26, no. 1, pp. 355–364, 2018, doi: 10.1007/s10924-017-0936-2.

[84]    I. Ismail, D. Sa, P. Rahajeng, and A. Suprayitno, "Extraction of Cellulose Microcrystalline from Galam Wood for Biopolymer," vol. 020072, 2018, doi: 10.1063/1.5030294.

[85]    J. P. Reddy and J. Rhim, "Extraction and Characterization of Cellulose Microfibers from Agricultural Wastes of Onion and Garlic," *J. Nat. Fibers*, vol. 00, no. 00, pp. 1–9, 2018, doi: 10.1080/15440478.2014.945227.

[86]    Z. Florencia and C. Menegalli, "Isolation and characterization of cellulose nanofibers from cassava root bagasse and peelings," *Carbohydr. Polym.*, 2016, doi: 10.1016/j.carbpol.2016.10.048.

[87]    J. L. Amaming, S. C. C. Hew, R. H. Ashim, O. S. Ulaiman, and T. S. Ugimoto, "Extraction of Microcrystalline Cellulose from Oil Palm Trunk," pp. 513–518, 2017.

[88]    H. Celebi and A. Kurt, *Effects of processing on the properties of chitosan/cellulose nanocrystal films*, vol. 133. Elsevier Ltd., 2015.

[89]    D. Wang, W. Cheng, Y. Yue, L. Xuan, X. Ni, and G. Han, "Electrospun cellulose nanocrystals/chitosan/polyvinyl alcohol nanofibrous films and their exploration to metal ions adsorption," *Polymers (Basel).*, vol. 10, no. 10, 2018, doi: 10.3390/polym10101046.

[90]    M. Fardioui, I. Meftah Kadmiri, A. el kacem Qaiss, and R. Bouhfid, "Bio-active nanocomposite films based on nanocrystalline cellulose reinforced styrylquinoxalin-grafted-chitosan: Antibacterial and mechanical properties," *Int. J. Biol. Macromol.*, vol. 114, no. 2017, pp. 733–740, 2018, doi: 10.1016/j.ijbiomac.2018.03.114.

[91]    S. Sheng, Z. Meiling, L. Chen, H. Wensheng, and Y. Zhifeng, "Extraction and characterization of microcrystalline cellulose from waste cotton fabrics via hydrothermal method," *Waste Manag.*, vol. 82, pp. 139–146, 2018, doi: 10.1016/j.wasman.2018.10.023.

[92]    A. Jiménez, M. J. Fabra, P. Talens, and A. Chiralt, "Polysaccharides as Valuable Materials in Food Packaging," *Funct. Polym. Food Sci. From Technol. to Biol.*, vol. 1, pp. 211–251, 2015, doi: 10.1002/9781119109785.ch7.

[93]  Y. Li, G. Li, Y. Zou, Q. Zhou, and X. Liamn, "Preparation and characterization of cellulose nanofibers from partly mercerized cotton by mixed acid hydrolysis," pp. 301–309, 2014, doi: 10.1007/s10570-013-0146-6.

[94]  A. F. Jozala, R. Aparecida, N. Pértile, and C. Alves, "Bacterial cellulose production by Gluconacetobacter xylinus by employing alternative culture media," 2014, doi: 10.1007/s00253-014-6232-3.

[95]  N. Stepanov and E. Efremenko, "'Deceived' Concentrated Immobilized Cells as Biocatalyst for Intensive Bacterial Cellulose Production from Various Sources," 2018, doi: 10.3390/catal8010033.

[96]  X. Wang *et al.*, "Physical properties and antioxidant capacity of chitosan/epigallocatechin-3-gallate films reinforced with nano-bacterial cellulose," *Carbohydr. Polym.*, vol. 179, pp. 207–220, 2018, doi: 10.1016/j.carbpol.2017.09.087.

[97]  E. F. Douglass, H. Avci, R. Boy, O. J. Rojas, and R. Kotek, "A Review of Cellulose and Cellulose Blends for Preparation of Bio-derived and Conventional Membranes, Nanostructured Thin Films, and Composites," *Polym. Rev.*, vol. 58, no. 1, pp. 102–163, 2018, doi: 10.1080/15583724.2016.1269124.

[98]  P. Taylor, Q. Lin, X. Chen, and X. Chen, "Bacterial Cellulose Production from the Litchi Extract by Gluconacetobacter Xylinus," no. November, pp. 37–41, 2014, doi: 10.1080/10826068.2014.958163.

[99]  S. Dima *et al.*, "Bacterial Nanocellulose from Side-Streams of Kombucha Beverages Production : Preparation and Physical-Chemical Properties," pp. 5–10, 2017, doi: 10.3390/polym9080374.

[100] R. Machado *et al.*, "Komagataeibacter rhaeticus as an alternative bacteria for cellulose production," *Carbohydr. Polym.*, 2016, doi: 10.1016/j.carbpol.2016.06.049.

[101] C. Huang *et al.*, "Utilization of Corncob Acid Hydrolysate for Bacterial Cellulose Production by Gluconacetobacter xylinus," no. 2, 2014, doi: 10.1007/s12010-014-1407-z.

[102] I. Reiniati, A. N. Hrymak, and A. Margaritis, "Kinetics of cell growth and

crystalline nanocellulose production by Komagataeibacter xylinus," *Biochem. Eng. J.*, vol. 127, pp. 21–31, 2017, doi: 10.1016/j.bej.2017.07.007.

[103] A. Grzabka-Zasadzinska, W. Smulek, E. Kaczorek, and S. Borysiak, "Chitosan Biocomposites with enzymatically produced nanocrystalline cellulose," *Polym. Polym. Compos.*, vol. 16, no. 2, pp. 101–113, 2017, doi: 10.1002/pc.

[104] Z. Kassab, H. Ben youcef, H. Hannache, and M. El Achaby, "Isolation of cellulose nanocrystals from various lignocellulosic materials: Physico-chemical characterization and Application in Polymer Composites Development," *Mater. Today Proc.*, vol. 13, pp. 964–973, 2019, doi: 10.1016/j.matpr.2019.04.061.

[105] V. C. Souza, E. Niehues, and M. G. N. Quadri, "Development and characterization of chitosan bionanocomposites containing oxidized cellulose nanocrystals," *J. Appl. Polym. Sci.*, vol. 133, no. 7, pp. 1–9, 2016, doi: 10.1002/app.43033.

[106] F. A. Corsello, P. A. Bolla, P. S. Anbinder, M. A. Serradell, J. I. Amalvy, and P. J. Peruzzo, "Morphology and properties of neutralized chitosan-cellulose nanocrystals biocomposite films," *Carbohydr. Polym.*, vol. 156, pp. 452–459, 2017, doi: 10.1016/j.carbpol.2016.09.031.

[107] M. El Achaby, Z. Kassab, A. Barakat, and A. Aboulkas, "Alfa fibers as viable sustainable source for cellulose nanocrystals extraction: Application for improving the tensile properties of biopolymer nanocomposite films," *Ind. Crops Prod.*, vol. 112, no. December 2017, pp. 499–510, 2018, doi: 10.1016/j.indcrop.2017.12.049.

[108] R. E. Abou-Zeid, E. A. Hassan, F. Bettaieb, R. Khiari, and M. L. Hassan, "Use of Cellulose and Oxidized Cellulose Nanocrystals from Olive Stones in Chitosan Bionanocomposites," *J. Nanomater.*, vol. 2015, 2015, doi: 10.1155/2015/687490.

[109] A. Grza, "Influence of the polymorphism of cellulose on the formation of nanocrystals and their application in chitosan / nanocellulose composites," vol. 42864, pp. 1–9, 2016, doi: 10.1002/app.42864.

[110] A. Grzabka-Zasadzińska, T. Amietszajew, and S. Borysiak, "Thermal and mechanical properties of chitosan nanocomposites with cellulose modified in ionic liquids," *J. Therm. Anal. Calorim.*, vol. 130, no. 1, pp. 143–154, 2017, doi: 10.1007/s10973-017-6295-3.

[111] Y. Liu *et al.*, "Biological–chemical modification of cellulose nanocrystal to prepare highly compatible chitosan-based nanocomposites," *Cellulose*, vol. 26, no. 9, pp. 5267–5279, 2019, doi: 10.1007/s10570-019-02486-x.

[112] Y. Liu, M. Li, M. Qiao, X. Ren, T. S. Huang, and G. Buschle-Diller, "Antibacterial membranes based on chitosan and quaternary ammonium salts modified nanocrystalline cellulose," *Polym. Adv. Technol.*, vol. 28, no. 12, pp. 1629–1635, 2017, doi: 10.1002/pat.4032.

[113] Z. Deng, J. Jung, J. Simonsen, and Y. Zhao, "Cellulose nanocrystals Pickering emulsion incorporated chitosan coatings for improving storability of postharvest Bartlett pears (Pyrus communis) during long-term cold storage," *Food Hydrocoll.*, vol. 84, no. June, pp. 229–237, 2018, doi: 10.1016/j.foodhyd.2018.06.012.

[114] M. C. Etty *et al.*, "New immobilization method of anti-PepD monoclonal antibodies for the detection of Listeria monocytogenes p60 protein – Part A: Optimization of a crosslinked film support based on chitosan and cellulose nanocrystals (CNC)," *React. Funct. Polym.*, vol. 146, no. April, p. 104313, 2020, doi: 10.1016/j.reactfunctpolym.2019.06.021.

[115] M. A. Smirnov *et al.*, "Green method for preparation of cellulose nanocrystals using deep eutectic solvent," *Cellulose*, vol. 27, no. 8, pp. 4305–4317, 2020, doi: 10.1007/s10570-020-03100-1.

[116] V. Rubentheren, T. A. Ward, C. Y. Chee, P. Nair, E. Salami, and C. Fearday, "Effects of heat treatment on chitosan nanocomposite film reinforced with nanocrystalline cellulose and tannic acid," *Carbohydr. Polym.*, vol. 140, pp. 202–208, 2016, doi: 10.1016/j.carbpol.2015.12.068.

[117] V. Rubentheren, T. A. Ward, C. Y. Chee, and P. Nair, "Physical and chemical reinforcement of chitosan film using nanocrystalline cellulose and tannic acid," *Cellulose*, vol. 22, no. 4, pp. 2529–2541, 2015, doi: 10.1007/s10570-015-0650-y.

[118] X. Tian, F. Hua, C. Lou, and X. Jiang, "Cationic cellulose nanocrystals (CCNCs) and chitosan nanocomposite films filled with CCNCs for removal of reactive dyes from aqueous solutions," *Cellulose*, vol. 25, no. 7, pp. 3927–3939, 2018, doi: 10.1007/s10570-018-1842-z.

[119] X. Tian and X. Jiang, "Preparing water-soluble 2, 3-dialdehyde cellulose as a bio-

origin cross-linker of chitosan," *Cellulose*, vol. 25, no. 2, pp. 987–998, 2018, doi: 10.1007/s10570-017-1607-0.

[120] S. K. Bajpai, S. Ahuja, N. Chand, and M. Bajpai, "Nano cellulose dispersed chitosan film with Ag NPs/Curcumin: An in vivo study on Albino Rats for wound dressing," *Int. J. Biol. Macromol.*, vol. 104, pp. 1012–1019, 2017, doi: 10.1016/j.ijbiomac.2017.06.096.

[121] Z. Deng, J. Jung, J. Simonsen, Y. Wang, and Y. Zhao, "Cellulose Nanocrystal Reinforced Chitosan Coatings for Improving the Storability of Postharvest Pears Under Both Ambient and Cold Storages," *J. Food Sci.*, vol. 82, no. 2, pp. 453–462, 2017, doi: 10.1111/1750-3841.13601.

[122] F. Hossain, P. Follett, S. Salmieri, K. D. Vu, C. Fraschini, and M. Lacroix, "Antifungal activities of combined treatments of irradiation and essential oils (EOs) encapsulated chitosan nanocomposite films in in vitro and in situ conditions," *Int. J. Food Microbiol.*, vol. 295, no. July 2018, pp. 33–40, 2019, doi: 10.1016/j.ijfoodmicro.2019.02.009.

[123] F. Hossain, P. Follett, S. Salmieri, K. D. Vu, M. Harich, and M. Lacroix, "Synergistic Effects of Nanocomposite Films Containing Essential Oil Nanoemulsions in Combination with Ionizing Radiation for Control of Rice Weevil Sitophilus oryzae in Stored Grains," *J. Food Sci.*, vol. 84, no. 6, pp. 1439–1446, 2019, doi: 10.1111/1750-3841.14603.

[124] J. Y. M. Wong and M. Y. Chan, "Influence of bleaching treatment by hydrogen peroxide on chitosan/durian husk cellulose biocomposite films," *Adv. Polym. Technol.*, vol. 37, no. 7, pp. 2462–2469, 2018, doi: 10.1002/adv.21921.

[125] J. R. Rodríguez-Núñez, T. J. Madera-Santana, D. I. Sánchez-Machado, J. López-Cervantes, and H. Soto Valdez, "Chitosan/Hydrophilic Plasticizer-Based Films: Preparation, Physicochemical and Antimicrobial Properties," *J. Polym. Environ.*, vol. 22, no. 1, pp. 41–51, 2014, doi: 10.1007/s10924-013-0621-z.

[126] H. M. C. Azeredo *et al.*, "Nanocellulose reinforced chitosan composite films as affected by nanofiller loading and plasticizer content," *J. Food Sci.*, vol. 75, no. 1, pp. 1–7, 2010, doi: 10.1111/j.1750-3841.2009.01386.x.

[127] H. Li, X. Gao, Y. Wang, X. Zhang, and Z. Tong, "Comparison of chitosan/starch

composite film properties before and after cross-linking," *Int. J. Biol. Macromol.*, vol. 52, no. 1, pp. 275–279, 2013, doi: 10.1016/j.ijbiomac.2012.10.016.

[128] E. T. Thostenson and T. Chou, "Microwave and Conventional Curing of Thick-Section Thermoset Composite Laminates: Experiment and Simulation," vol. 22, no. 2, 2001.

[129] Y. Xu, S. Willis, K. Jordan, and E. Sismour, "Chitosan nanocomposite films incorporating cellulose nanocrystals and grape pomace extracts," *Packag. Technol. Sci.*, vol. 31, no. 9, pp. 631–638, 2018, doi: 10.1002/pts.2389.

[130] E. Jahed, M. A. Khaledabad, M. R. Bari, and H. Almasi, "Effect of cellulose and lignocellulose nanofibers on the properties of Origanum vulgare ssp. gracile essential oil-loaded chitosan films," vol. 117, no. April, pp. 70–80, 2017, doi: 10.1016/j.reactfunctpolym.2017.06.008.

[131] S. Y. Rong, N. M. Mubarak, and F. A. Tanjung, "Structure-property relationship of cellulose nanowhiskers reinforced chitosan biocomposite films," *J. Environ. Chem. Eng.*, vol. 5, no. 6, pp. 6132–6136, 2017, doi: 10.1016/j.jece.2017.11.054.

[132] E. Sogut and H. Cakmak, "Utilization of carrot (Daucus carota L.) fiber as a filler for chitosan based films," *Food Hydrocoll.*, vol. 106, no. December 2019, p. 105861, 2020, doi: 10.1016/j.foodhyd.2020.105861.

[133] J. S. Smith, D. Bedrov, and G. D. Smith, "A molecular dynamics simulation study of nanoparticle interactions in a model polymer-nanoparticle composite," vol. 63, pp. 1599–1605, 2003, doi: 10.1016/S0266-3538(03)00061-7.

[134] T. Huq *et al.*, "Nanocrystalline cellulose ( NCC ) reinforced alginate based biodegradable nanocomposite film," *Carbohydr. Polym.*, vol. 90, no. 4, pp. 1757–1763, 2012, doi: 10.1016/j.carbpol.2012.07.065.

[135] A. Dorigato, Y. Dzenis, and A. Pegoretti, *Filler Aggregation as a Stiffening Mechanism in Polymer Nanocomposites*, no. January. 2013.

[136] S. Wang *et al.*, "Characteristics and biodegradation properties of poly ( 3-hydroxybutyrate- co -3-hydroxyvalerate )/ organophilic montmorillonite ( PHBV / OMMT ) nanocomposite," vol. 87, pp. 69–76, 2005, doi: 10.1016/j.polymdegradstab.2004.07.008.

[137] V. Tanrattanakul and D. Jaroendee, "Comparison Between Microwave and Thermal Curing of Glass Fiber-Epoxy Composites : Effect of Microwave-Heating Cycle on Mechanical Properties," 2006, doi: 10.1002/app.24245.

[138] N. Detduangchan, W. Sridach, and T. Wittaya, "Enhancement of the properties of biodegradable rice starch films by using chemical crosslinking agents," vol. 21, no. 3, pp. 1225–1235, 2014.

[139] M. Ghasemlou *et al.*, "Physical, mechanical and barrier properties of corn starch films incorporated with plant essential oils," *Carbohydr. Polym.*, 2013, doi: 10.1016/j.carbpol.2013.07.026.

[140] T. S. Franco *et al.*, "Carboxymethyl and Nanofibrillated Cellulose as Additives on the Preparation of Chitosan Biocomposites: Their Influence Over Films Characteristics," *J. Polym. Environ.*, vol. 28, no. 2, pp. 676–688, 2020, doi: 10.1007/s10924-019-01639-0.

[141] A. Adel, A. El-Shafei, A. Ibrahim, and M. Al-Shemy, "Extraction of oxidized nanocellulose from date palm (Phoenix Dactylifera L.) sheath fibers: Influence of CI and CII polymorphs on the properties of chitosan/bionanocomposite films," *Ind. Crops Prod.*, vol. 124, no. July, pp. 155–165, 2018, doi: 10.1016/j.indcrop.2018.07.073.

[142] J. Yang, C. Dahlström, H. Edlund, B. Lindman, and M. Norgren, "pH-responsive cellulose–chitosan nanocomposite films with slow release of chitosan," *Cellulose*, vol. 26, no. 6, pp. 3763–3776, 2019, doi: 10.1007/s10570-019-02357-5.

[143] K. Zhao *et al.*, "Using cellulose nanofibers to reinforce polysaccharide films: Blending vs layer-by-layer casting," *Carbohydr. Polym.*, vol. 227, no. August 2019, 2020, doi: 10.1016/j.carbpol.2019.115264.

[144] B. Amalia, C. Imawan, and A. Listyarini, "Fabrication and characterization of thick films made of chitosan and nanofibrillar cellulose derived from pineapple leaf," *IOP Conf. Ser. Mater. Sci. Eng.*, vol. 496, no. 1, pp. 4–9, 2019, doi: 10.1088/1757-899X/496/1/012021.

[145] M. Ghazanfari, I. Ranginkar Jahromi, A. Moallemi-Oreh, H. Ebadi-Dehaghani, and M. Akbarzadeh, "Evaluation of mixing efficiency in elaborating of chitosan/cellulose nanocomposite via statistical analyses," *Int. J. Biol. Macromol.*,

vol. 93, pp. 703–711, 2016, doi: 10.1016/j.ijbiomac.2016.09.010.

[146] R. Kumar, B. Rai, and G. Kumar, "A Simple Approach for the Synthesis of Cellulose Nanofiber Reinforced Chitosan/PVP Bio Nanocomposite Film for Packaging," *J. Polym. Environ.*, no. 0123456789, 2019, doi: 10.1007/s10924-019-01588-8.

[147] J. Liang, R. Wang, and R. Chen, "The impact of cross-linking mode on the physical and antimicrobial properties of a chitosan/bacterial cellulose composite," *Polymers (Basel).*, vol. 11, no. 3, 2019, doi: 10.3390/polym11030491.

[148] X. Zheng *et al.*, "Efficient removal of anionic dye (Congo red) by dialdehyde microfibrillated cellulose/chitosan composite film with significantly improved stability in dye solution," *Int. J. Biol. Macromol.*, vol. 107, no. PartA, pp. 283–289, 2018, doi: 10.1016/j.ijbiomac.2017.08.169.

[149] K. Choo, Y. C. Ching, C. H. Chuah, S. Julai, and N. Liou, "Preparation and Characterization of Polyvinyl Alcohol-Chitosan Composite Films Reinforced with Cellulose Nanofiber," pp. 1–16, 2016, doi: 10.3390/ma9080644.

[150] B. Soni, E. B. Hassan, M. W. Schilling, and B. Mahmoud, "Transparent bionanocomposite films based on chitosan and TEMPO-oxidized cellulose nanofibers with enhanced mechanical and barrier properties," *Carbohydr. Polym.*, vol. 151, pp. 779–789, 2016, doi: 10.1016/j.carbpol.2016.06.022.

[151] E. Jahed, M. A. Khaledabad, H. Almasi, and R. Hasanzadeh, "Physicochemical properties of Carum copticum essential oil loaded chitosan films containing organic nanoreinforcements," *Carbohydr. Polym.*, vol. 164, pp. 325–338, 2017, doi: 10.1016/j.carbpol.2017.02.022.

[152] S. Chen, M. Wu, C. Wang, S. Yan, P. Lu, and S. Wang, "Developed chitosan/oregano essential oil biocomposite packaging film enhanced by cellulose nanofibril," *Polymers (Basel).*, vol. 12, no. 8, 2020, doi: 10.3390/polym12081780.

[153] E. Sogut and A. C. Seydim, "The effects of chitosan- and polycaprolactone-based bilayer films incorporated with grape seed extract and nanocellulose on the quality of chicken breast fillets," *Lwt*, vol. 101, pp. 799–805, 2019, doi: 10.1016/j.lwt.2018.11.097.

[154] Z. Deng, J. Jung, and Y. Zhao, "Development, characterization, and validation of chitosan adsorbed cellulose nanofiber (CNF) films as water resistant and antibacterial food contact packaging," *LWT - Food Sci. Technol.*, vol. 83, pp. 132–140, 2017, doi: 10.1016/j.lwt.2017.05.013.

[155] L. Ren, X. Yan, J. Zhou, J. Tong, and X. Su, "Influence of chitosan concentration on mechanical and barrier properties of corn starch/chitosan films," *Int. J. Biol. Macromol.*, vol. 105, pp. 1636–1643, 2017, doi: 10.1016/j.ijbiomac.2017.02.008.

[156] S. Sun, P. Liu, N. Ji, H. Hou, and H. Dong, "Effects of various cross-linking agents on the physicochemical properties of starch/PHA composite fi lms produced by extrusion blowing," pp. 1–12, 2017, doi: 10.1016/j.foodhyd.2017.11.046.

[157] Adel, El-Shafei, Al-Shemy, Ibrahim, and Rabia, "Influence of Cellulose Polymorphism on Tunable Mechanical and Barrier Properties of Chitosan/Oxidized Nanocellulose Bio-Composites," vol. 60, no. 4, pp. 639–652, 2017.

[158] M. Pereda, G. Amica, I. Rácz, and N. E. Marcovich, "Structure and properties of nanocomposite films based on sodium caseinate and nanocellulose fibers," *J. Food Eng.*, vol. 103, no. 1, pp. 76–83, 2011, doi: 10.1016/j.jfoodeng.2010.10.001.

[159] D. Dehnad, Z. Emam-djomeh, H. Mirzaei, S.-M. Jafari, and S. Dadashi, "Optimization of physical and mechanical properties for chitosan-nanocellulose biocomposites," *Carbohydr. Polym.*, vol. 105, pp. 222–228, 2014, doi: 10.1016/j.carbpol.2014.01.094.

[160] E. D. Alvarado, M. G. P. Juárez, C. P. Pérez, E. Pérez, and J. A. G. Calderón, "Improvement in the dispersion of TiO2 particles inside Chitosan-Methyl cellulose films by the use of silane coupling agent," *J. Mex. Chem. Soc.*, vol. 63, no. 2, pp. 154–168, 2019, doi: 10.29356/jmcs.v63i2.741.

[161] N. R. Savadekar and S. T. Mhaske, "Synthesis of nano cellulose fibers and effect on thermoplastics starch based films," *Carbohydr. Polym.*, vol. 89, no. 1, pp. 146–151, 2012, doi: 10.1016/j.carbpol.2012.02.063.

[162] E. Fortunati *et al.*, "Microstructure and nonisothermal cold crystallization of PLA composites based on silver nanoparticles and nanocrystalline cellulose," *Polym. Degrad. Stab.*, vol. 97, no. 10, pp. 2027–2036, 2012, doi:

10.1016/j.polymdegradstab.2012.03.027.

[163] C. M. Yeng, S. Husseinsyah, and S. S. Ting, "Modified Corn Cob Filled Chitosan Biocomposite Films," no. December 2014, pp. 37–41, 2013, doi: 10.1080/03602559.2013.820752.

[164] E. Abdul, N. Muhd, and W. Yehye, "Nanocellulose reinforced as green agent in polymer matrix composites applications," no. January, pp. 1–16, 2018, doi: 10.1002/pat.4264.

[165] S. K. Bajpai, N. Chand, and S. Ahuja, "Investigation of curcumin release from chitosan/cellulose micro crystals (CMC) antimicrobial films," *Int. J. Biol. Macromol.*, vol. 79, pp. 440–448, 2015, doi: 10.1016/j.ijbiomac.2015.05.012.

[166] M. Lubis, A. Gana, S. Masysrah, M. Ginting, and M. Harahap, "Production of bioplastic from jackfruit seed starch (Artocarpus heterophyllus ) reinforced with microcrystalline cellulose from cocoa pod husk ( Theobroma cacao L .) using glycerol as plasticizer," pp. 0–9, 2018, doi: 10.1088/1757-899X/309/1/012100.

[167] X. Ma, M. Lv, D. P. Anderson, and P. R. Chang, "Natural polysaccharide composites based on modified cellulose spheres and plasticized chitosan matrix," *Food Hydrocoll.*, vol. 66, pp. 276–285, 2017, doi: 10.1016/j.foodhyd.2016.11.038.

[168] S. K. Bajpai, N. Chand, S. Ahuja, and M. K. Roy, "Vapor induced phase inversion technique to prepare chitosan/microcrystalline cellulose composite films: synthesis, characterization and moisture absorption study," *Cellulose*, vol. 22, no. 6, pp. 3825–3837, 2015, doi: 10.1007/s10570-015-0775-z.

[169] R. Gaudreault, "Salt Necessary for PEO-Cofactor Association : The Role of Molecular Modelling in Salt Necessary for PEO-Cofactor Association : The Role of Molecular Modelling in PEO Flocculation Mechanisms," no. August, 2005.

[170] C. C. S. Coelho *et al.*, "Effect of moderate electric fields in the properties of starch and chitosan films reinforced with microcrystalline cellulose," *Carbohydr. Polym.*, vol. 174, pp. 1181–1191, 2017, doi: 10.1016/j.carbpol.2017.07.007.

[171] X. Huang, F. Xie, and X. Xiong, "Surface-modified microcrystalline cellulose for reinforcement of chitosan film," vol. 201, no. June, pp. 367–373, 2018, doi: 10.1016/j.carbpol.2018.08.085.

[172] S. K. Bajpai, N. Chand, S. Ahuja, and M. K. Roy, "Curcumin/cellulose micro crystals/chitosan films: Water absorption behavior and in vitro cytotoxicity," *Int. J. Biol. Macromol.*, vol. 75, pp. 239–247, 2015, doi: 10.1016/j.ijbiomac.2015.01.038.

[173] A. M. Slavutsky and M. A. Bertuzzi, "Water barrier properties of starch films reinforced with cellulose nanocrystals obtained from sugarcane bagasse," *Carbohydr. Polym.*, vol. 110, pp. 53–61, 2014, doi: 10.1016/j.carbpol.2014.03.049.

[174] B. W. S. Souza, M. A. Cerqueira, J. T. Martins, A. Casariego, J. A. Teixeira, and A. A. Vicente, "Influence of electric fields on the structure of chitosan edible coatings," *Food Hydrocoll.*, vol. 24, no. 4, pp. 330–335, 2010, doi: 10.1016/j.foodhyd.2009.10.011.

[175] A. Kutvonen, G. Rossi, S. R. Puisto, N. K. J. Rostedt, and T. Ala-nissila, "Influence of nanoparticle size , loading , and shape on the mechanical properties of polymer nanocomposites," vol. 214901, 2012, doi: 10.1063/1.4767517.

[176] S. Fu *et al.*, "Acceleration of dermal wound healing by using electrospun curcumin-loaded poly(e-caprolactone)-poly(ethylene glycol)- poly(e-caprolactone) fibrous mats," pp. 1–10, 2013, doi: 10.1002/jbm.b.33032.

[177] X. Xiong, J. Duan, W. Zou, X. He, and W. Zheng, "A pH-sensitive regenerated cellulose membrane," *J. Memb. Sci.*, vol. 363, no. 1–2, pp. 96–102, 2010, doi: 10.1016/j.memsci.2010.07.031.

[178] Y. Tian, P. Zhu, M. Zhou, R. Guo, and F. Cheng, "Microfibrillated cellulose modified with urea and its reinforcement for starch-based bionanocomposites," *Cellulose*, vol. 0123456789, 2019, doi: 10.1007/s10570-019-02505-x.

[179] M. Quaresimin, M. Salviato, and M. Zappalorto, "Strategies for the assessment of nanocomposite mechanical properties," *Compos. Part B*, vol. 43, no. 5, pp. 2290–2297, 2012, doi: 10.1016/j.compositesb.2011.12.012.